IOM

Leibniz-Institut für
Oberflächenmodifizierung e.V.

Biennial Report
2012 / 2013

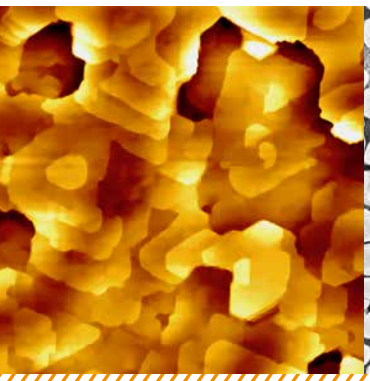
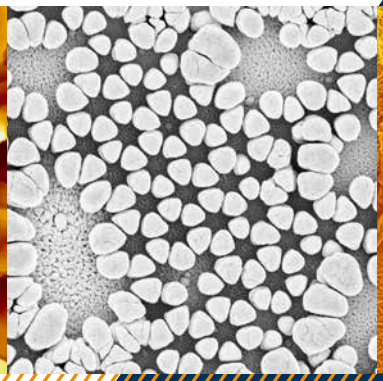
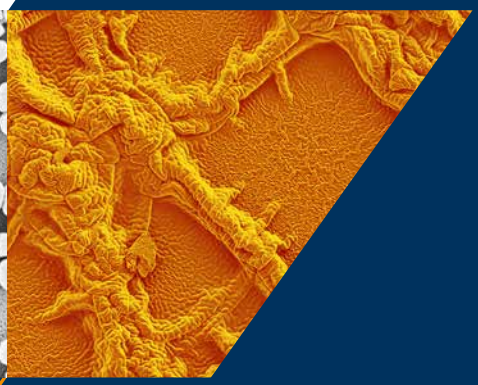

IOM

Leibniz-Institut für
Oberflächenmodifizierung e.V.

Biennial Report
2012 / 2013

Executive Board

Director
Prof. Dr. Dr. h. c. Bernd Rauschenbach

Telefon: +49 341 235-2308
Telefax: +49 341 235-2313

E-Mail: bernd.rauschenbach@iom-leipzig.de

Leibniz-Institut für Oberflächenmodifizierung e. V.
Permoserstraße 15 / D-04318 Leipzig / Germany

Telefon: +49 (0) 341 235-2308
Telefax: +49 (0) 341 235-2313

www.iom-leipzig.de

Members of the Board of Trustees

- **Freistaat Sachsen, Minister für Wissenschaft und Kunst**
  vertreten durch Frau ROR'in Cathrin Liebner
- **Bundesrepublik Deutschland, Bundesminister für Bildung und Forschung**
  vertreten durch Herrn MinR Dr. Herbert Zeisel
- **Verein des Leibniz-Instituts für Oberflächenmodifizierung e. V.**
  vertreten durch Prof. Dr. Rüdiger Szargan

Members of the Scientific Advisory Board

- **Dr.-Ing. Markus Roth (Chairman)**
  Osram GmbH, Business Unit UV/IR, Wipperfürth
- **Prof. Dr. Andre Anders**
  University of California and Lawrence Berkeley National Laboratory, USA
- **Dr. Klaus-Friedrich Beckstette**
  Carl-Zeiss Oberkochen
- **Dr. Kurt Dietliker**
  ETH Zürich and BASF Schweiz AG, Switzerland
- **Prof. Dr. Roger Gläser**
  Universität Leipzig, Fakultät für Chemie und Mineralogie
- **Prof. Dr. Marius Grundmann**
  Universität Leipzig, Fakultät für Physik und Geowissenschaften
- **Prof. Dr. Hans-Gerd Löhmannsröben**
  Universität Potsdam
- **Tino Petsch**
  3D-Micromac AG, Chemnitz
- **Prof. Dr. Christina Trautmann**
  GSI Darmstadt
- **Prof. Dr. Andreas Tünnermann**
  Institut für Angewandte Physik der Universität Jena und
  Fraunhofer Institut für Angewandte Optik und Feinmechanik, Jena

Organisational Structure of the Institute

Contents

Preface

In this biennial report, the Leibniz Institute of Surface Modification (IOM) a member of the Leibniz Association, summarizes its scientific activities for the years 2012 and 2013. In last two years we successfully continued our scientific work in many topics in the research field ion, plasma, electron and photon interaction with surfaces and thin films. The particular strength of the 150 employees of the IOM lies in the skillful connection of research and technology development.

The number of scientific publications was maintained at a high level with a significant fraction of them being published in renowned international journals. The scientists of the IOM contributed a large number of presentations at international conferences and colloquia. In addition to international workshops and conferences organized by the institute, the increased number of invited lectures and foreign visitors hosted by the IOM during the last two years demonstrates the positive development.

Furthermore, in the years 2012 and 2013 the scientists of the institute succeeded in raising third-party funds for projects to advance their research work and technological development. With a total of about 12 million, the third-party funds reached an unprecedented peak. Here, the IOM strongly emphasizes collaborations with the chemical, optical and semiconductor industries.

Particular highlights in 2012 and 2013 were:

- An outstanding event in 2012 certainly represented the 20th anniversary of our institute, which was celebrated in the presence of the Minister of Science and Art of the Free State of Saxony Prof. S. von Schorlemer, the President of the Leipzig University, Prof. B. A. Schücking, President of the Leibniz Association, Prof. K. U. Mayer and many other guests from the Government, BMBF, Leipzig University and industry.
- We extend a warm welcome to Prof. Dr. Bernd Abel who started as the new deputy director and head of the chemical department at the Leibniz Institute of Surface Modification in May 2012. Prof. Abel is also Chair for Chemical Engineering of Polymers at Leipzig University.
- The Leipziger nanoAnalytikum (LenA) at our institute was opened in the presence of the Minister of Science and Art of the Free State of Saxony, Prof. S. von Schorlemer, in May 2012. The LenA center houses high-performance electron microscopes, like STEM and SEM, powerful instruments in material science for studies down to atomic levels.
- Another highlight in 2013 was the opening of a new laboratory and office building at the institute. With an area of approximately 3.000 square meters, there are located a very large laser laboratory, several clean rooms and different laboratories for physical and chemical measuring systems, together with a new lecture hall as well as offices for scientists and visiting guests.
- In August 2013, the Prime Minister of the Free State of Saxony, S. Tillich, visited the Leibniz Institute of Surface Modification together with members of the Bundestag and the Landtag of Saxony.

Our primary objectives remain unchanged: We will join fundamental research together with application oriented research to contribute to the advancement of innovative technologies.

Finally we would like to thank all partners, colleagues and partners from industry and science who supported our progress in 2012 and 2013. Special thank are due to the Members of the Board of Trustees and the Scientific Advisory Board.

Leipzig, in the spring 2014
Prof. B. Rauschenbach

20TH ANNIVERSARY OF IOM LEIPZIG

/ The IOM Leipzig celebrated the foundation of the institute 20 years ago in the presence of the Minister of Science and Art of the Free State of Saxony Prof. S. v. Schorlemer, the President of the Leipzig University, Prof. B. A. Schücking, President of the Leibniz Association, Prof. K. U. Mayer and many other guests from the Government, BMBF, Leipzig University and industry in May 2012.

THE OPENING OF THE LenA CENTER

LenA
Leipziger nanoAnalytikum

/ On the occasion of IOM celebration in May 2012 the Leipziger nanoAnalytikum (LenA) at our institute was opened in the presence of a many guests. The LenA center houses high-performance electron microscopes, like scanning transmission electron microscope and scanning electron microscope and SEM, powerful instruments in material science for studies down to atomic levels.

OPENING CEREMONY OF A NEW IOM BUILDING

/ A highlight in 2013 was the opening of a new laboratory and office building at the institute. With an area of approximately 3,000 square meters, there are located a very large laser laboratory, several clean rooms and different laboratories for physical and chemical measuring systems, together with a new lecture hall as wellas offices for scientists and visiting guests.

PRIME MINISTER OF THE FREE STATE OF SAXONY AT THE IOM LEIPZIG

/ In August 2013, the Prime Minister of the Free State of Saxony, S. Tillich, visited the Leibniz Institute of Surface Modification together with members of the Bundestag and the Landtag of Saxony.

NEW AT THE INSTITUTE

/ A warm welcome to our new colleague Prof. Dr. Bernd Abel. Since May 2012 he is the deputy director of the IOM Leipzig and head of the Chemical Department. We are glad that he joined us and wish him success and good luck for his future.

SOME IMPRESSIONS OF THE »LANGE NACHT DER WISSENSCHAFTEN« AT IOM LEIPZIG, JUNE 2012

AWARDS OF THE INSTITUTE

/ Science and Technology Award 2012
Dr. Frank Frost

For his contribution to the topic
»Formation of Nanostructures by low-energy ion irradiation«

/ Young Scientist Award 2012
Dr. Chinmay Khare

For his thesis with the title
»Growth of Ge, Ag and multilayered Si / Ge nanostructures by ion beam sputter glancing angle deposition«

/ Science and Technology Award 2013
Dipl.-Phys. Horst Neumann

For his contribution to the topic
»Application of the ion beam technology in industry«

/ Young Scientist Award 2013
Dipl.-Phys. Alexander Malwin Jacob

For his contributions to the topic
»Investigation of the local mechanical properties of surfaces«

Scientific and Technology Results

Reports

Selected Results

Macroporous electron-beam generated polymeric cryogels for biotechnological applications

S. Reichelt, C. Abe, U. Decker, A. Prager, R. Konieczny, Ch. Elsner, W. Knolle
in collaboration with
M. Schnabelrauch, J. Becher, J. Weisser, INNOVENT Jena

Introduction

Cryogels are three-dimensional networks with interconnected macropores in the range of 1 - 200 µm. Their spongelike morphology makes them attractive supports for tissue engineering application. Nutrients and metabolomic waste can be easily transported to and from the cells. Typically cryogels are synthesized in frozen aqueous systems by free radical polymerization. The driving force of the reaction is a phase separation process between the ice crystals and a non-frozen liquid microphase there the reactants are concentrated. Mostly double bond containing monomers like acrylates or methacrylates serve as monomers. Thereby the pores are templated by the ice crystals. During the freezing the ice-crystals grow to a certain point forming an interconnected frozen network. The pore walls are shaped in the liquid microphase by the reacting (macro)monomers. Established protocols published in the literature use an activator/initiator system (ammoniumperoxodisulfate/N,N,N',N'-tetramethyl-ethylene diamine) for the initiation of the reaction. [1] The disadvantages of this reaction type are the long reaction time up to 16 h hours and the immediate initiation of the polymerization, which can result in systems with lower porosity. UV initiated approaches are faster but limited to transparent devices and by the low penetration depth of the photons. However, both approaches require the use of initiators, which are expensive, mostly toxic and remain as fragments in the backbone after reaction.

A new route which overcomes all this drawbacks is the electron-beam induced cryogel synthesis. The reaction time is shorter (here < 10 min) and the penetration depth of the electrons is only limited by the energy of the accelerator (here up to 7 cm in the case of two-side- irradiation). The major improvement is the absence of initiators. The synthesis of macroporous materials by electron-beam irradiation is an inexpensive and environmentally friendly approach to macroporous materials of high purity. Electron beam irradiation has not been used to prepare initiator and crosslinker-free (like glutardialdehyde) cryogels till now.

In this paper we report on the development of a new electron-beam (EBeam) derived approach to macroporous cryogels. In the first part, the synthesis and evaluation of the reaction parameters of polyethylene glycol (PEG) based cryogels is described, followed by a method to tailor the porosity of the cryogels. Then, one route to amine functionalized cryogels is introduced. Finally, an outlook regarding the application as cytocompatible matrices in biotechnology is given. The prepared cryogels were thoroughly characterized by dynamic mechanical analysis (DMA), scanning electron microscopy (SEM), microtomatography (µCT), thermogravimetric analysis (TGA) and X-ray photoelectronspectroscopy (XPS). We also studied their in-vitro cytocompatibility to understand the potential application of these materials in tissue engineering.

Experimental

Materials. Poly(ethylene glycol) methacrylate (PEGMA), tetraethylene glycol diacrylate (TEGDA), poly(allyl amine) (PAAm) and two derivated natural polymers, methacrylated dextran and hyaluronan (degraded, 65 kDa) were the (macro)monomers. Poly(ethylene glycol)s (PEG) of different molecular weight (6 kDa, 20 kDa, 200 kDa) were used as additional pore forming agents. Millipore water was applied as solvent and in the frozen state as porogen.

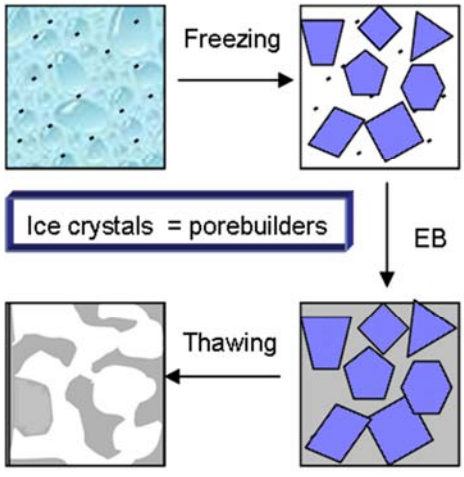

Figure 1: Synthesis of EBeam-generated cryogels [2].

Synthesis. The principle of the reaction is schematically shown in Figure 1. The cryogels were synthesized according the following standard protocol. The (macro)monomers (and PAAm or PEG) were dissolved in water in a certain concentration and degassed by flushing with nitrogen and ultrasound treatment for each 5 min. Then the systems were frozen (e.g. in centrifugal or eppendorf tubes, capillaries or micro plates), using a common lab cryostat (Lauda, Germany), at -20 °C for 0.5 – 2 h. The frozen formulations were transferred to the linear electron-beam accelerator (Elektronika, Torjy Company, Russia) and irradiated in a home built cooling box applying a dose of 12 or 21 kGy (applied in 3 kGy dose steps). After the reaction the cryogels were allowed to thaw and the resulting porous cryogels were flushed with water several times and dried in vacuum for the further characterization.

Methods. The yield of gelation was determined as follows: The freshly prepared and washed cryogels were dried in vacuum at 40 °C to constant weight. The gel content was calculated by referring the weight of the dried cryogels to the mass of the reactands. The cryogel morphology was studied by SEM (Ultra 55, Carl Zeiss SMT, Germany) and the chemical composition by XPS with an AXIS Ultra (Kratos Analytical, England). The interconnectivity of the cryogels was studied by µCT at the Scanco Medical AG in Switzerland. The column back pressures of the cryogels prepared in silanized fused silica capillaries (length 10 cm) were measured by µHPLC performed on a Dionex UltiMate 3000 system at a flow rate of 1-100 µl/min in HPLC grade water. The elastic moduli and the T_g values were determined by the DMA 800 (Perkin Elmer, USA) in compression mode (1 and 10 Hz). The thermal stability was measured by TGA using the Pyris 1 TGA (Perkin Elmer, USA).

The cytotoxicity was investigated by the seeding of 3T3 cells (mouse fibroblasts) onto the cryogels, cultivation under cell culture conditions and viability staining after 1 and 4 days. The cells were seeded at 25,000 cells/cm^2 and cultured in DMEM containing 10% fetal calf serum under 5% CO_2 atmosphere at 37 °C. After 1 and 4 days, the samples were withdrawn and the cells were stained at the samples by adding a twofold concentrated solution consisting of 30 µg/mL fluorescein diacetate (FDA) and 2fold GelRed. Fluorescence micrographs of green fluorescent viable cells and red fluorescent nuclei from dead cells were taken using an Observer Z1m microscope (Carl Zeiss Microscopy, Jena, Germany).

Results and Discussion

PEG-based cryogels

In the beginning of the study a suitable reference cryogel system for parameter optimization was developed. Several water soluble mono- or multifunctional acrylates or methacrylates of different chemistry and backbone flexibility were tested. In most cases, cryogels with different pore sizes could be successfully generated. [3] Finally, a system containing 5 wt.-% PEGMA and 5 wt.-% TEGDA was chosen as model system. [2] Such systems could be synthesized in yields above 90 %. An image of an electron-beam generated cryogel is presented in Figure 2. As can be seen in Figure 3 the samples are characterized by the typical spongelike morphology. An increase in the (macro)monomer concentration results in cryogels with lower porosity and lower pore sizes. (Figure 3), followed by an increase of the crosslinking density and the elastic moduli from 0.08 MPa

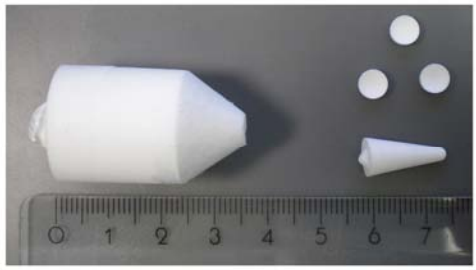

Figure 2: Cryogels synthesized in different shapes.

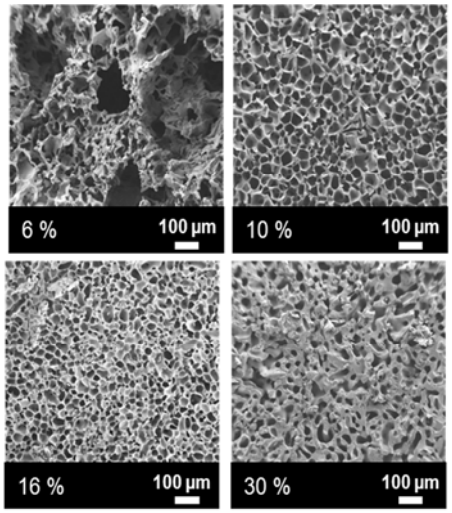

Figure 3: Effect of the concentration on the cryogel morphology [2].

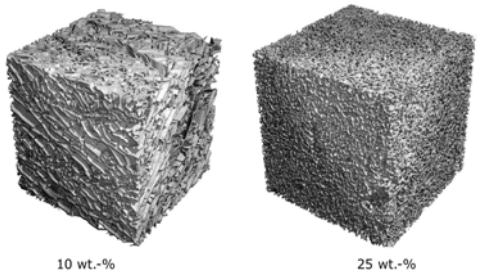

Figure 4: µCT studies of PEG cryogels independence on the monomer concentration.

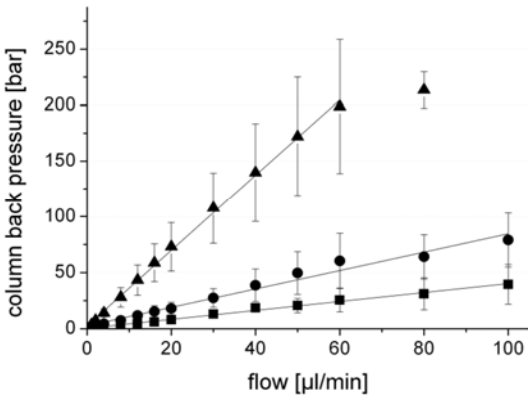

Figure 5: Column back-pressure of cryogel capillaries (ID=200 µm) in dependence on the (macro)monomer concentration [2]. Triangle: 25wt.%, filled circles:15wt.%, filled squares: 10wt.%.

(10 wt.-%) to 10 MPa (30 wt.-%), indicating that mechanical properties can be tailored within orders of magnitude. [2] The optimal freezing temperature was found to be between -20 and -30 °C. Above this temperature the acrylate formulation might not be fully frozen due to the supercooling effect. Below the eutectic point of the multicomponent system the acrylates are also solid and no phase separation between ice crystals and acrylates is occurring.

The morphology and interconnectivity were also studied by µCT. As indicated in Figure 4 a network of interconnected pores could be confirmed as expected from the SEM image.

These cryogel types were synthesized in silanized fused silica capillaries for further investigation. As visualized in Figure 5 the column back pressure increases as a function of the flow rate. Especially the lower concentrated cryogels were stable at all studied flow rates. The pressure reached at the maximum flow rate of the HPLC system was about 40 bar. At the standard instrument flow rate of 4 µl/min the cryogel columns (10 and 15 wt.-%) do not show a back pressure. The back pressure is orders of magnitudes lower than for common particle based HPLC columns. This study also proves that the porous materials are consisting of a system of interconnected pores.

Influence of pore forming agents

High porosity three-dimensional materials are of interest for biotechnological applications. This might improve the efficient transport of nutrients and metabolomics waste in cell cultivation. The high material porosity of about 80-90 % can be increased by the addition of pore forming agents like pure PEGs of different molecular weight. [3] Low molecular mass PEGs introduce a large amount of small pores (<100 nm) inside the pore walls. The higher the molar mass, the smaller the pores (Fig. 6). At low molar masses free hydroxyl groups inhibit the incorporation of the PEG chains and pores are formed. At higher molecular weight (M_w = 200 kDA) the effect of the functional groups is less pronounced and the PEG molecules are incorporated in the cryogel network. This leads to the formation of PEG droplets on the cryogel pore walls (not shown here). [3]

Amine functionalized cryogels

For various application functional surfaces are of interest, e.g. for the interaction of tissue material with the cryogel surface. Therefore poly(allyl) amine, an amine containing polymer, was incorporated in-situ as macromonomer or EBeam grafted to the cryogel surface from an aqueous solution. The simplest approach is the in-situ incorporation in a “one-pot” approach. 5 wt.-% PAAm were added to the 10 wt.-% concentrated PEGMA/TEGDA system. It was proven by XPS that PAAm was incorporated almost quantitatively in the cryogel matrix. The interesting fact is, that

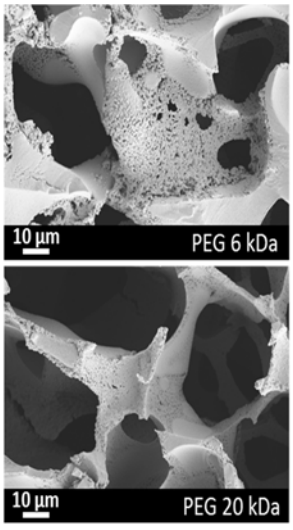

Figure 6: Influence of PEGs as pore forming agents on the porosity of PEG cryogels [3].

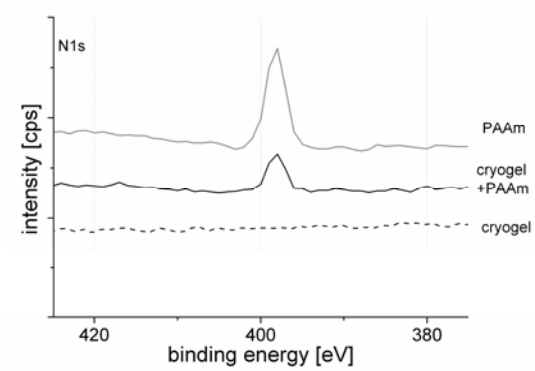

Figure 7: Proof of the successful incorporation of amine groups by XPS [2].

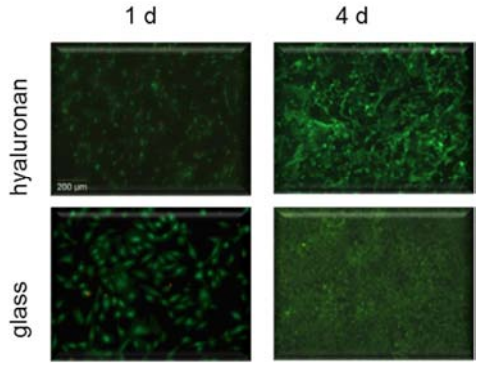

Figure 8: Fluorescence micrographs of 3T3 cells cultured at hyaluronan cryogels (5 wt.-%) and glass as control for 1 and 4 days [4].

PAAm does not contain any polymerizable amine groups. [2] In Figure 7 the newly occurring N1s peak of PAAm-modified cryogels is shown.

Cytocompatible cryogels

The most simple approach to biocompatible materials is to use natural polymers for the synthesis. Materials of interest are for instance polysaccharides like dextran or components of the extracellular matrix like glycosaminoglycans (e.g. hyaluronan). Methacrylated derivatives were provided by INNOVENT Jena. Porous cryogels were successfully synthesized in different forms and concentrations.[3] Mechanical and thermal stable (up to 315 °C, 2 h at 120 °C) materials with the typical porous structure were synthesized. The results of the in-vitro cytocompatibility of hyaluronan cryogels are provided in Figure 8. The cytotxicity of the cryogels was studied by seeding 3T3 mouse fibroblast cells on the surface of the materials and estimating their adhesion and viability after 1 and 4 days of cultivation. The results of cytotoxicity testing of the MPCs allowed an evaluation and comparison under different points of view. Starting with missing to moderate cytotoxicity at day 1 in most cases a layer of adherent viable cells developed as a result of undisturbed proliferation and washing off or dilution of cytotoxic components possibly present at the beginning. However, there were some differences. Cryogels from hyaluronan showed the highest cell density and best morphology of cells compared to dextran. A cytotoxic effect was detectable for neither hyaluronan nor dextran, but a higher increase of cell density was found after 4 days on the hyaluronan cryogel. Furthermore the microscopic analyses show that cells may also grow inside the pores of the cryogels. Altogether, all of the prepared dextran and hyaluronan based cryogels show an excellent cytocmpatibility.

Conclusion

In the course of this study we developed a new method for the generation of macroporous, polymeric materials by electron beam initiated crosslinking polymerization at subzero temperatures without additional crosslinkers, potentially toxic initiators or leaching agents. Cytocompatible polymeric cryogels were prepared from nature-based polysaccharides The fabricated macroporous materials were sufficiently stable to handle them in cell cultivation procedures without special care. First in-vitro cytotoxicity testing with mouse fibroblasts illustrated their excellent cytocompatibility which makes them attractive scaffold materials for tissue engineering.

Acknowledgement

The authors greatful acknowledge the analytical department of the IOM and the DFG for the financial support (RE 3184/1-1). We thank the SCANCO Medical AG for performing the µCT measurements.

Literature

[1] F.M. Plieva, H. Kirsebom, B Mattiasson, B. 34. J Sep Sci, (2011) 2164.
[2] S. Reichelt, C. Abe, S. Hainich, W. Knolle, U. Decker, A. Prager, R. Konieczny, 9 Soft Matter (2013) 2484.
[3] S. Reichelt, A. Prager, C. Abe, W. Knolle, 94 Rad. Phys. Chem. (2014) 40.
[4] S. Reichelt, J. Becher, J. Weisser, A. Prager, U. Decker, S. Möller, A. Berg, M. Schnabelrauch, 35 Mat. Sci. Eng. C (2014) 164.

Photochemical approach to thin barrier films for the encapsulation of flexible laminar electronic devices

L. Prager, U. Helmstedt, A. Pender
in collaboration with
H. Herrnberger, M. Münch, Solarion AG, Zwenkau,
O. Kahle, M. Stasiak, Fraunhofer-Einrichtung für Polymermaterialien und Composite, Teltow,
F. Kita, AZ Electronic Materials (Germany) GmbH, Wiesbaden

Introduction

Sensitive laminar electronic devices, such as inorganic and organic photovoltaic (PV and OPV) cells as well as organic light-emitting diodes (OLEDs) and displays, have to be protected against oxygen and moisture. Because of demands on flexibility, reduction of weight and cost minimization, rigid glass front panes usually applied have to be replaced by flexible and transparent encapsulation films. A common approach for the production of such films is the deposition of inorganic oxide layers with a thickness of about 50 - 100 nm (Al_2O_3, SiO_x, $ZnSn_xO_y$, or other metal oxides) onto polymer films by different methods like CVD, PVD, sol-gel techniques or ALD. In recent years, an alternative approach has been developed at IOM which is based on the photochemical conversion of perhydropolysilazane (PHPS) layers to silica layers at moderate temperature (< 80 °C) and normal pressure [1, 2]. Within the frame of preceding research projects, step by step a pilot plant has been designed for the production of barrier films on polymer films from roll to roll (R2R), 200 mm wide. In this way, transmission rates for oxygen (OTR /cm^3 m^{-2} d^{-1} bar^{-1}) and water vapor (WVTR /g m^{-2} d^{-1}) in the order of $10^0 – 10^{-1}$ could be achieved. However, for the protection of inorganic thin-film solar cells, barrier films should possess transmission rates WVTR < 5 x 10^{-4}, in case of OPV and OLEDs even less.

One way to enhance barrier properties is the lamination of 2 or more mono-layer barrier films, each consisting of a polymeric substrate film coated with an inorganic barrier layer, like explained above, to a stack [3, 4] which fulfills ambitious demands regarding, e. g., barrier properties, long-term stability, weather resistance, transparency. This can be done in industrial scale by a R2R process. The choice of the lamination adhesive depends on a couple of demands towards its properties: wetting of the surface, strong bonding to the surface after curing, low shrinking in the curing process in order to avoid mechanical stress, sufficient elasticity after curing, technological compatibility within the production process and chemical compatibility. Furthermore, for PV applications durability at outdoor conditions with respect to temperature variation (heating, freezing) and solar radiation is claimed.

At this point, we will report on our research and development on the design of flexible high-barrier laminates based on single barrier films produced using PHPS as the precursor for thin SiO_x-layers on polymer films. The targets of the investigations were, (i) to improve the barrier properties of the mono-layer barrier films, (ii) to design laminates based on single barrier films for the application as encapsulation films for flexible thin-film solar cells, (iii) to evaluate these films regarding barrier properties, and (iv) to develop and establish a test sequence for evaluation of these films on encapsulated solar modules regarding weatherability and durability for outdoor applications projected to last over 20 years.

Results

The barrier properties could be sufficiently improved by several activities. First, the pilot plant was upgraded by (i) the installation of an air-conditioning to minimize hydrolysis of the structural polysilazane units leading to the formation of silanol groups which are not accessible to the VUV initiation of the conversion process instead of that facilitate permeation of water molecules, (ii) replacement of Xe_2* excimer lamps by an improved version (XERADEX/L40/375/DB-SX48/90, Radium GmbH, Wipperfürth) with increased radiant exitance in the VUV spectral range and (iii) housing of the station for slit-nozzle application of the PHPS solution by a laminar flow box for minimizing dust particle concentration which are the source of many defects. Different polymers as substrate films have been evaluated regarding their resistance against the impact of VUV-irradiation during the conversion process of the PHPS coating to silica. In the case of polymethylmetacrylate and polycarbonate, radia-

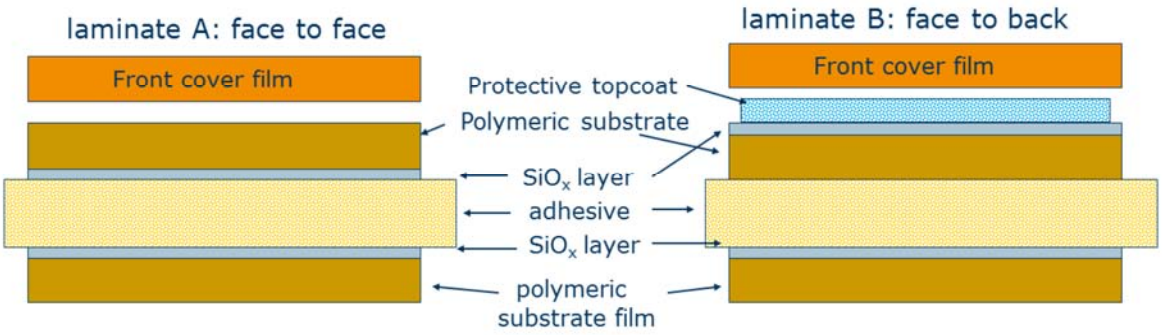

Figure 1: Schema of the face-to-face (left) and the face-to-back (right) lamination of two mono-layer barrier films.

tion damage close to the interface between substrate and coating causes substantial adhesion problems.

The wavelength-dependent penetration depths of VUV photons in acrylates and epoxides intended to use as planarization layers between the polymer substrate and the PHPS based silica layer were measured and found to be in the range of 100 nm – 1 µm, whereby the less the wavelength of the VUV photons the less the penetration depth [5]. Beside of silica layers, thin films of other metal oxides are also promising materials for the use as inorganic barrier layers (s. introduction). As a first attempt, the photochemical conversion of a polymeric hexanoato aluminium complex using VUV irradiation has been investigated. XPS depth profiles of thin homogeneous films prepared by spin-coating of a precursor solution showed that VUV irradiation (at T < 80°C and normal pressure) in the presence of oxygen leads to the mineralization of the precursor and the formation of almost carbon free layers having a homogeneous composition close to AlO_2 and a density of about 2.1 g cm^{-3} [6].

For a technical application, the required radiant exposure of 36 J cm^{-2} is still too high. Nevertheless, this approach seems to be an interesting alternative to vacuum-based or sol-gel deposition methods.

The breakthrough concerning barrier properties of mono-layer barrier films could be finally achieved by selecting and applying special polymer films as substrate films, e.g. PVD pre-coated PEN or PET films. Ultimately, barrier films exhibiting WVTR < 5 x 10^{-2} with high reproducibility can be produced on polymer films PEN and PET, 50 – 100 µm thick, 250 mm wide at velocities up to 10 m/min.

Suchlike produced barrier films have been used as basic components for the design of high-barrier encapsulation laminates exhibiting the principle designs shown in Fig. 1, and a SEM image in Fig. 2. The complete encapsulation stack for a PV module includes a front cover film, which protects the module against weathering. The advantage of the face-to-back lamination consists in the fact that the first barrier layer is close to the top of the stack and protects the polymeric substrate against uptake of water. But on the other hand, the lamination of the hydrophilic silica layer with the rather hydrophobic substrate film is more challenging than the lamination of two equal, in terms of free surface energy, silica layers.

As adhesives both self-made (IOM, Fraunhofer PYCO) and commercially available UV curable formulations had been used respectively developed, and tested. In this context, epoxide and acrylate based formulations, organic/inorganic hybrid systems based on organosilazanes and acrylates/epoxides as well as organic/inorganic hybrid systems based on thiol-ene reactions with vinyl-functionalized polysilazanes had been investigated. Fabricated laminates were tested regarding barrier properties. For the measurement of high-barrier films with WVTR < 2 x 10^{-3} at Fraunhofer PYCO, the so called Calcium mirror test had been installed. Thereby, the reaction of water

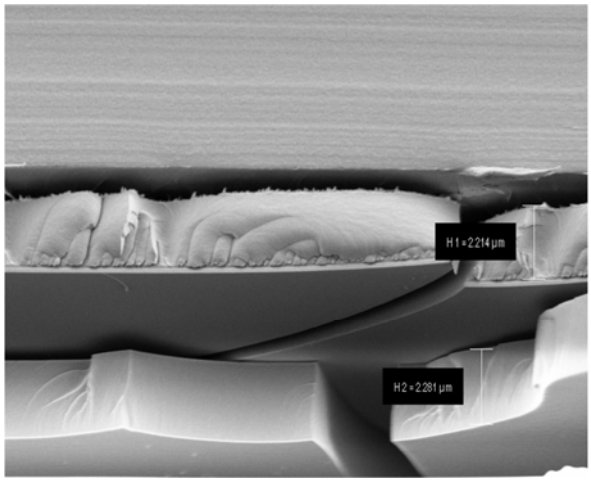

Figure 2: SEM image of laminated barrier films.

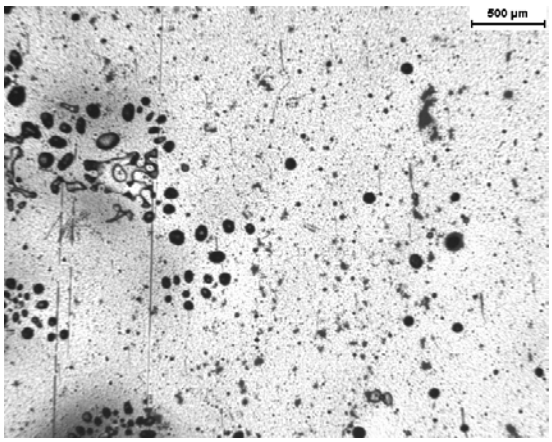

Figure 3: Image of a barrier film after Ca test - visualization of defects.

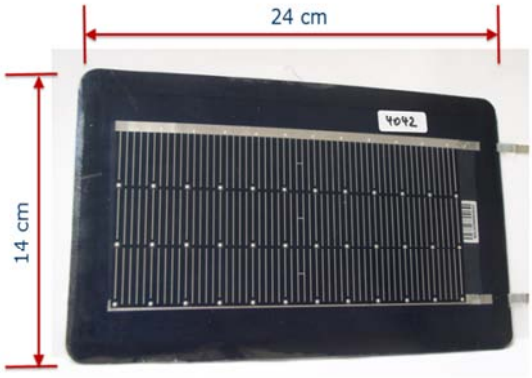

Figure 4: Minimodule fabricated at Solarion AG and used for several climate tests.

molecules permeating through the barrier film with the Ca layer evaporated onto the barrier film can be used. This reaction leads to the change of the optical properties of the Ca mirror from reflecting to transparent and can be evaluated quantitatively. Depending on the quality of the barrier, this process can be accelerated by means of sample storage at enhanced temperature and relative humidity. The detection limit of this method is in the range of 10^{-5} g m^{-2} d^{-1}. Beside of measuring transmission rates, this method allows for the visualization of defects, e.g. pinholes and microcracks (Fig. 3), and for fault diagnostics in the production line.

Applying various polymer films and laminating adhesives, high-barrier laminates were produced and subjected to several tests regarding e.g. barrier properties, peeling and optical criteria. Using positive evaluated high-barrier films as encapsulation films, photovoltaic test modules were fabricated at Solarion AG (Fig. 4) by various encapsulation methods (various adhesives, lamination temperature and pressure) and tested regarding weatherability applying several climate tests: damp-heat test at 85 °C and 85 % r. H., a combined test consisting of alternating damp-heat exposure and thermo-cycle exposure (-40 °C – 85 °C) including wetting and freezing, and a second combined test with UV exposure and wetting.

After exposure to all these tests, some encapsulated modules showed excellent durability. In Fig. 5 results of a combined climate test of PV mini-modules encapsulated with face-to-back laminated high-barrier laminates are shown. Laminates based on PEN films showed the best results with a durability of more than 2700 h preserving more than 90 % of PV power compared to the initial value measured immediately after encapsulation. These films proved to be suitable for the encapsulation of flexible thin-film PV modules with a required outdoor durability of more than 20 years [7]. At the same time, these laminates exhibited excellent transparency (T > 85 %) in the

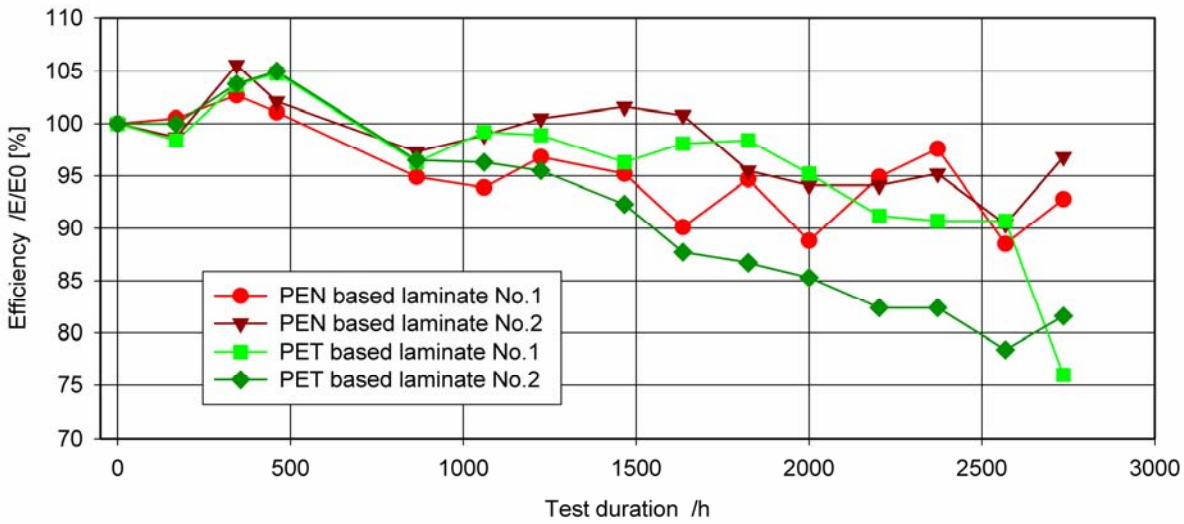

Figure 5: Results of the combined climate test consisting of alternating damp-heat and thermo-cycle exposure including wetting and freezing.

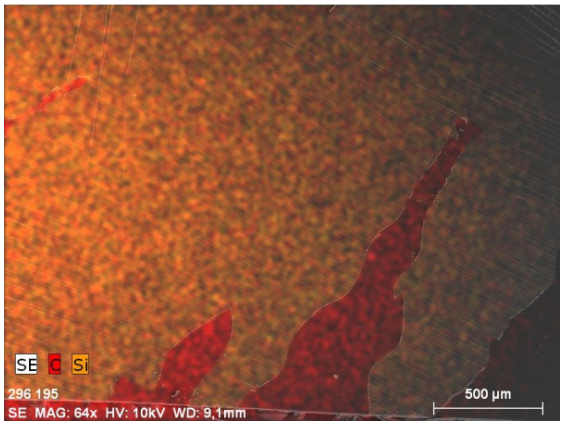

Figure 6: SEM-EDX image of the delaminated interface protecting topcoat – silica layer showing that the silica layer remained almost completely on the top of the PET substrate.

spectral range of interest 375 nm < λ < 1.2 µm successfully competing with the best commercially available encapsulation films.

On tested laminates appeared faults have been analyzed. Applying SEM-EDX analysis on deficient laminates, delaminating interfaces have been investigated. In the case of PET based barrier films, weak sticking interfaces are those between encapsulation adhesive and protective coating, between protective coating and silica layer (Fig. 6), and between silica layer and substrate film. The latter, for instance, is caused by irradiation damage of the PET surface during VUV initiated conversion of the PHPS layer. Besides these findings, PET films are known to be not stable against UV damage and hydrolytic degradation under outdoor conditions. Recent works at the project partner Solarion aim on the utilization of high-barrier laminates for flexible solar cells. Now, it is possible to design extremely light solar modules which are applicable in mobile carriers as well as for integration in construction materials, for instance roof components and facade claddings. Real products close to commercialization stage are solar clapboards, modules which can be integrated in thermal insulation boards, and solar modules on metallic roof elements.

Conclusion and outlook

In the course of the described R&D activities, durable, weatherproof, flexible, transparent high-barrier films suitable for the encapsulation of flexible thin-film photovoltaic modules have been developed. Commercial PV products using flexible encapsulation films are in the development stage. Further investigations will be focused on the improvement of barrier properties and the possible application as flexible OLED encapsulation films. Additionally, future technological developments aim for a cost-efficient integrated R2R process on a competitive basis compared to developments of other R&D groups. Research on the photochemical generation of other metal oxides (e.g. Al, Ti, Zn) has to be continued.

Acknowledgement

The investigations had been carried out within the framework of a corporate project (033RI0905 A-E) funded by the Bundesministerium für Bildung und Forschung (BMBF).

Literature

[1] L. Prager, A. Dierdorf, H. Liebe, S. Naumov, S. Stojanović, R. Heller, L. Wennrich, M.R. Buchmeiser, Chem. Eur. J. 13 (2007) 8522.
[2] W. Knolle, L. Wennrich, S. Naumov, K. Czihal, L. Prager, D. Decker, M.R. Buchmeiser, Phys. Chem. Chem. Phys. 12 (2010) 2380.
[3] J. Greener, K.C. Ng, K.M. Vaeth, T.M. Smith, J. Appl. Polym. Sci. 106 (2007) 3534.
[4] M. Schmidt, N. Rodler, O. Miesbauer, M. Rojahn, T. Vogel, R. Dorfler, E. Kucukpinar, H.C. Langowski, J. Adhes. Sci. Techn. 26 (2012) 2405.
[5] L. Prager, L. Wennrich, W. Knolle, S. Naumov, A. Prager, Mater. Chem. Phys. 134 (2012) 235.
[6] L. Wennrich, H. Khalil, C. Bundesmann, U. Decker, J.W. Gerlach, U. Helmstedt, D. Manova, S. Naumov, L. Prager, Mater. Chem. Phys. 137 (2013) 1046.
[7] L. Prager, U. Helmstedt, H. Herrnberger, M. Münch, O. Kahle, F. Kita, A. Pender, M. Stasiak, In *pro flex 2013*, Dresden, 2013.

Analytical characterization of surfaces

A. Freyer, E. Bilz, A. Prager, N. Steffens, I. Reinhardt, U. Decker
in collaboration with
H. Hildebrand, K. Franke, Helmholtz-Center Dresden-Rossendorf

Introduction

In order to obtain material surfaces with special properties often coatings are employed, which are specifically modified, e.g. by adding small amounts of nanoparticles (1 - 30%). The analysis of these technical surfaces requires high-end analytical techniques. Also, the impact of released nanoparticles on biological systems is not yet clear. For the analysis and quality control of these systems powerful and sensitive techniques have to be developed and applied. In particular, only a combination of several methods can provide the desired information of the complex systems. This will be demonstrated here for three different examples,

- UV-coatings modified by TiO_2 or Ag nanoparticles, which are weathered to monitor the stress of the coating and the release of nanoparticles by the radiation (Xenon tests),
- Photoinitiator-free UV curing of acrylate-based nano-composite coatings, and
- Investigations of printed inks to obtain information about migrating and evaporating species.

TiO_2 and Ag UV-coatings [1]

The photocatalytic properties of TiO_2 give much faster results to simulate the degradation of coatings during UV irradiation. For UV-coatings on PET samples (Melinex505, DuPont, Luxembourg) several commercially available TiO_2 nanoparticles were tested. P25 (Anatase: Rutil= 80:20, Evonik) was chosen with a primary size of 21 nm. The P25 system was selected because of its photocatalytic activity. Normally, the UV stress tests will last up to 24 to 42 months. Standard industrial coatings are protected for UV-degradation and so a model system of an ethoxylated triacrylate SR 454 (Sartomer) is used to develop useful methods, describing the loss of nanoparticles. The coatings are applied manually -25 µm and the industrial coatings had thicknesses of 4 µm. Infrared spectroscopy, as well as colour, gloss and thermo-gravimetric measurements clearly show that the model system is completely destroyed after 200-300h. With this system a special wet chemical method was developed to collect the small amounts of nanoparticles, which leave the coatings. Common analytical methods could not detect these nanoparticles and any concentration process can give unwanted aggregations.

A special highly sensitive radiochemical method was developed - [^{48}Ti] was activated to [^{48}V] with a half live time of 15.97d. Auto radiographic and scanning electron microscopy data show that the nanoparticles are homogeneous distributed in the marked and unmarked coatings. The activity of the model and industrial coatings (1% P25) and the extracted products during UV-irradiation are measured and compared with the ones that were not irradiated. The investigations clearly show that the decomposition starts around the TiO_2 nanoparticles and depends on the composition of the coating and the size of the particles. Here the standard industrial formulation CET6 (Cetelon Germany) with 1% P25 and 12.3% $Si0_2$ (Aerosil ox 50 (Evonik industries) nanoparticles for scratch

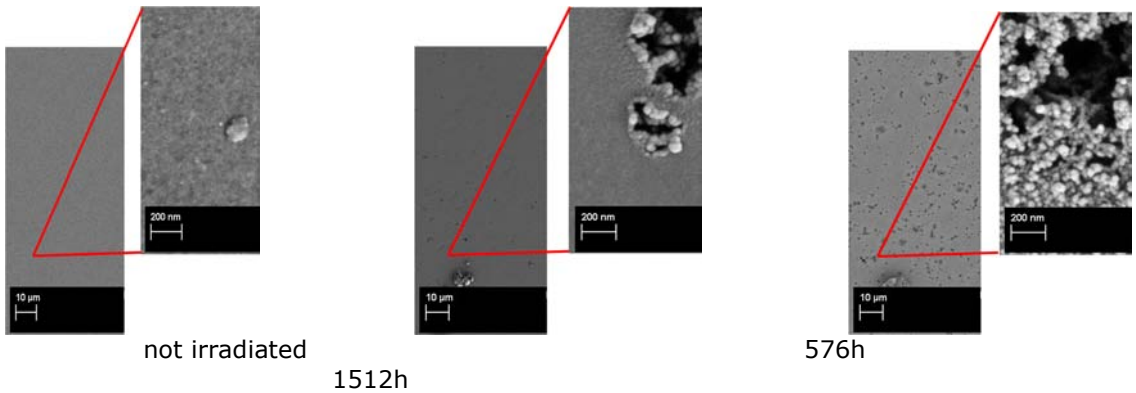

Figure 1: Scanning electron microscopy images displaying the development of the destruction of a commercial coating CET6 (Cetelon, Germany) by UVA irradition with added 1% P25.

resistance) is not yet destroyed after 2000h in comparison to the model system. The scanning microscopy pictures in Figure 1 show this clearly. Similar investigations have been done for coatings with Ag nanoparticles with concentrations less than 0.5%, which are assumed to have antibacterial properties. The sensitivity of radiochemicaly activated Ag was estimated to be one order of magnitude higher than measured for instance by inductively coupled plasma optical emission spectroscopy at about 0.1µg/l. Differing from the previous investigations there is no photocatalytic activity, which destroys the coating and so the loss of Ag will be much slower. Until now the results are not so clear and further investigations are needed.

Photoinitiator-free UV curing

Transparent, scratch and abrasion resistant topcoats control the quality of wood flooring products for some years. To maximize mechanical, optical and chemical performance a proper selection of the lacquer components is very important and the embedding of inorganic micro- and/or nano-sized particles has attracted increasing attention. For curing such high solid formulations, photopolymerization is an effective approach owing to its advantages such as high curing speed, low energy consumption, low operation temperature, and less environmental pollution by avoiding volatile organic solvents. Some serious drawbacks of UV cured coatings such as unpleasant odour, harmful toxicity, and a more or less strong yellowing/darkening may originate from photoinitiator residues and limits the industrial applications of UV-curable coatings in some specific areas, where the low migration of photo-cleavage side products is required, e.g. coatings for food, cosmetic, and tobacco packaging, as well as printing inks for such-like packaging materials. To minimize the mentioned drawbacks, flushing the UV curing chamber with inert gases, such as nitrogen or carbon dioxide, is one of the most efficient methods for obtaining high curing rates at low photoinitiator amounts. Nevertheless, several users of UV curing technology are looking for photopolymerization systems without using any external photoinitiators. In the absence of any photoinitiator or any other additives, the self-initiation of acrylic and methacylic acids as well as several acrylic monomers has been observed during long-term irradiation with a conventional medium pressure Hg-lamp. Depending on the acrylate used, conversions between 50 and 90 % were reached after 30 seconds irradiation. However, no acrylate conversion occurred by using a cut-off filter for wavelengths < 300 nm. Due to quantum chemical calculations, the excitation of acrylate molecules by high energy photons (with wavelengths below 267 nm) can generate radicals resulting in the self-initiation of acrylic C=C photopolymerization reactions. Most photocurable acrylate-based resins and diluting acrylates or monomers do not or only weakly absorb in the spectral region of the usual mercury arc lamp. Hence, the application of short-wavelength vacuum UV (VUV) irradiation, e.g. emitted by a monochromatic 172 nm (Xe_2*) excimer lamp, meets two challenges: (i) the photoinitiator-free UV curing and (ii) the manufacture of matt finished coatings. Silk matt and matt clear coatings that diffuse light, offer an authentic appearance of the wood's character in wood and parquet flooring by accentuating its natural structure. On the other hand, high gloss finishes that reflect light and give a shiny appearance offer a more elegant appearance. UV curing is commonly regarded as being less effective in producing matt finished coatings by adding matting agents compared to solvent-containing lacquers. These investigations are continued [2].

Fortunately, VUV/UV curing by a dual lamp set-up consisting of a 172 nm excimer lamp and a conventional medium pressure mercury lamp can generate a micro-structured surface in such a way that the light falling on it is scattered. Real-time attenuated transmission reflection fourier transform infrared (RT-ATR-FTIR) studies on radiation curing of acrylate formulations by a monochromatic 172 nm (Xe2*) excimer lamp and a polychromatic medium pressure mercury arc lamp revealed that under oxygen-free curing conditions photopolymerization reactions take place at high reaction rates even in the absence of a photoinitiator. For example, Fig. 2 shows the ATR-FTIR spectra of the curing of tripropylenglycoldiacrylate (TPGDA-CYTEC Surface Specialties) during 60 sec of 172 nm irradiation. Significant changes in the typical regions of C=C bands (1636, 1408, and 810 cm^{-1}) and CH_2 bands (2934 and 1453 cm^{-1}) point to the onset of the photoinitiator-free photopolymerization by 172 nm irradiation. Thus, the C=C double bond conversion vs. irradiation time profile of TPGDA (Fig. 3) demonstrates that an irradiance of 15 $mWcm^{-2}$ by the monochromatic 172 nm excimer lamp is sufficient to generate enough free radicals for high acrylate conversion (> 85 %) during an exposure time of < 10s.

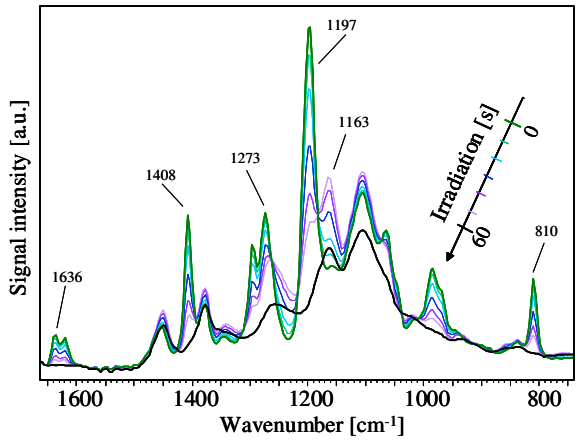

Figure 2: Changes in the fingerprint region of ATR-FTIR spectra of TPGDA during photoinitiator-free curing by a 172 nm excimer lamp.

2D correlation analysis of the ATR-FTIR data makes the irradiation time-dependent correlation between acrylic C=C conversion and wave-number shifts of C=O and C-O-C bonds evident. Using a dual VUV/UV lamp set-up, through cure of photoinitiator-free acrylate-based nano-composites of about 60 µm thickness has been performed.

In Figure 4 the RT-ATR-FTIR clearly shows that after conversion of double-bonds a second reaction takes place, which gives higher crosslinking densities. Post-curing irradiation of thoroughly cured acrylate coatings by the 172 nm excimer lamp referred to an excitation of C=O groups within thin surface layers. Radical formation via absorption of high-energy photons (having wavelengths below 219 nm) by C=O bonds is assumed finally yielding a higher network density via radical recombination reactions.

Thus, VUV matted acrylate coatings show enhanced surface hardness, improved chemical resistance, and hydrophilic surface properties.

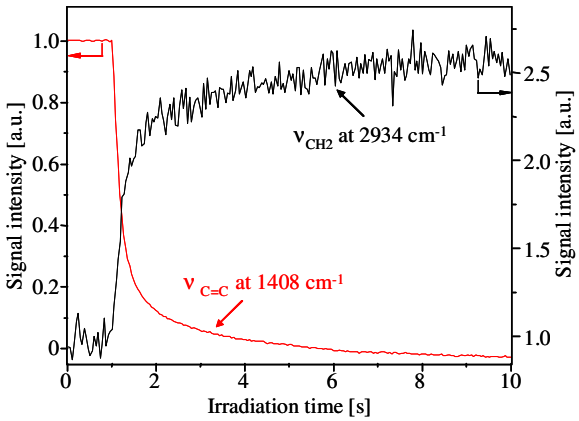

Figure 3: Double bond conversion $\nu_{C=C}$ at 1408 cm^{-1} changes of ν_{CH2} at 2934 cm^{-1} TPGDA during 172 nm excimer irradiation.

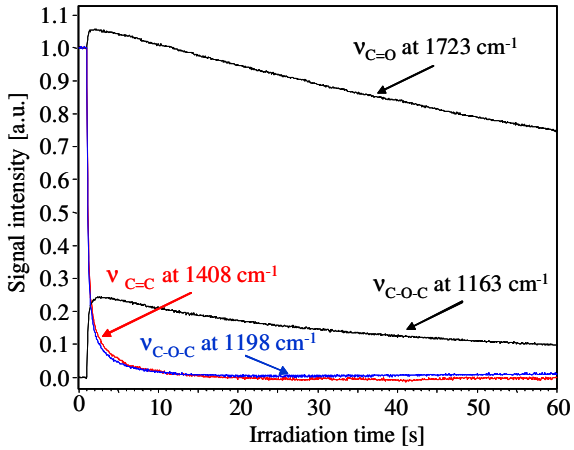

Figure 4: Changes in signal intensities $\nu_{C=C}$ at 1408 cm^{-1}, $\nu_{C=O}$ at 1723 cm^{-1}, ν_{C-O-C} at 1198 cm^{-1} and ν_{C-O-C} at 1163 cm^{-1} TPGDA during 60s 172 nm excimer irradiation.

Table 1: Surface properties of VUV/UV-matted acrylate-based nano-composites.

	matted and cured by dual VUV/UV lamp set-up **	cured by (Hg) UV lamp *
Gloss (at 60°)	6	59
Microhardness (N/mm^2)	264 ± 10	249 ± 12
Water contact angle (°)	90	95
Surface energy (mN/m^2)	29	23
Chemical resistance (iodine/ ethanol, 1h)	good	traces are seen

**2 wt.-% photoinitiator (Darocure 1173 / Ciba), ** photoinitiator-free.*

A practical application is shown in Figure 5, where clearly is seen the matting effect.

Migration investigations

In food package industry are of interest the substances, which can migrate into food and the global migration limit for this is 10 mg/dm^2 for non-toxic substances. To prevent this migration special multilayer materials with or without barrier layers and or low migrating coatings (inks) are developed. These systems are analysed by determining the global or specific migration by extraction under definite conditions with different solvents. Important are substances with molecular mass below 1000 Dalton.

Figure 5: Reflectance behavior of acrylate-based nano-composite clear coats on laminate cured by a (Hg) UV lamp (left) and the dual VUV/UV lamp system (right). The gloss levels at 60º are 87 and 4 units, respectively.

One of the most sensitive analysis techniques for volatile and semi-volatile migrating substances is the solid phase micro-extraction (SPME) coupled with gas chromatography mass spectrometry (GC-MS). Here no further steps of preparation are necessary. Small parts of the package material (1-5 cm^2) are inserted in a vial, which is then closed. Together with a special fibre it was heated over a definite time. The volatiles and semivolatiles are enriched on the fibre. Depending on the substances several types of fibres are available (Supelco, USA).

One of the most sensitive analysis techniques for volatile and semi-volatile migrating substances is the solid phase micro-extraction (SPME) coupled with gas chromatography mass spectrometry (GC-MS) [3]. Here no further steps of preparation are necessary. Small parts of the package material (1-5 cm^2) are inserted in a vial, which is then closed. Together with a special fibre it was heated over a definite time. The volatiles and semivolatiles are enriched on the fibre. Depending on the substances several types of fibres are available (Supelco, USA).

The fibre is injected into the GC-MS, where the substances desorb at higher temperatures. Going through the GC the substances are separated to give a chromatogram (total ion current) and can be identified and analyzed by their mass spectrum. Every time an empty sample in a series is measured under the same conditions to show that the effects really come from the samples. Exist possibilities to quantify the components. The Figure 6 shows such an example under different UV irradiation conditions. At higher conveyer speed (50 m/min and lower dose) higher concentrations of unconverted monomer is seen (17 min). On the other side at lower speed (higher conversions) the monomer peak is lower but one can find more destruction products of the stabilizer (15.5 min). This method is very effective and in short times many samples can be automatically analyzed qualitatively. By mass spectrometry many products can be identified. For quantification a calibration had to be done. In comparison to normal GC-Headspace or the standard methods higher values are estimated by SPME-GC-MS.

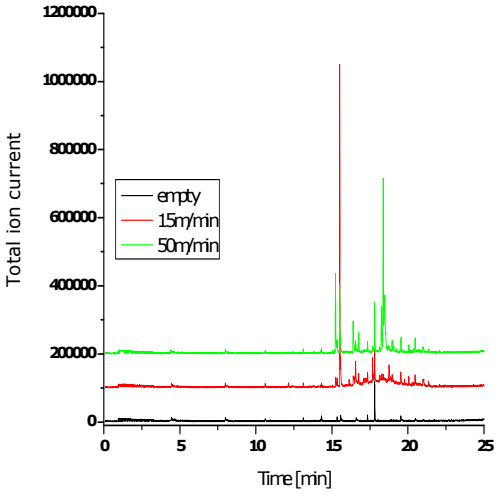

Figure 6: GC-MS chromatograms of different UV-irradiated samples after solid phase micro-extraction.

Literature

[1] R. Mehnert, E. Mai, A. Freyer, E.Bilz, Farbe + Lack 118-4 (2012) 31.
[2] F. Bauer, U. Decker, S. Naumov, C. Riedel, Prog. Org. Coat. 69 (2010) 287.
[3] C. P. de Oliveira, A. Rodriguez-Lafuente, N. de F. F. Soares, C. Nerin, Journal of Chromatography A, 1244 (2012) 61.

Electric propulsion - development of diagnostics, modelling and related components at IOM

F. Scholze, C. Bundesmann, C. Eichhorn, H. Neumann
in collaboration with
H. Leiter, Astrium ST GmbH, F. Scortecci Aerospazio Tecnologie s.r.l., R.Y. Gnizdor EDB Fakel

Introduction

Electric propulsion (EP) thrusters replace more and more conventional chemical thrusters onboard of spacecrafts. The main applications for EP thrusters are north-south station keeping of geostationary satellites, orbit raising or new formation flying missions, which can be done only by EP [1]. Even though EP thrusters are limited in maximum thrust, they use the propellant very efficiently, and the low thrust is counterbalanced by a long firing time and higher exhaust velocity. The later is, especially, interesting for long distance missions, such as “Deep Space One” of NASA or “BepiColombo” of ESA. EP thrusters are designed for a life time of more than 20,000 h [2]. Validated tools for life time prediction as well as for plasma and beam modeling support scientists and engineers within the design phase and shorten the development time. During the formal qualification process the thrusters have to be operated 1.5 times the nominal life time in a vacuum facility on ground. At present, there exists a strong need for new, standardized in-situ diagnostic concepts for tests on ground for making experimental results comparable. In-situ measurements are superior to ex-situ measurements, because in-situ measurements avoid breaking the vacuum and dismounting or, even worse, dismantling the thruster. Performance data of a firing thruster, which can measured only in-situ, are essential for the thruster optimization and qualification process, which usually includes validated modeling [3].

Diagnostics development

An advanced in-situ diagnostic system for EP thrusters and terrestrial ion beam sources has been developed at IOM together with European industrial partners [4]. The system is modular such that it can be easily adapted to special needs of the vacuum testing chamber or of the test article. The diagnostic system utilizes a high-precision 5-axis positioning system. So far, the following diagnostic tools have been tested: a telemicroscope for high-resolution optical imaging (TMS), a triangular laser head (TLH) for surface profile scanning, a pyrometer for temperature

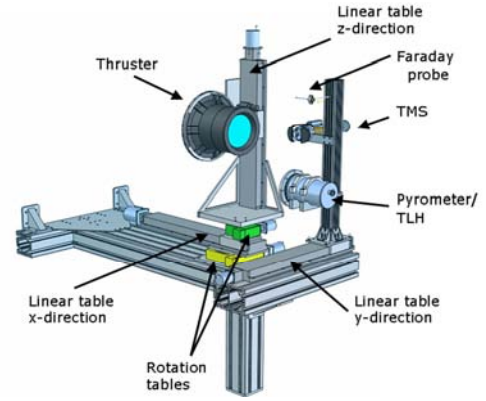

Figure 1: Drawing of the diagnostic system with 5-axis positioning system, diagnostic heads and a thruster. Not shown is the ESMS, which is mounted to one of the chamber walls.

scanning, a Faraday probe for current density mapping, and an energy-selective mass spectrometer (ESMS) for beam characterization (energy and mass distribution, composition). Therefore, our system can provide a comprehensive set of parameters, which are all measured in-situ. The system has been successfully tested with two thrusters: a Hall Effect thruster SPT-100D EM1 (FAKEL, Russia, [6]) and a gridded ion thruster RIT-22 (Astrium ST, Germany, [7, 8]). The positioning system (Figure 1) consists of a modular bar setup and uses in total three stepper-motor driven linear tables (maximum travel range 700 mm, maximum tested travelling speed 50 mm/s, positioning reproducibility better than 0.1 mm) and two stepper-motor driven rotation tables (360 deg, 3 deg/s, better 0.5 deg). By that, thruster and diagnostic tools can be positioned and oriented very precisely relative to each other. The x-axis allows adjusting the distance between thruster and diagnostic heads, the y- and z-axis define the observation spot on the thruster. In addition to single spot measurements, line scans or even 2D maps are possible. Furthermore, the two rotation tables allow to perform angular resolved measurements. All axes are computer controlled. The TMS uses a telephoto lens (focal length f = 135 mm), a monochrome CCD sensor with a resolution of 1280 x 960 pixels, and an extension tube with a length of 150 mm in order to improve the lateral and axial resolution, which are

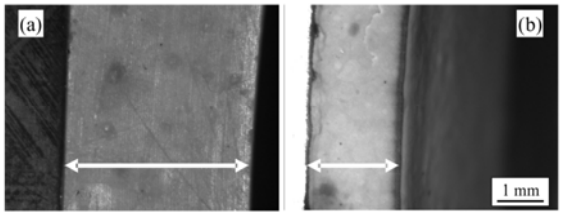

Figure 2: TMS images of an outer ceramics wall of the SPT-100D EM1 at the beginning (a) and at the end (b) of the test campaign. The top plane of the ceramics walls is indicated by double arrows.

found to be 0.01 mm and 0.4 mm, respectively. The total field of view is about 5.8 x 4.4 mm^2 at a working distance of about 250 mm. For safety reasons, the TMS is placed inside a vacuum-sealed housing with a borosilicate window and a shutter mechanism. The TLH measures the distance to an object upon the triangulation effect. By performing scans across an object's surface, a surface profile and its change can be recorded. The working distance of the TLH is 150 mm ± 40 mm, the laser spot diameter is 0.12 mm and resolution during operation in vacuum is found to be better than 0.1 mm. The pyrometer measures the radiation intensity in a certain spectral range. Here commercial pyrometer, which operates in the spectral range from 2.0 µm to 2.8 µm, is used. The measured temperature range is between 100°C and 700°C. The pyrometer optics is selected such that the pyrometer has a small spot size at a moderate distance (1.3 mm at 150 mm). The temperature reproducibility (considering also window effects) is better than 5°C. The TLH as well as the pyrometer are placed inside a second vacuum-sealed housing with a standard quartz window (TLH) and window made of SUPRASIL (Pyrometer), and two separate shutters for protection of both entrances windows. The Faraday probe has been developed at IOM. It has a graphite collector with a diameter of 2 mm within an Alumina separator together in a small stainless steel tube with a length of 101 mm in

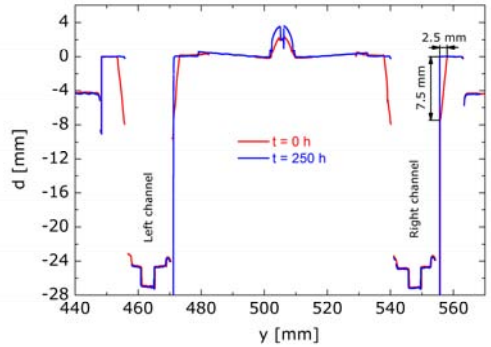

Figure 3: TLH line scans across the centre of the SPT 100D EM1 at the beginning (a) and at the end (b) of the test campaign.

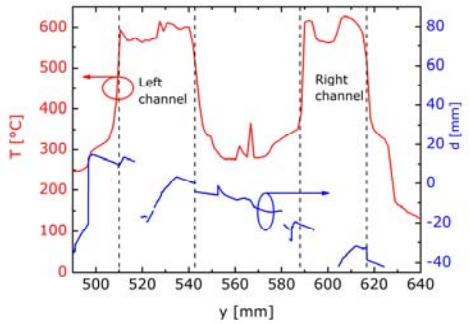

Figure 4: Pyrometer (solid line) and TLH scan (dashed line) across the diameter of the SPT-100D EM1. The scans are recorded immediately after switching-off the thruster which is operated at U = 750 V and I = 2.6 A. The thruster is tilted by 25°. The vertical dotted lines mark the left and right plasma channel.

order to get only small interactions with the thruster itself, especially, when measuring at small distances. Current densities up to 50 mA/cm^2 can be measured. Because of the small secondary electron emission coefficient of graphite no bias voltage needs to be applied. Therefore, the Faraday probe measures the net current density including effects of space charge compensation as well as the well-known charge transfer loss. The commercially available ESMS can measure ion energies up to E* = 5000 eV (resolution 0.5 eV) and atomic masses up to M* = 300 amu (resolution 1 amu). The energy distribution of the beam ions (related to the generation places of the ions), the mass distribution of the beam (i.e. beam composition or contaminations) and the amount of higher charged ions in relation to single charged ions can be studied. The ESMS is mounted at the chamber wall. The use of the 5-axis positioning system allows ESMS measurements across the whole beam and at different entrance angles for measure the divergence of the beam ions. In the following, selected results of a test campaign with a Hall Effect thruster SPT-100D EM1 are presented in order to demonstrate the capabilities of our diagnostic system. The total test time was 250 h. Figure 2 shows TMS images of the special Boron Nitride (BN) plasma channel wall at the beginning and at the end of the test campaign. The radial erosion can be seen clearly, the axial erosion can be obtained by using the depth of field (not shown here). The radial and axial erosion at the end of the test campaign was found to be 2.5 mm ± 0.1 mm and 7.5 mm ± 0.5 mm, respectively. Figure 3 presents surface profile scans, as measured with the TLH, at the beginning and at the end of the test campaign. Again the radial and axial erosion can be seen clearly. The absolute

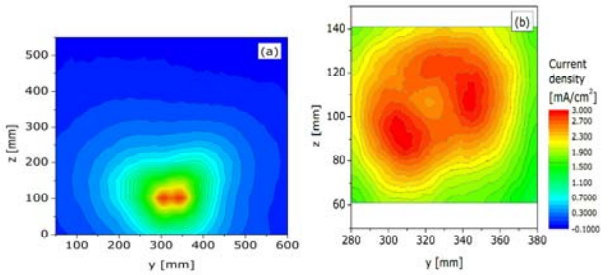

Figure 5: Current density maps of the SPT-100D EM1 operated at U = 750 V and I = 2.6 A measured with the Faraday probe at a distance of d = 600 mm. Panel (a) shows a map plotted from horizontal line scans measured at Δz = 50 mm, panel (b) is a centre map with Δz = 2 mm and a reduced y-range.

numbers agree very well with the TMS results: radial and axial erosion at the end is 2.5 mm ± 0.2 mm and 7.5 mm ± 0.4 mm, respectively. The TLH has difficulties measuring surfaces parallel to the laser beam. Therefore, the TLH scan curves are no continuous lines. Figure 4 presents a pyrometer line scan and a TLH line scan measured simultaneously across the diameter of the SPT-100D EM1. The thruster is tilted by 25° in order to get the opportunity to measure the temperature of the plasma channel walls in depth, which can be resolved clearly. The right part of the pyrometer scan curve is smoother due to a lower lateral resolution of the pyrometer, because only the top part of the left plasma channel is in the focal plane of the pyrometer optics. Figure 5 shows two Faraday probe maps of the SPT-100D EM1, exemplarily, at a distance of 600 mm. In Figure 5 (a) the vertical resolution is lower than in panel (b). Thus, the image in panel (a) looks fairly rotationally symmetric. However, in the more detailed map in panel (b) two spots of high current density appear. The lack of rotational symmetry is assigned to a non-symmetric injection of electrons from the neutralizer and a complex plasma generation scenario. In Figure 6 (a) a selected energy scan of the SPT-100D EM1 is plotted. The energy distribution is rather broad and can reveal even multiple peak structures with energy variations of several 100 eV (not shown here) depending on the measurement position and operation parameters of the thruster. In Figure 6 (b) and (c) two mass scans are plotted, the first at the energy of the maximum of the energy curve in Figure 6 (a) and the second at an energy slightly below. First of all, the mass spectra show contributions of multiple charged Xenon ions up to charge number 5. However, the fraction of multiple charged ions is higher for an ion energy of E* = 710 eV than for E* = 753 eV. Again, these results indicate the very complex plasma generation mechanism. The AEPD is of great interest, because a strong need for standardization of thruster characterization is announced by ESA. Therefore, further developments are content of a current ESA contract. The activities are concentrated on reducing possible interactions of diagnostics and thruster by reducing the dimension of the heads and by testing new measurement strategies, and on integration of additional or alternative tools. One of these- the emission spectroscopy probe for the system is under development at IOM and ready for integration. [5]

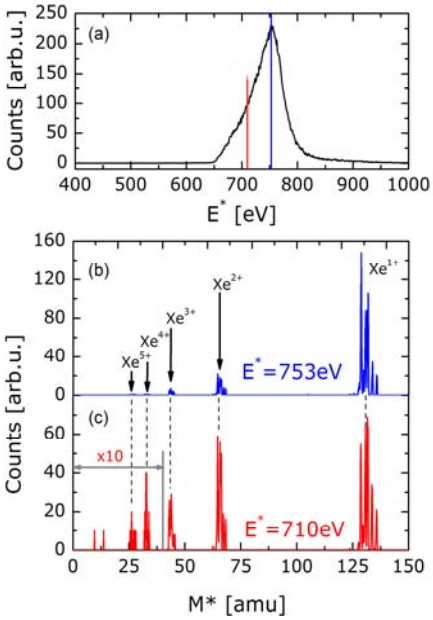

Figure 6: ESMS energy scan (a) and mass scans (b,c) of the SPT-100D EM1 operated at U = 750 V and I = 2.6 A. The mass scans are measured at two energies as indicated in panel (a) (E = 753 eV, E* = 710 eV).*

Modelling

For gridded RF-thrusters the grid erosion is the life time dominating factor [6]. In this context the investigation of grid system life time optimization in dependence on geometry and performance is a very important task of the qualification process of gridded ion thrusters. Experimental life time tests are very time and budget consuming processes, while a validated modelling method allows an optimization of thruster performance well adapted on the mission profile. One main requirement for this modelling is the knowledge of the sputter yield of the grid material under the realistic impact condition, namely ion energy and incidence angle. A typical grid material is graphite. Figure 7 summarizes experimental sputter yield data of graphite in dependence on ion energy and incidence angle measured at IOM and used in an own grid erosion simulation code. It is based on the com-

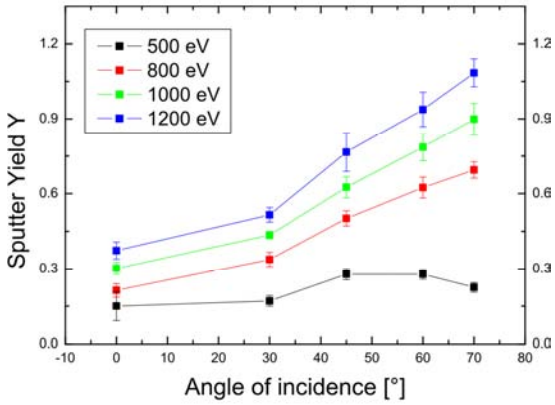

Figure 7: Graphite sputter yield in dependence on the angle of incidence and energy of the Xe-ions.

mercial 2D ion trajectory code IGUN© [7], which simulate the ion extraction and beamlet formation. The neutral flow through the extraction channel is modeled assuming molecular flow conditions and diffuse collisions with walls. From the ion beamlet density and the neutral density the density of charge-exchange ions is calculated and their trajectories are modeled again using the IGUN© code. The erosion rate profile of the grids is obtained by summarizing the grid impinging ions and applying an angular- and energy dependent sputter model. But this erosion rate is not constant over the grid system lifetime. For reasonable grid erosion modeling and lifetime estimations it is therefore necessary to simulate the grid evolution dynamically instead of extrapolating the begin-of-life (BOL) erosion properties. The grid profile is changed according to the erosion rate profile for a defined time step and then the simulation is started again with the new geometry. This iterative procedure allows to model the grid hole geometry and finally the life time dynamically adapted on the mission. The simulation was validated by experiments. Data from 3 thruster lifetime-tests were available for the validation of the dynamical life-time modeling: A 3,000 h accelerated subscale wear test at IOM the RIT-10 lifetime-test for the ARTEMIS mission for 20,000 h and finally, a 5,000 h endurance test of the RIT-22. All test data comprise time-dependent accelerator grid hole diameters at various positions on the grids for different grid configurations and operation conditions. For all long-duration test cases an excellent agreement was achieved between simulation results and the experimental data. One example is shown in Figure 8.

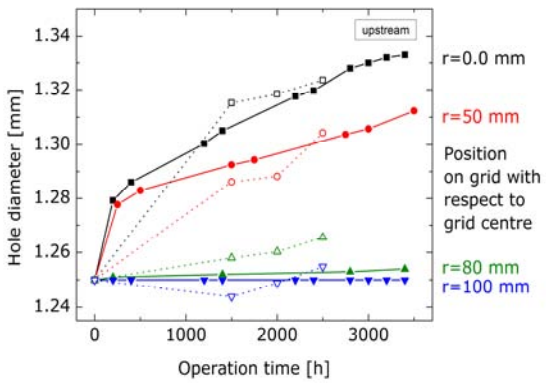

Figure 8: Comparison between measured (open symbols) and simulated (closed symbols) accelerator grid hole diameters of a RIT-22 for different radial positions of the hole on the grid.

Neutralizer

Any thruster needs a neutralizer for neutralizing the positive charge generated by the propellant ions. Typically hollow cathodes are used for this task. However, these neutralizers have severe disadvantages, i.e. they are very sensitive to mechanical and environmental influences. Therefore, an inductively coupled RF-neutralizer has been developed at IOM [8]. It was successfully tested together with a RIT-22 thruster, representing the first European cathodeless thruster system on laboratory level. The basics for a new call were prepared at IOM for integration in the special harmonization procedure for the Basic Technology Research Program (TRP) of ESA and it was realized within the last quarter of 2013 as a subject of a new ESA proposal. Here the aim is to raise the development to a higher qualification level, i.e. an engineering model. These activities are a European collaboration together with Astrium ST (Germany) and Sgenia (Spain) under leadership of IOM and currently in a review process.

Literature

[1] E.Y. Choueiri, J. Propul. Power 20, 193 (2004).
[2] H.J. Leiter, R. Kukies, R. Killinger, E. Bonelli, S. Scaranzin, F. Scortecci, H. Neumann, M. Tartz, Proc. 43rd Joint Propulsion Conf. 2007, AIAA-2007-5198 (2007).
[3] M. Tartz, E. Hartmann, H. Neumann, Rev. Sci. Instrum. 79, 02B905 (2008).
[4] C. Bundesmann, M. Tartz, F. Scholze, H. Neumann, H.J. Leiter, F. Scortecci, J. Propul. Power 27, 532 (2011).
[5] C. Eichhorn, F. Scholze, C. Bundesmann, H. Neumann, Proc. 33rd IEPC Washington D.C. (2013), 295.
[6] M. Tartz, H. Neumann, Proc. 42nd Joint Propulsion Conf. 2006, AIAA-2006-5001(2006).
[7] R. Becker, W.B. Herrmannsfeldt, Rev. Sci. Instrum. 63, 2756 (1992).
[8] F. Scholze, M. Tartz, H. Neumann, Rev. Sci. Instrum. 79, 02B724 (2008).

Improving the Biocompatibility of CoCr Alloys by Plasma Immersion Ion Implantation

S. Mändl, D. Manova, J.W. Gerlach
in collaboration with
C. Díaz, J. A. García, Asociación de la Industria Navarra, Spain

Introduction

Artificial biomaterials are gaining more and more importance as the average lifetime, as well as the demands on the quality of life, are continuously increasing. There is a challenge for the next generation of materials to include as many functions and properties as possible within one kind of material: stimulation of autointegration, biomechanic adjustment, adaptive growth response, together with individualization. However, the concept of biocompatibility itself is still easy to understand and difficult to define, necessitating further fundamental research on surface interactions. Presently, a third generation of smart biomaterials designed to stimulate specific cellular responses is under development and testing.

Several interaction modes have been identified, while no concise explanation of their respective mechanisms is available up to now: (i) surface roughness on the µm- and nm-scale is determining the adhesion of cells and receptor molecules. (ii) the electronic density of state at the surface responsible for electron transfer and the distribution of the electrical potential which can interrupt normal cell behaviour. (iii) outdiffusion of metallic cations leading to toxic effects and apoptosis in the surrounding tissue. (iv) generation of wear particles and their transport towards a final agglomeration in tissue and organs.

When analyzing biocompatibility from a materials science viewpoint, the microstructure and chemical composition of the surface can be viewed as the decisive factors. Hence a physical surface modification can be a suitable tool to influence several factors simultaneously. Thus a process consisting of several, distinct physical, chemical and biochemical steps with their respective, enhanced costs and regulation complexities can be avoided.

Plasma immersion ion implantation (PIII), a thermochemical surface modification process operating at elevated temperatures allows a versatile modification by adjusting temperature, time, ion energy and ion flux to improve the biocompatibility of titanium alloys [1]. The underlying physical processes include diffusion, phase formation and, as a result, modified mechanical properties of the resulting surface layers.

Experiment

The experiments focused on medical grade CoCr alloys, especially L605 (10 wt.% Ni, 20 wt.% Cr, 15 wt.% W, 3 wt.% Fe, bal. Co) and SY21med (28 wt.% Cr, 5 wt.% Mo, bal. Co), together with HS188 (22 wt.% Ni, 22 wt.% Cr, 14 wt.% W, 3 wt.% Fe, bal. Co) for general comparisons on the influence of alloying elements. For fundamental investigations, flat polished coupons were used.

The PIII experiments were carried out in a ultrahigh vacuum chamber with a base pressure better than 10^{-5} Pa at a nitrogen gas flow of 150 sccm, resulting in a working pressure of 0.15 Pa. Plasma generation by an ECR source operating at 2.45 GHz resulted in a plasma density around 6 – 10 × 10^9 cm^{-3} and an electron temperatures of 1.0 – 1.5 eV. The high voltage pulses with a rise time of less than 0.5 µs and a length of 15 µs were fixed at 10 kV across the presented experiments, resulting in incident ion fluences of 2 × 10^{11} atoms/cm^2 per pulse. By changing the pulse repetition rate, the sample temperature during implantation could be adjusted between 200 and 600 °C. Additional experiments were carried out using an auxiliary heating system to maintain the process temperature while varying the ion flux. Beside the nitrogen PIII experiments, oxygen or nitrogen + oxygen PIII was studied to enhance the corrosion protection.

The phase composition was studied by x-ray diffraction (XRD) using Cu K_α radiation. Additional experiments were performed using *in situ* XRD diagnostics during low energy broad beam ion implantation [2]. The elemental concentration distributions were measured with time-of-flight secondary ion mass spectrometry (ToF-SIMS) with Ga^+ as primary beam for analysis and O_2^+ as a secondary ion beam for depth profiling and enhancing the secondary ion yield.

Wear tests on coupons were performed using a rotating ball-on-disc configuration with an alumina

ball, diameter 0.476 cm, in continuous sliding contact. A track diameter of 0.65 cm and a rotation speed between 50 and 200 rpm translates into a speed of 1.7 – 6.8 cm/s. The applied loads were between 0.66 and 9.07 N, corresponding to contact pressures of 0.42 – 1.0 GPa.

Ringer solution, a useful tool to predict the in-vivo corrosion, was prepared according to the standard protocol suggested. Pure electrochemical corrosion experiments, together with fretting wear experiments were conducted in this solution.

Results and Discussion

The initial aim was to determine the nitrogen uptake, diffusion and phase formation. Similar to austenitic stainless steel, an unusually fast nitrogen diffusion at moderate temperatures with a rather constant nitrogen content was observed. Fig. 1 gives an overview of the observed diffusion [3] when assuming a diffusion controlled layer growth ($D = L^2/4t$). A thermally activated process is observed with an activation energy of about 0.8 – 1.0 eV when assuming a single activation energy. This activation energy is identical to the value observed for austenitic stainless steel, while a slightly lower prefactor for the diffusivity is found experimentally.

While no influence of the alloys composition on the diffusion during PIII was observed, some effect is found during plasma nitriding at low pressures without pulsing the substrate. For stainless steel, no nitriding is possible, as the surface oxide presents an impenetrable barrier. In contrast, this barrier is not present for CoCr, where a strong influence of the alloy composition is observed. This indicates that the additional step of surface adsorption of low energy ion from the plasma [4], the breaking of the molecular bond and the uptake into the bulk material below the surface is the rate limiting factor for the diffusion process [5].

For investigating this process in more detail, *in situ* XRD experiments were performed where this additional nitrogen uptake from the plasma is suppressed. The time resolved intensity of the substrate alone is sufficient to determine the temporal evolution of the layer growth. High current densities, respective nitrogen supply, lead to a diffusion controlled, inverse parabolic layer formation while lower current densities lead to a linear, supply controlled behaviour [6].

The phase formation is characterized by the appearance of expanded austenite, i.e. an fcc lattice expanded by about 5 – 8% (see Fig. 2) normal to the surface. Stress and stress gradient are additionally found in the material, together with dislocation formation and twinning [7], indicating that the stress is actually limited by the yield strength of the material.

Depending on the process time and temperature, a decay of the metastable expanded austenite is observed. Using *in situ* x-ray measurements, it can be deduced that the expanded austenite phase is disappearing without any additional phases appearing. Only after a time delay, the formation of CrN and Cr_2N is visible, as shown in Fig. 3 [6]. Apparently, the lattice is decaying into nanosized precipitates which are subsequently growing. This process is dissimilar to a spinodal decomposition observed in carbon-rich iron and steel alloys. While the atomic composition after nitriding seems to allow a stoichiometric CrN phase, a detailed analysis indicates that there is either excessive nitrogen or insufficient nitrogen, especially when Cr_2N is formed. At the same time, the rather small and intermixed precipitates complicate a definite analysis. Additional work is still in progress, similar to the decay into CrN and ferrite of expanded austenite in stainless steel.

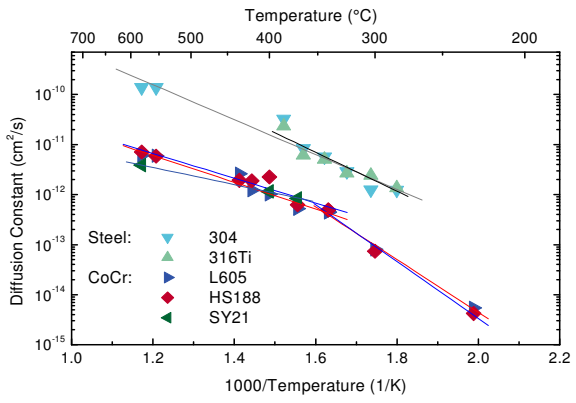

Figure 1: Arrhenius plot of resulting diffusion constants as a function of temperature for three CoCr alloys as well as two stainless steel alloys.

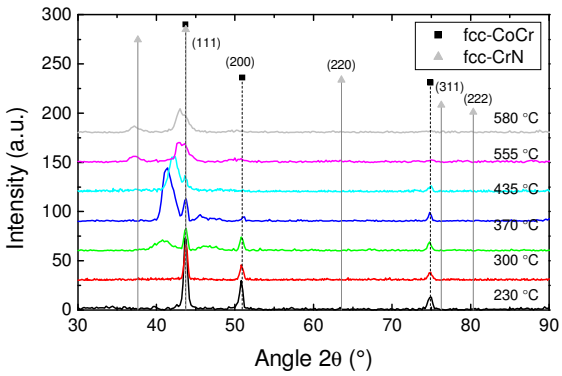

Figure 2: XRD spectra for CoCr alloy HS188 after nitrogen PIII for temperatures between 230 °C and 580 °C.

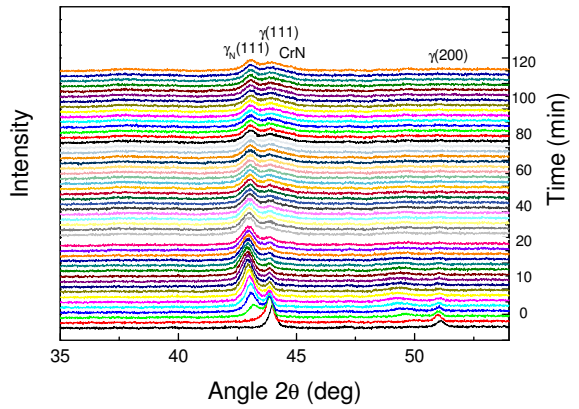

Figure 3: Time evolution of XRD spectra during low energy nitriding at 550 °C.

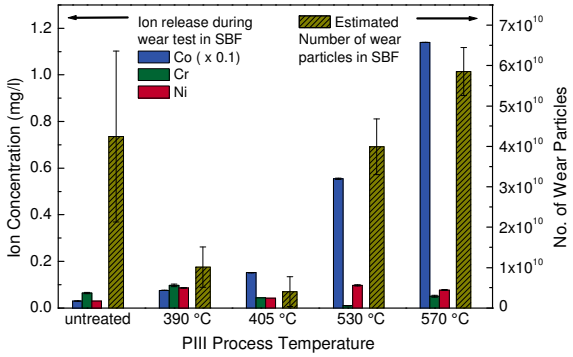

Figure 4: Comparison of metal ion release during wear tests in SBF with number of wear particles. Please note that the cobalt concentrations were multiplied by a factor of 0.1 for clarity.

This beginning decay, starting around 1 hour after the beginning of nitrogen insertion at a temperature of around 400 °C is also reflected in the corrosion data. While CoCr alloys are forming a protective, closed Cr_2O_3 surface layer even for chromium concentrations of only around 20 at.% due to the thermodynamically driven migration of Cr atoms to the surface, is the formation of precipitates containing CrN reducing this mobility [8]. Correspondingly, a degradation of the tribochemical behaviour is observed at elevated temperatures where these precipitates are present.

The surface hardness itself is not influenced by the phase formation after nitrogen insertion into CoCr alloys at elevated temperatures. Starting from a base value of 5 GPa, an increase to 12 – 16 GPa is always observed, independent of the implantation conditions. However, it must be ascertained that the hardness of the surface layer is measured without any influence of the substrate, e.g. by reducing the load to 10 – 20 mN for the nanoindentation measurements. The hardening itself is either due to solution-strengthening or precipitations, perhaps with additional influence from work hardening due to the formation of dislocations during the anisotropic materials expansion.

Corresponding to the increased surface hardness, the abrasive wear rate under dry conditions is reduced after nitrogen PIII of CoCr alloys. While the untreated alloys show a strong dependence of the wear rate (against alumina balls in ball-on-disc configuration), correlated with their original development history, these differences disappear after nitrogen insertion. The wear mechanism is still abrasive with a similar energy deposition into the surface as the friction coefficient remains rather high and unchanged with values of 0.50 – 0.55. Nevertheless, a reduction of the wear by a factor of 20 – 500 is observed, in agreement with the strengthened surface structure after nitrogen insertion. Due to the high friction coefficient, the maximum of the contract stress is still residing within the modified surface layer and not the base material. At the same time, an excellent adhesion of the expanded austenite layer can be inferred as no flaking or delamination was observed in SEM micrographs.

While the investigations under dry conditions are instructive for fundamental processes, applications, especially biomedical ones, are always in lubricated conditions, either with synovial or serum fluid. When reproducing the dry wear tests with Ringer solution, a strong reduction of the wear rate was observed for the untreated samples while obtaining similar values for the samples treated with PIII at 350 °C as under dry conditions. Thus, the effect of the PIII treatment on the tribology is partially compensated when changing the measurement conditions.

When increasing the PIII implantation temperature, a strong increase of the wear rate is observed, even up to values larger than that of the untreated material (see Fig. 4). A closer inspection of the wear tracks reveals a transition from abrasive wear towards fretting wear with increasing the nitrogen implantation temperature. As the passivating behaviour of the surface is lost, a combination of mechanical and electrochemical attack and their synergy effect leads to higher corrosion and wear. As can be seen, the corrosion is characterized by a highly selective increase in the release rate of Co ions with neither Cr nor Ni being influenced by the nitriding temperature during these wear tests in simulated body fluid.

Thus, a compromise between reduced wear and reduced ion release has to be found for biomedi-

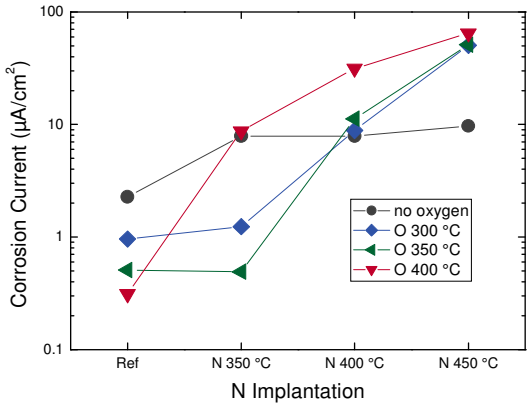

Figure 5: Corrosion rates calculated from the polarisation curves as function of nitrogen and oxygen implantation temperature. The samples labelled as "ref" are only implanted with oxygen (with indicated temperature), together with a sample from untreated base material (black circle).

cal applications. When investigating the cellular response only to cobalt ions, a significant detrimental effect has been observed [9]. A higher cell activity seems to compensate the damage from these ions.

One alternative to avoid the loss of corrosion protection after nitrogen insertion, while maintaining the wear resistance, is to use a duplex nitrogen + oxygen PIII process. Here, the passivation layer is artificially formed in a second step after formation of the hard and wear resistant diffusion layer. As no diffusion is occurring for the oxygen implantation in the temperature range between 300 and 500 °C, the phase formation is restricted to the immediate surface with a thin oxide layer of a few nanometers covering the surface. Hence, the nanostructure formed during nitrogen ion implantation with a roughness exceeding 100 nm is preserved, keeping the primary bioactivity intact.

As shown in Fig. 5, pure oxygen implantation reduces the corrosion current compared to untreated reference material. A similar effect is found for 350 °C pre-implantation with nitrogen. However, for higher nitrogen implantation temperatures, an adverse effect is observed with the secondary oxygen implantation leading to a deteriorating corrosion behaviour despite forming a closed oxide layer on the surface.

When using x-ray photoelectron spectroscopy for surface analysis, the following results have been found [10]: in all cases, a thickening of the native oxide layer is observed, together with a partial depletion of Co, Ni and W at the surface even after the nitrogen implantation step. When adding additional oxygen to the surface during the second step of the duplex treatment, no qualitative differences are found in the XPS spectra. Qualitatively, the Co segregation immediately below the surface is more pronounced, followed by a thicker chromium oxide layer when using additional oxygen implantation as the native oxide was formed at room temperature, albeit for a longer time.

One possible explanation for this apparently contradictory behaviour may be found in the microstructure of the oxide layer. While polycrystalline grains dominate the surface morphology, there will be grain boundaries, dislocations and other defects. These sites could act as an additional conduit for corrosion reactions with a corrosion current density much higher along these defects than for the average surface.

Conclusion

Nitrogen PIII of CoCr alloys allows the formation of a hard and wear resistant surface layer. However, the corrosion protection is compromised for rather low processing temperatures as CrN precipitates start to form on a nanoscale, difficult to observe experimentally. Either a carefully supervised compromise between wear and corrosion has to be achieved or a duplex nitrogen + oxygen PIII treatment can be applied to restore the protective oxide layer.

Literature

[1] J. Lutz, A. Lehmann, S. Mändl, Surf. Coat. Technol. 202 (2008) 3747.
[2] D. Manova, A. Bergmann, S. Mändl, H. Neumann, S. Rauschenbach, Rev. Sci. Instrum. 83 (2012) 113901.
[3] J. Lutz, J.W. Gerlach, S. Mändl, phys. stat. sol. (a) 205 (2008) 980.
[4] J. Lutz, S. Mändl, Nucl. Instrum. Meth. B 267 (2009) 1522.
[5] G. Ertl, J. Vac. Sci. Technol. A 1 (1983) 1247.
[6] C. Wesemann, Master Thesis, Leipzig University, 2013.
[7] J. Lutz, D. Manova, J.W. Gerlach, M. Störmer, S. Mändl, IEEE Trans. Plasma Sci. 39 (2011) 3056.
[8] J. Lutz, C. Díaz, J.A. García, C. Blawert, S. Mändl, Surf. Coat. Technol. 205 (2011) 3043.
[9] K. Schröck, H. Schneider, J. Lutz, M. Hacker, S. Mändl, M. Kamprad, M. Schulz-Siegmund, J. Biomed. Mater. Res. A 102 (2014) 34842.
[10] S. Mändl, C. Díaz, J.W. Gerlach, J.A. García, Nucl. Instrum. Meth. B 307 (2013) 305.

Microstructure of porous GaN thin films

A. Lotnyk, D. Poppitz, J.W. Gerlach, B. Rauschenbach

Introduction

In the last years, an increasing number of GaN based nanosized structures like nanowires or nanorods were prepared and investigated with the particular aim of adapting them for solid state lighting purposes. The expected superior crystalline and optical quality of such nanosized structures allows the design of advanced high-brightness optoelectronic devices.

In this work, porous GaN thin films consisting of irregular nanowall arrays were epitaxially grown on 6H-SiC(0001) or on c-plane Al_2O_3 substrates by ion-beam assisted molecular beam epitaxy at different substrate temperatures. The surface topography, crystalline structure, microstructure and morphology of the thin films were studied in detail by scanning electron microscopy and state of the art aberration corrected scanning transmission electron microscopy (STEM). In particular, the local structure of the nanowalls and the GaN-SiC interface was analyzed by advanced high-resolution STEM techniques. Based on the results, a growth mechanism of porous GaN thin films is discussed.

Experimental

The GaN thin films were produced in a self-designed ultra-high vacuum system for ion-beam assisted molecular-beam epitaxy (IBA-MBE) as described in [1]. Polished SiC substrates oriented in (0001) were used. For the growth of GaN layers, the chamber was equipped with a conventional Ga effusion cell and a hollow anode N ion-beam source [2] which produces ions with a maximum kinetic energy of 25 eV. The N ion flux onto the sample was 6.3×10^{14} $cm^{-2}s^{-1}$. The Ga effusion cell was operated at temperatures between 970 °C and 1020 °C, corresponding to Ga fluxes onto the sample from 1×10^{14} $cm^{-2}s^{-1}$ to 2.3×10^{14} $cm^{-2}s^{-1}$. At the beginning of the film deposition, a positive gradient of the Ga flux was established to prefer hexagonal GaN growth. The substrate temperature was kept constant during the deposition and was in the range of 750 °C to 850 °C. Deposition times of up to 7 h were used, resulting in a maximum film thickness of 700 nm.

The surface topography of the films was investigated with a field emission scanning electron microscope (SEM, FEI Quanta 250) equipped with secondary and backscatter electron detectors. Transmission electron microscopy (TEM) was performed with a Titan^3 G2 60-300 (FEI). This microscope is equipped with a probe Cs-corrector and a high-brightness electron gun (X-FEG), bright-field (BF), dark-field (DF) and high-angle annular dark field (HAADF) STEM detectors as well as a post-column Gatan imaging filter (GIF Quantum 963/P with DualEELS and fast shutter). The TEM was operated at 80 kV and 300 kV acceleration voltages. Energy dispersive X-ray (EDX) analysis was performed by using a SuperX detector. Cross-sectional samples for TEM analysis were prepared by focused ion beam (FIB) technique (Auriga CrossBeam FIB-SEM, Carl Zeiss Microscopy GmbH) so that all investigated samples were oriented in the w-GaN [2-1-10] zone axis. To improve the quality of TEM specimens, a focused low-energy argon ion milling using NanoMill system (Model 1040, Fischione Instruments) was applied. Ion energies from 900 eV down to 200 eV were used to achieve final sample thicknesses between 10 and 30 nm as well as to remove Ga ion-implanted and amorphized regions caused by the FIB process [3, 4].

Results and Discussion

Fig. 1a gives SEM image of GaN thin film grown on 6H-SiC(0001) substrate at substrate temperature of 850 °C. The surface topography of the film shows a rough and porous structure. The pore size varies with changing substrate temperature. The diameter of pores is 40±10 nm for the sample grown at a substrate temperature of 750 °C and ranges from 100 to 500 nm for the sample deposited at a substrate temperature of 850 °C (Fig. 1a). Fig. 1b gives a FIB cross-section of the sample shown in Fig. 1a. From Fig. 1b it can be seen that the pores penetrate into the film down to the

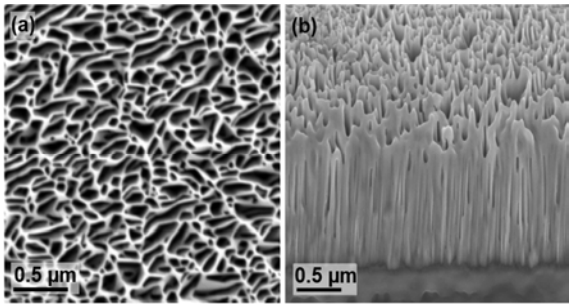

Figure 1: (a) SEM image of poreus GaN thin film. (b) FIB cross-section of the sample shown in (a).

substrate without branching or crossing. It should be noted that similar porous structures were also observed for GaN thin film grown on c-plane oriented sapphire at substrate temperatures of 700 °C and 750 °C.

In order to gain insight into the growth mechanism of porous GaN thin films, partially protected areas of the GaN films were studied by SEM imaging (Fig. 2). During the deposition process clamps were used to fix the SiC substrate on a sample holder. Below these clamps the substrate is largely protected from Ga atom and N ion fluxes. Thus, less GaN material can reach the substrate surface at the shielded regions (Fig. 2a). Fig. 2b shows a SEM image of GaN islands nucleated under the clamp. This region is far away from the area where the porous GaN thin film growth occurs (see e.g. Fig. 1). With approaching to the areas of porous GaN, the density of islands is increasing (Fig. 2c and 2d). Concomitantly, the height of the GaN islands increases and a network characterized by laterally elongated islands emerges (Fig. 2d).

TEM analysis was done to gain access to detailed local information. Fig. 3 shows EDX elemental maps at the nanometer scale of the porous GaN film grown at a substrate temperature of 750 °C. The shown elemental maps have a size of 300x300 pixels with a pixel size of 153 pm and a pixel time of 4 µs (frame time of 43 s). For the quantification of the elemental maps the K-lines were used for nitrogen, silicon and carbon and the L-line for gallium quantification. The GaN is present with a chemical composition close to 1:1. No

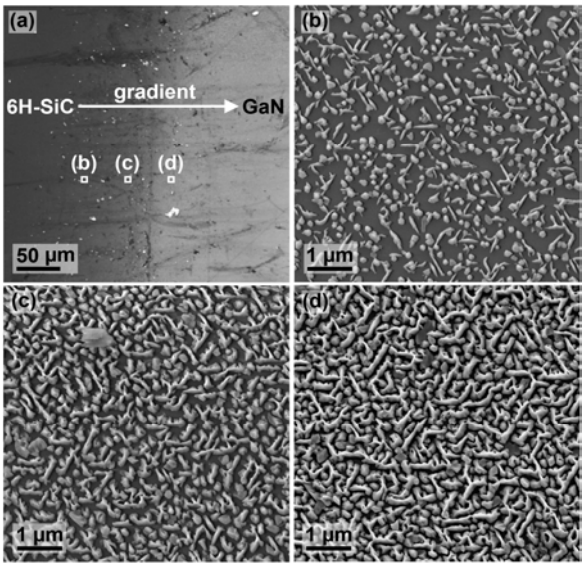

Figure 2: SEM images of (a) area protected by a clamp and (b),(c), (d) enlarged images of the areas marked in (a).

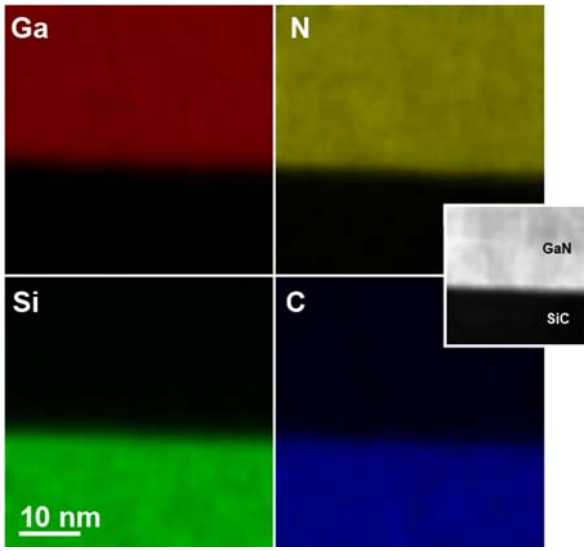

Figure 3: EDX elemental maps of Ga, N, Si and C element distributions at the GaN-SiC interface. The inset shows the STEM image of the acquired area.

intermixing or diffusion effects at the thin film-substrate interface were observed. The interface is not sharp due to a roughness of the normally polished substrate surface which leads to slight blurring at the interface.

Fig. 4 presents a cross-sectional bright-field TEM image of a porous GaN film grown at a substrate temperature of 750 °C. The porous film consists of nanowalls, which are clearly discernible. Selected area electron diffraction pattern in Fig. 4b of the GaN film shows the hexagonal GaN pattern oriented parallel to the [2-1-10] with weak streaks in c axis direction. No diffraction spots originating from the cubic polytype (z-GaN) were found. The streaks between the diffraction spots in c- axis direction indicate c-plane stacking faults in the GaN thin film. Selected area electron diffraction pattern in Fig. 4c illustrates epitaxial growth of

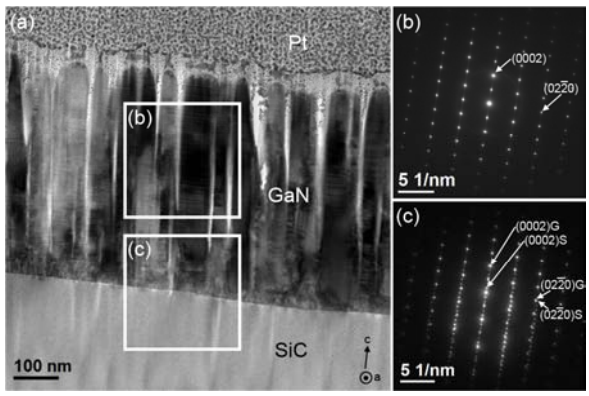

Figure 4: (a) Bright-field TEM micrograph of a porous GaN film grown on 6H-SiC(0001) at a substrate temperature of 750 °C taken at 80 kV acceleration voltage. (b) and (c) electron diffraction patterns of the film and the interface region, respectively.

GaN film on SiC substrate. The c-axis and a-axis of w-GaN and 6H-SiC are oriented in parallel to each other. Further FFT analysis of single GaN nanowalls (not shown here) reveals a slight tilt of the walls against each other as well as a tilt against the normal of the substrate material.

Fig. 5 shows a high-resolution HAADF-STEM image of a pore in GaN epitaxially grown on 6H-SiC at a substrate temperature of 850 °C. The onset of the pore is located at the substrate-film interface. At the beginning of the FIB preparation process of the TEM sample a platinum protection layer was deposited on top of the film to protect the film from Ga ion beam irradiation induced damage. The platinum filled the pores during its deposition down to the substrate surface. The polycrystalline platinum particles between the GaN walls in Fig. 5 indicate that the formation of pores is started at the SiC surface. Cross-sectional STEM images of the same porous GaN film as in Fig. 4 are shown in Fig. 6. Fig. 6a presents a BF-STEM image taken from the upper part of the film near the film surface, whereas Fig. 6b presents a HAADF-STEM image of a region close to the GaN-SiC interface. Both images demonstrate high crystalline quality of the GaN nanowalls. Fig. 6a illustrates c-plane stacking faults in the GaN film. No other defects or inclusions were found in this part of the GaN film. In contrast, a high density of a variety of defects, like cubic inclusions and stacking faults, was observed in regions close to the substrate surface as shown in Fig. 6b (see also Fig. 7).

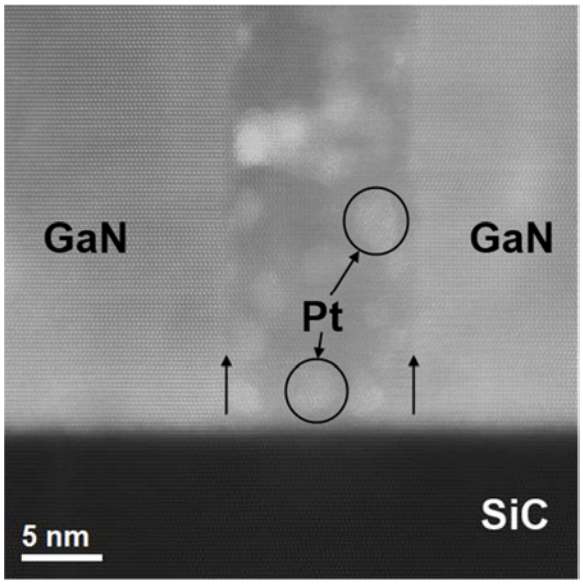

Figure 5: Cross-sectional HAADF-STEM image of a pore in a GaN thin film. The arrows indicate the sidewalls of the pore which occurs directly at the 6H-SiC substrate surface.

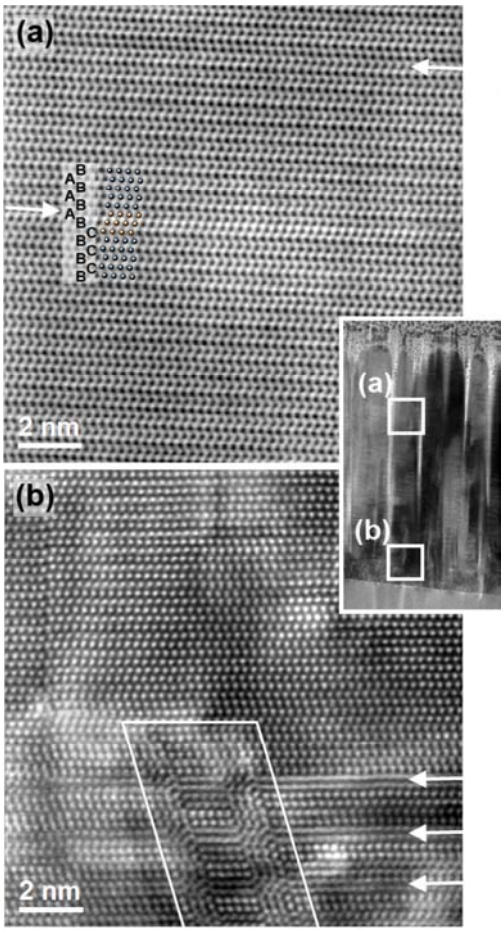

Figure 6: (a) High-resolution BF-STEM image (Wiener filtered) of an area close to the top of the porous GaN film with two stacking faults (white arrows). (b) High-resolution HAADF-STEM image of the film close to the SiC substrate with cubic GaN inclusions and stacking faults (white arrows).

Fig. 7 shows a Wiener-filtered high-resolution HAADF-STEM image of the GaN-SiC interface region. The image demonstrates a good match of two lattices and clearly illustrates the stacking order of the 6H-SiC substrate and the hexagonal GaN film. The stacking order changes only in the first two monolayers where an additional c-position of the Ga atoms is inserted. The interface between the substrate and the porous GaN film in the image is locally atomically sharp. In addition, sharp contrast between GaN and SiC indicates no intermixing effects (also confirmed by EDX analysis in Fig. 3).

In the following, we propose a possible growth mechanism of porous GaN thin films investigated in this work. Recently, a relation between the N ion to Ga atom ratio and the growth mode was reported [2]. It is known that gallium-rich growth conditions promote a two-dimensional growth mode, whereas nitrogen-rich growth conditions lead to three-dimensional growth [5-7]. Thus, the nucleation of three-dimensional GaN islands was

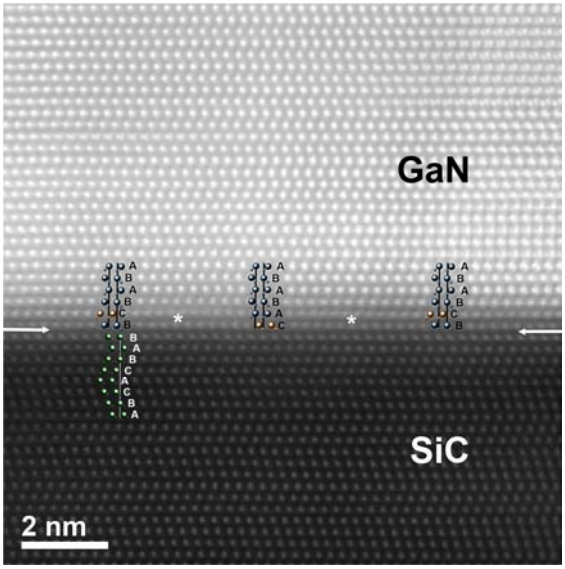

Figure 7: HAADF-HRSTEM image of the GaN-SiC interface. A model of stacking sequence in SiC is also inserted. The white arrows mark the interface. The asterisks mark the areas in GaN where the stacking sequence from BCB to CAB and back is changing.

enhanced. It can be derived from SEM analysis that the islands grow faster in height than in lateral direction (see Fig. 2). This was also reported in literature regarding the growth of nanorods and nanowires by the MBE technique with N-rich growth conditions [8]. The size of the formed islands can be increased by increasing the energy of the Ga adatoms or by increasing the Ga flux until the islands coalesce and form a dense GaN layer. Under extremely N-rich conditions, the coalescence of GaN islands can be inhibited and height growth is preferred. Additionally, Ga atoms reach the top of the crystallites by sidewall diffusion, where they get incorporated due to the energetically favorable low index lattice plane. By this the formed GaN islands grow further in height and do not coalesce [7-9]. Due to the observed formation of laterally elongated islands a network of nanowalls is created (Fig. 2c to d). As another result of our study, we find a substrate temperature dependent increase of the pore size (see Fig. 1). Diffusion length of adatoms increases with increasing substrate temperature or increasing kinetic energy of the adatoms by using hyperthermal ions. The resulting pore size is larger for the porous GaN film. The high-resolution TEM investigations as well as the electron diffraction patterns (see Figs. 4, 6 and 7) prove the high crystalline quality and well- oriented growth of the porous GaN films.

Conclusion

Porous GaN thin films consisting of nanowalls were deposited by ion-beam assisted molecular beam epitaxy on 6H-SiC(0001) substrates at different substrate temperatures in N-rich conditions. The porous films were characterized by SEM and Cs-corrected STEM. The results showed that the porous GaN films grew epitaxially on 6H-SiC substrates with a high crystalline quality. FIB and cross-sectional STEM revealed that the origin of the porosity is located at the GaN-SiC interface. The GaN nanowalls consist of w-GaN, whereas cubic GaN was observed by HRSTEM only close to the GaN-SiC interface. Sparsely distributed defects in the GaN nanowalls were identified as c-plane stacking faults. Variation of the substrate temperature affected the pore size. The growth mechanism of porous GaN thin films was also discussed. The extremely N-rich growth conditions in combination with the high substrate temperature and the energetic N ion irradiation during growth are the main reasons for the formation of nanowall networks of the investigated GaN thin films. Conclusively, owing to the high surface area of the GaN nanowall networks, applications of the structures as gas sensors with high sensitivity or as optical devices with potentially high performance are possible.

Acknowledgements

The financial support of the European Union and the Free State of Saxony (LenA project; project no. 100074065) is greatly acknowledged.

Literature

[1] Y.V. Trushin, D.V. Kulikov, K.L. Safonov, J.W. Gerlach, B. Rauschenbach, J. Appl. Phys. 103 (2008) 114904.
[2] A. Anders, N. Newman, M. Rubin, M. Dickinson, E. Jones, Rev. Sci. Instrum. 67 (1995) 905-907.
[3] D. Poppitz, A. Lotnyk, J. Gerlach, B. Rauschenbach, MC 2013 Proceedings 617-618 (URN number: urn:nbn:de:bvb:355-epub-287343).
[4] A. Lotnyk, D. Poppitz, J. Gerlach, B. Rauschenbach, MC 2013 Proceedings 305-306 (URN number: urn:nbn:de:bvb:355-epub-287343).
[5] J.W. Gerlach, r: Schwertberger, D. Schrupp, B. Rauschenbach, H. Neumann, M. Zeuner, Surf. Coat. Technol. 128-129 (2000) 286-291.
[6] L. Neumann, J.W. Gerlach, B. Rauschenbach, Thin Solid Films 520 (2012, 3936-3945.
[7] B. Heying et al., J. Appl. Phys. 88(4) (2000) 1855-1860.
[8] T. Gotschke, T. Schumann, F. Limbach, T. Stoica, R. Calarco, Appl. Phys. Lett. 98 (2011) 103102.
[9] J.W. Gerlach, R. Schwertberger, D. Schrupp, S. Sienz, W. Attenberger, B. Rauschenbach, IPAP Conf. Ser. 1 (2000) 202.

Enzyme Immobilization on Polymer Membranes

A. Schulze, S. Starke, M. Went

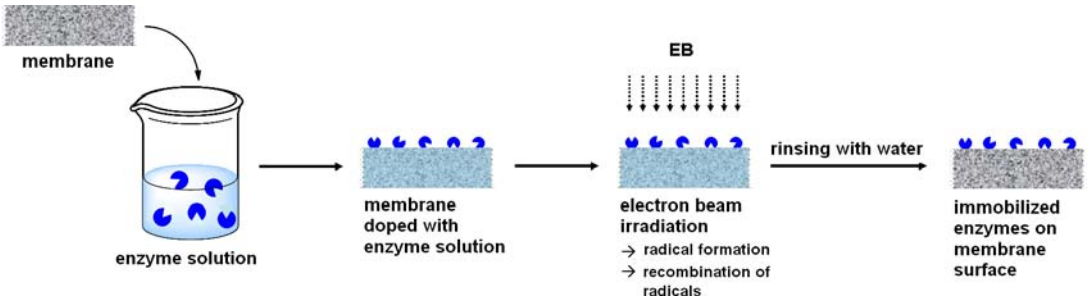

Figure 1: Procedure for the coupling of trypsin on polymer membranes using electron beam irradiation.

The use of enzymes such as trypsin has proven to be of great importance, particularly for industrial and biochemical applications. However, the use of free enzymes is limited due to the labile nature of native enzymes which makes a reuse therefore difficult. In contrast, immobilized enzymes exhibit several advantages, e.g. they offer improved thermal and operational stability and a better availability of the active site to the substrate. Furthermore, immobilized enzymes can be easily removed from the reaction mixture, and thus enable the reuse preventing a contamination of the product at the same time. Enzyme-membrane reactors take advantage of the membrane having the simultaneous task of supporting the biocatalyst as well as acting as a selective barrier for the products to be separated. Many approaches for the immobilization of enzymes on membranes have been described in the literature including adsorption, covalent coupling, cross-linking and incorporation in the polymer substrate. We have reported that electron beam (EB) technology can be efficiently used for surface activation of the matrix polymer and the simultaneous immobilization of small molecules on the membrane surface [1, 2].

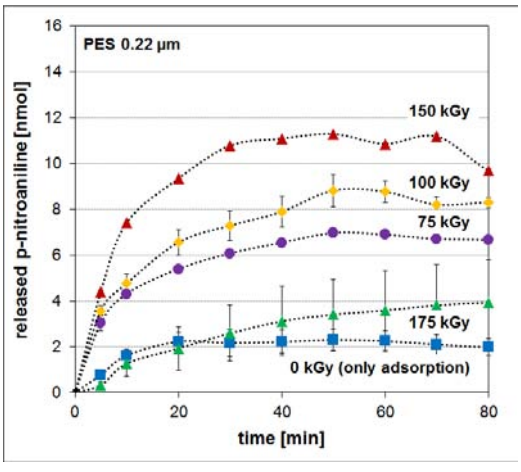

Figure 2: Trypsin activity after immobilization on a polyethersulfone (PES) membrane with different electron beam doses.

This approach (Figure 1) has now been successfully applied on the immobilization of trypsin on polymer membranes in a one-step reaction [3]. It was demonstrated that the resulting membranes showed a significantly higher enzymatic activity as compared to trypsin immobilization per adsorption on the membrane surface (Figure 2). So we assume that EB irradiation within the chosen conditions does not negatively impact the enzyme activity and furthermore, EB treatment is an efficient method for trypsin immobilization on polymer membrane surfaces.

Since the use of EB activation allows for operating independently from specific functionalities present at the matrix polymer's surface, this method can be generally adopted to different membrane polymers, e.g., polyethersulfone and polyvinylidene fluoride.

Fortunately, we could not detect any fouling caused by pore blocking or formation of a coating layer by the enzyme proteins on the membrane surface as demonstrated by pure water flux experiments, SEM and mercury porosimetry measurements. The membrane performance in terms of water permeability and bulk porosity was not decreased by the enzyme immobilization.

Literature

[1] A. Schulze, B. Marquardt, S. Kaczmarek, R. Schubert, A. Prager, M. R. Buchmeiser, Macromol. Rapid Commun. 31 (2010) 467.
[2] A. Schulze, B. Marquardt, M. Went, A. Prager, M.R. Buchmeiser, Water Sci. Technol. 65 (2012) 574.
[3] S. Starke, M. Went, A. Prager, A. Schulze, React. Funct. Polym. 73 (2013) 698.

On the Regioselectivity of Insertion in the Ru-Alkylidene Catalyzed Cyclopolymerization of 1,6-Heptadiynes

S. Naumov

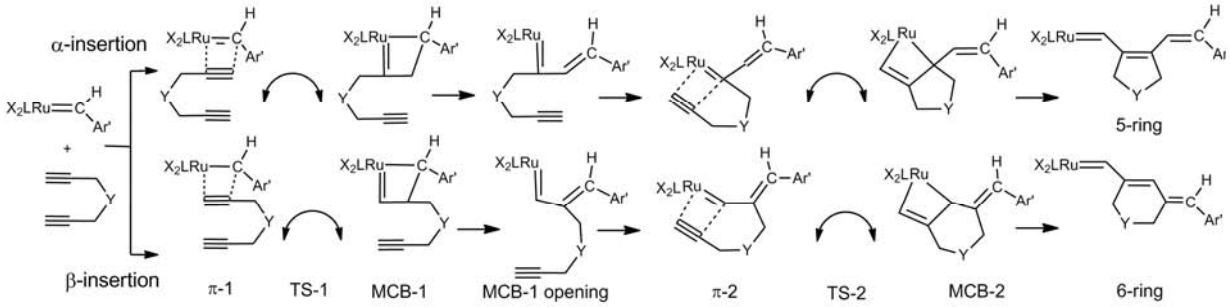

Figure 1: The two possible reaction pathways (α- and β–insertion) leading to the formation of five- and six-membered repeat units.

The experimentally observed high α-addition selectivity of 1,6-heptadiynes to modified Grubbs-Hoveyda initiatorswas elucidated with quantum chemical calculations [1]. For these purposes, the two possible pathways of initiation in the Ru-alkylidene triggered cyclopolymerization (CP) of 1,6-heptadiynes, resulting in either 5- membered (α-insertion) or 6-membered (β–insertion) repeat units were treated as a multi-step process (Fig. 1). The first reaction cascade entails the activation of a precatalyst ($RuX_2(IMesH_2)(CH\text{-}2\text{-}(2\text{-}PrO\text{-}C_6H_4))$, (1; X=F, Cl, Br, I, CF_3COO, $IMesH_2$=1,3-dimesitylimidazolin-2-ylidene) (Fig. 2), reaction with a 1,6-heptadiyne (π-1 complex formation) and further transformation into the first metallacyclobutene (MCB-1) followed by ring opening.

The second reaction cascade entails again the formation of a π complex (π-2) through binding of the second alkyne moiety of the 1,6-heptadiyne and further transformation into MCB-2 followed by ring opening of MCB-2. The energies of the transition structures for both MCB-1 and MCB-2 formation (TS-1 and TS-2), which are considered the rate determining steps in CP, are systematically lower for an α-insertion of a monomer than for a β–insertion. In addition, the geometrical parameters of the most stable structure of the βπ-2 complex are systematically less favourable for MCB-2 formation than in the case of an απ-2 complex resulting in very high activation energies for βMCB-2 formation. Finally, the formation of the βMCB-2 needs an additional step, namely the endergonic formation of the intermediate βMCB-2*. Since a halogen exchange to “pseudo-halides” in Grubbs-Hoveyda initiators is required to turn them into active initiators in CP, the effect of electronegativity (EN) of the X-ligands on the stability of the π-1 complex was calculated for X=I, Br, CF_3COO and F. There, an increase in EN results in lower energies for the α-insertion-derived π-1 complexes. For α-insertion, the energies of transitions states for MCB-1 formation decrease in the order (I>Br>Cl≈CF_3COO≈F). Furthermore, the use of CF_3COO ligands results in a preorientation of the alkyne group in TS(π) parallel to the Ru-alkylidene. Together, all findings are consistent with the experimentally observed [2, 3] preference for α-insertion in the cyclopolymerization of 1,6-heptadiynes with modified Grubbs-Hoveyda initiators.

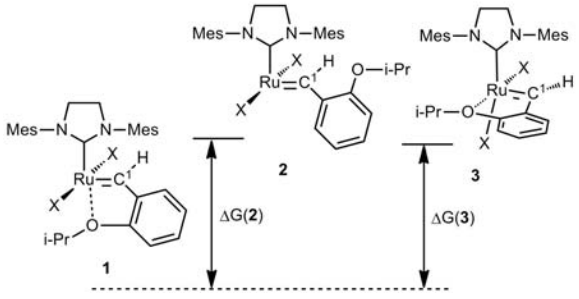

Figure 2: Three stable structures 1 - 3 of the initiator. The most stable structure (1) is stabilized through Ru-O interaction.

Literature

[1] S. Naumov, M.R. Buchmeiser, Organometallics 31(2012) 847.
[2] M.R. Buchmeiser, D. Wang, Y. Zhang, Naumov, K. Wurst, Eur. J. Inorg. Chem. (2007) 3988.
[3] M.R. Buchmeiser, D. Wang, S. Naumov, K. Wurst, J. Organomet. Chem. 691(2006) 5391.

Controlling the function of surfaces with light

D. Hintzen, S. Naumov, K. Siefermann
in collaboration with
Y. Riyad, J. Griebel, Universität Leipzig

Polymer surface coatings can be controlled by light if they contain molecular chromophors, such as azobenzene. Illumination of azobenzene-containing polymer films with light interference patterns can, e.g., create a defined periodic relief structure on the film surface. This technique bears great potential for fast sub-micrometer structuring of large area surfaces. Recently, periodic structures on the 100nm scale were achieved [1]. However, the full power of structuring possibilities is still limited by the fact that the molecular mechanism is not yet adequately understood. The same holds for other light controlled features of polymeric films. The goal of this project is to use (ultrafast) spectroscopic techniques to answer important questions on the mechanism of switching, energy transfer after light absorption, and final structure formation in polymeric films containing azobenzene or other photosensitive units. This knowledge will be directly used to develop new illumination concepts and to create polymeric materials with superior properties regarding structuring possibilities, light control, and stability.

It is believed that efficient light-induced cis-trans isomerization of the photosensitive (e.g. azobenzene) units in the polymeric material is crucial for rapid surface structuring. While a number of azobenzene-compounds with great switching properties are known from experiments in solution, it is unclear how these properties change quantitatively when the azobenzene-molecules are incorporated into a polymer network. We have thus performed a systematic study in order to quantify the impact of a polymeric environment on the dynamics of light-induced trans-cis isomerization. The

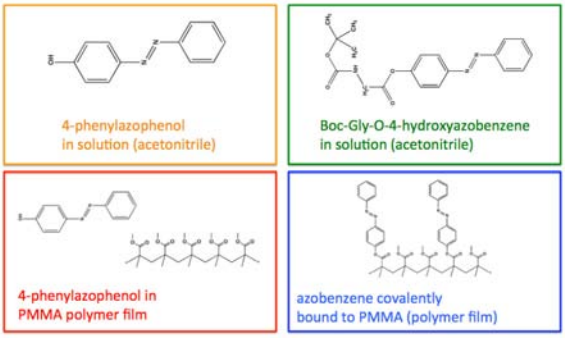

Figure 1: Systematic study of light induced cis-trans isomerization dynamics of azobenzene in four different systems.

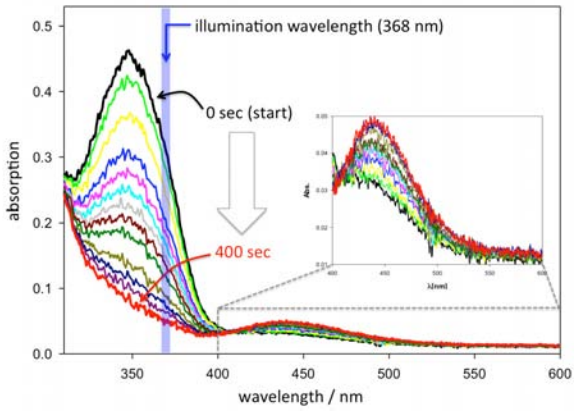

Figure 2: Change of absorption spectrum of 4-phenylazophenol in PMMA polymer film during illumination with 368 nm light. The change in absorption directly reflects the light induced switching from trans to cis isomer.

study was performed on 4 different azobenzene systems (see Figure 1) and it allowed insights into the impact of chemical modification of the azobenzene unit as well as chemical environment. An exemplary measurement is shown in Figure 2.

The measurements are accompanied by quantum chemical calculations to gain insights into the molecular origin of observed differences in switching properties. This combination of experiment and theory will yield crucial information for the rational design of new polymeric materials with superior properties.

In particular, fs-pump-probe spectroscopy will be very useful to shed light on the mechanisms of molecular switches in polymer layers at surfaces. A femtosecond pump-probe spectroscopy experiment with tunable light between 250nm and 720nm employing a home-build **n**oncollinear **o**ptical **p**arametric **a**mplifier (NOPA) and a continuum probe was designed and set up within the SFB-TR102 to investigate the mechanistic details of light-switchable polymer layers. The overall time resolution is about 80fs.

Literature

[1] N. S. Yadavalli, M. Saphiannikova, N. Lomadze, L. M. Goldenberg, S. Santer, Applied Physics A 113 (2013) 263.

Micro and Nanostructured Materials for Energy Applications

A. Varga, F. Lohmann, W. Knolle, S. Naumov, B. Abel

The control of materials on the micro- and nanometer scale is necessary to develop high performance solid-state electrochemical devices. Especially the modification and characterization of surfaces is a key to enhance our understanding of elementary electrochemical processes.

Among more traditional fuel cell technologies, solid acid fuel cells (SAFCs) represent a new and innovative type, with several key advantages. Namely, the state of the art solid acid electrolyte material, CsH_2PO_4, is cheap, non-toxic and an excellent proton conductor at an operating temperature of 240°C. However, as other intermediate temperature fuel cells, SAFCs are performance limited at the cathode. Significant amounts of platinum catalyst have been employed to achieve a power density of 415 mW/cm^2. [1]

Here we explore a dual strategy of increasing the platinum catalyst utilization and thus the electrode performance without increasing the catalyst loading and finding cheap and abundant alternatives to precious metals.

Aerosol methods have been shown to be a suitable method to deposit electrolyte nanoparticles on a conducting substrate [2]. Here we explore the creation and deposition of CsH_2PO_4 nanoparticles on SAFC current collectors and electrolyte thin films, Figure 1. In situ UV-treatment of the aerosol with a stabilizing polymer may provide a method to prevent agglomeration of nanoparticles in the sub 100 nm range, and thus enable an ideal microstructure. Unprecedented deposition rates of 50 mg/min may also enable the commercial application of the spray drying process to create SAFC electrodes.

Recently, nitrogen doped carbon nanotubes (CNTs) and graphene have been shown to exhibit remarkable catalytic activity in polymer electrolyte fuel cell electrodes. Here we also explore the chemical vapor deposition (CVD) method to grow catalytically active CNTs on carbon paper substrates and to fabricate SAFC electrodes without precious metal catalysts. [4] Controlled surface modification methods, such as MeV electron beam, UV irradiation and plasma treatment was explored to introduce catalytically active sites in as synthesized CNT surfaces. These active sites are characterized with surface analytical methods, such as photoelectron microscopy, atomic force microscopy, X-ray photoelectron spectroscopy, and Raman spectroscopy. The results are correlated with macroscopic measurements of electrode performance with impedance spectroscopy, Figure 2.

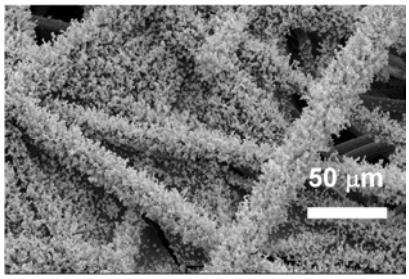

Figure 1: CsH_2PO_4 nanoparticles deposited via a nano-spraydryer, directly on a solid acid fuel cell current collector.

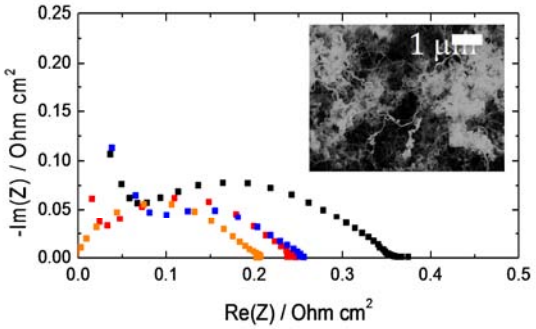

Figure 2: Impedance sectra for four sperate symmetric cells CNT-Electrode|CsH_2PO_4|CNT-Electrode, measured at 240°C and O_2 atmosphere. Inset showing SEM image of as grown, catalytically active CNTs. [3]

Controlled deposition of metal thin films via magnetron sputtering and atomic layer deposition allows mechanistic studies and the determination of rate limiting steps of electrode reactions. The effect of surface treatment on the specific catalytic activities of platinum binary and tertiary alloys is explored.

Literature

[1] T. Uda, S.M. Haile, Electrochemical and Solid State Letters 8 (2005) A245.
[2] A. Varga, N.A. Brunelli, M.W. Louie, K.P. Giapis, S.M.Haile, Journal of Materials Chemistry 10 (2010) 6309.
[3] A. Varga, California Institute of Technology, PhD- Thesis, 2013.
[4] A. Varga, M. Pfohl, N. A. Brunelli, M. Schreier, K. P. Giapis and S. M. Haile, *PCCP* 15 (2013) 15470-15476.

Towards sub-diffraction patterning of surfaces by pulsed laser irradiation

P. Lorenz, F. Frost, M. Ehrhardt, K. Zimmer

The sub-diffraction nanopatterning of surfaces by laser irradiation is a big challenge for laser methods. Especially self-assembling laser-induced processes like ripple formation, fs-laser metal nanostructuring, and ns-laser nanostructuring exhibit an outstanding potential for the fast and large-area nanomachining of surfaces [1]. Coupling the laser-induced formation of metal nanodroplets with the concept of the laser-induced front side etching (LIFE) process [2] permits the production of manifold complex nanostructures into dielectric surfaces.

This method is called IPSM-LIFE (laser-induced front side etching using in situ pre-structured metal structures), Fig. 1 [3].

A KrF excimer laser with a top hat beam profile was applied to irradiate magnetron-sputtered chromium layers with a thickness from 10 nm to 100 nm on fused silica substrates.

In a first step multi-pulse irradiation of the samples with low laser fluences (< 1 J/cm²) results in thin-film melting, melt flow, and finally in the formation of different shaped nano-sized metal features, e.g. droplets, onto the fused silica mainly due to dewetting (see Fig. 2) [3]. However, the multi-pulse irradiation at suitable parameters causes not only a formation of metal features but also the localized melting of the fused silica surface. These thermal processes can result in the formation of well-defined ring structures (see Fig. 2) due to the simultaneous melting and reorganisation of the metal film and the pattern formation in the fused silica [3, 4].

Single pulse irradiation of already nanostructured metal films on fused silica with high laser fluences (> 1 J/cm²) results in the transfer of the metal pattern structure into the fused silica (see Fig. 3) where the metal patterns are removed [5].

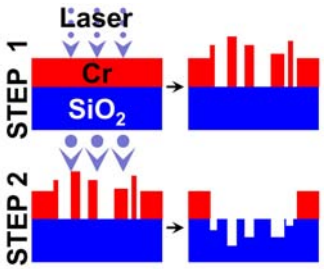

Figure 1: Schematic illustration of the IPSM-LIFE process (STEP 1: low fluence, STEP 2: high fluence treatment).

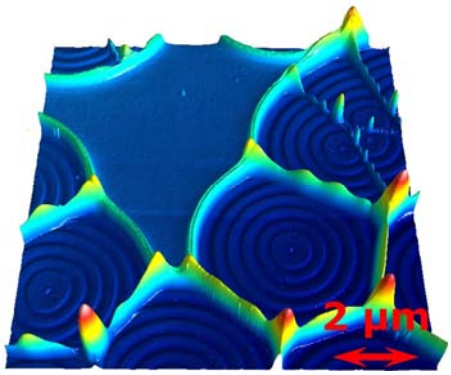

Figure 2: 3D AFM image of an irradiated 10 nm Cr/SiO_2 system (laser fluence Φ = (250 ± 50) mJ/cm², number of laser pulses N = 6).

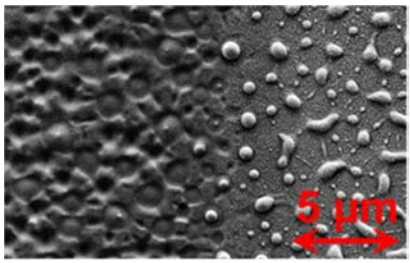

Figure 3: SEM image of an irradiated 20 nm Cr/SiO_2 sample; (right) only the pre-structured metal layer (Step 1: Φ = (200 ± 50) mJ/cm², N = 5) and (left) the structured fused silica surface (Step 2: Φ = (300 ± 50) mJ/cm², N = 9).

Furthermore, the simulation of the process comprising laser absorption, heating, and phase transition (heat equation: including melting and evaporation) and fluiddynamics of the liquid film (Navier-Stokes equation) allows a good explanation of the experimentally observed resultant nanostructures [4].

The IPSM-LIFE method allows the fabrication of randomly distributed structures with lateral sizes down to 10 nm suitable for different purposes, such as optical applications, cytology, and counterfeit security.

Literature

[1] D. Bäuerle, Laser Processing and Chemistry, Springer 2011, Berlin Heidelberg.
[2] P. Lorenz, M. Ehrhardt, K. Zimmer, Appl. Surf. Sci. 258 (2012) 9742.
[3] P. Lorenz, F. Frost, M. Ehrhardt, K. Zimmer, Appl. Phys. A 111 (2013) 1025.
[4] P. Lorenz, M. Klöppel, F. Frost, M. Ehrhardt, K. Zimmer, P. Li, Appl. Surf. Sci. 280 (2013) 933.

Alternative ion-beam based epitaxial GaN film formation route

J.W. Gerlach, L. Neumann, D. Hirsch, B. Rauschenbach

In growth of GaN films by nitrogen ion-beam assisted molecular beam epitaxy (IBA-MBE), two-dimensional growth can be provoked by using slightly Ga-rich conditions [1]. As a consequence, surplus Ga atoms will be present on the film surface. When the amount of these Ga adatoms is high enough, they will agglomerate to form extended Ga droplets. One common way to proceed with such droplets is to chemically wet etch them away. Another way to treat them is irradiating the droplets with the same type of hyperthermal N ions that were used to grow the GaN film, beforehand.

In order to study the limits of the latter way, Ga droplets were formed directly on 6H-SiC(0001) heated to 630°C, i.e. without any GaN film in between, and post-irradiated with low-energy N ions at the same substrate temperature [2]. In this two-step process (see Fig. 1), Ga atom flux and N ion flux are temporally entirely separated from each other. While during IBA-MBE growth Ga atoms come from the vapour phase to the surface of the growing film with a relatively homogeneous lateral distribution, in the process described here, instead, Ga droplets formed on the substrate surface act as the sole source of Ga. These locally

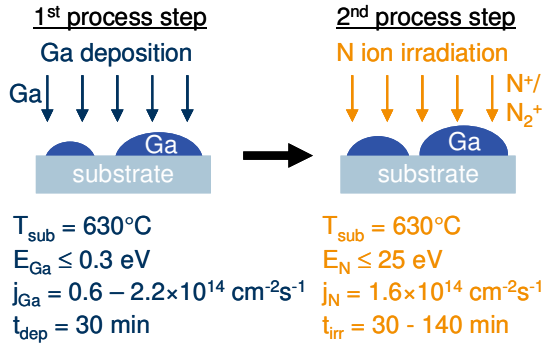

Figure 1: Schematic of the investigated two-step process and typical preparation parameters.

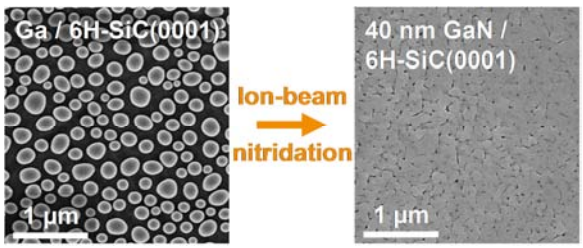

Figure 2: SEM micrographs of Ga droplets formed on a 6H-SiC(0001) substrate surface (left) and a GaN thin film obtained after hyperthermal ion-beam nitridation of such droplets (right).

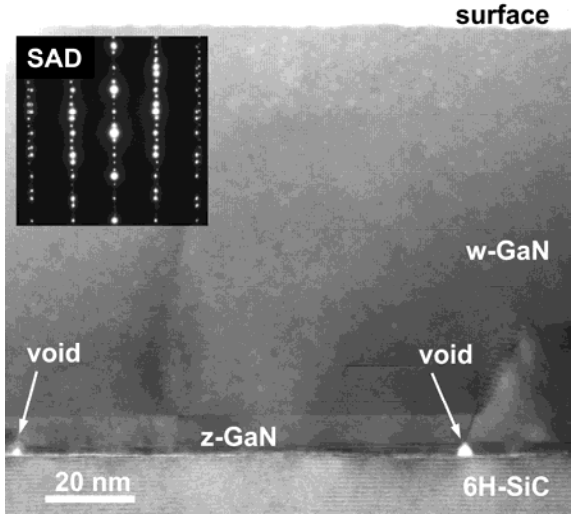

Figure 3: TEM micrograph of an almost 100 nm thick GaN film prepared by ion-beam nitridation of Ga droplets. The SAD pattern (inset) originates from the film-substrate interface region.

well defined but randomly dispersed droplets (Fig. 2, left) supply the GaN growth with Ga atoms. Nonetheless, after the ion-beam nitridation step an almost coalesced, epitaxial GaN film of relatively homogeneous thickness and of high crystalline quality is obtained (see Fig. 2, right and Fig. 3). Detailed investigation using different amounts of deposited Ga atoms resulted in correspondingly thick GaN films with thicknesses of up to 100 nm.

Taking into account results obtained *in situ* during the nitridation process and results from the characterization of the final GaN films, the following diffusion-driven film formation scheme is proposed: Nitrogen ions that reach the droplet surface are forced by the droplet curvature to diffuse at the surface to the droplet perimeter, where epitaxial GaN can nucleate. Diffusion of N through the droplet to the substrate is negligible. Further epitaxial GaN growth proceeds under ongoing consumption of the Ga droplet until the self-limiting process eventually stops, revealing coalesced GaN domains with characteristic voids at the film-substrate interface (Fig. 3).

Literature

[1] L. Neumann, J.W. Gerlach, B. Rauschenbach, Thin Solid Films 520 (2012) 3936.

[2] J.W. Gerlach, T. Ivanov, L. Neumann, Th. Höche, D. Hirsch, B. Rauschenbach, J. Appl. Phys. 111 (2012) 113521.

Pulsed laser deposition of phase change materials

E. Thelander, B. Rauschenbach
in collaboration with
H. Lu, University Wuhan, China

Ever since the late sixties, a number of investigations have been placed on Te-based alloys for optical information storage. Nowadays, chalcogenide-based phase-change materials are being used for commercial optical storage media (re-writable CD, DVD and Blu-Ray), and are growing in importance for use in non-volatile electronic memory. The operation principle of the memory media is based on a reversible transition between an amorphous and crystalline phase, where large changes in optical and electrical properties at different states can be used for saving information. Optical memories utilize the reflectivity contrast (about 20%), while electronic memories use the pronounced difference (>10^3) in electrical conductivity. The materials being used typically lies on the tie-line between GeTe and Sb_2Te_3 in the Ge-Te-Sb ternary phase diagram and particularly the $Ge_2Sb_2Te_5$ phase has received a lot of attention. This is due to its unique set of properties that renders is a god candidate for applications.

The PLD-setup is comprised of an excimer-laser (248 nm, 20 ns) and a UHV-deposition chamber. Our targets consist of pure stoichiometric GeTe or $Ge_2Sb_2Te_5$ and the composition is transferred to our films without any significant deviations. The laser plasma consists of energetic species and therefore it is also possible to deposit on temperature-sensitive substrates [1]. The influence of the energetic plasma also extends to a reduction in crystallization time and a decrease of the irradiation wavelength [2]. As-deposited samples of $Ge_2Sb_2Te_5$ were irradiated with a 20 ns second long laser pulse with a wavelength of 248 nm. This is much below the currently used wavelength of 405 nm in optical recording technology. The laser was defocused on the samples so that a large area was irradiated which realized the simultaneous structural determination with X-ray diffraction. As can be seen in Figure 1a the samples show distinct diffraction peaks for fluences up to 200 mJ/cm^2. However, above 100 mJ/cm^2 a reduction of intensity can be seen which is attributed to the melting/evaporation of the film. In Figure 1b, the lattice parameter evolution can be seen with respect to applied laser fluence. It can be seen that the lattice parameter is largely

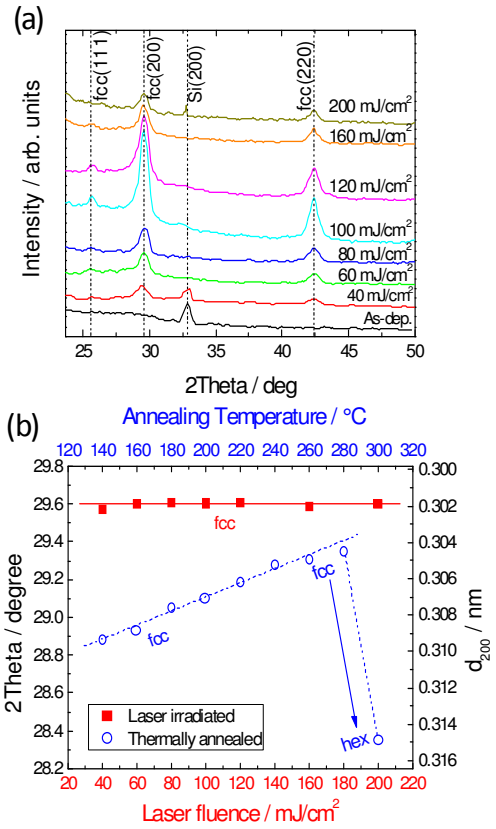

Figure 1: Laser crystallization of GST-films showing (a) T2T-measurement for samples crystallized with different fluence and (b) lattice parameter dependence on laser fluence and annealing temperature.

independent of the fluence which is an important factor for application since a large expansion upon crystallization induces unwanted stress in the material. This should be compared with the thermally annealed films where the lattice parameter is strongly dependent on annealing temperature. Irradiation of the samples with a second pulse of higher intensity brought the films back into an amorphous state thereby showing that a full switching cycle was possible.

This shows that pulsed laser deposition could have a large influence on the crystallization/amorphization behaviour and further studies on the growth modes are required.

Literature

[1] H. Lu, E. Thelander, J.W. Gerlach, D. Hirsch, U. Decker, B. Rauschenbach, Appl. Phys. Lett. 101, (2012) 031905.
[2] H. Lu, E. Thelander, J.W. Gerlach, U. Decker, B. Rauschenbach, Adv. Funct. Mater. 23, (2013) 3621.

Smart materials: ion beam assisted synthesis, characterization and functionalization

U. Allenstein, A. Arabi-Hashemi, A.M. Jakob, A. Landgraf, Y. Ma, S.G. Mayr

Fe_7Pd_3 is a magnetic shape memory alloy capable to perform strains of up to 5 % by applying a moderate external magnetic field. The magnetic shape memory effect due to variant reorientation is only observed within the FCT phase, since only this phase fulfills both the requirements of a high mobility of twinning dislocations and a high magneto-crystalline anisotropy. The metastable phase diagram of Fe_7Pd_3 can be shifted by stresses and deviations from the equilibrium short range order configuration [1]. A convenient method to manipulate both is ion irradiation. 500 nm thick Fe_7Pd_3 samples were deposited on MgO by molecular beam epitaxy. The as-deposited samples revealed the FCC austenite phase. We showed that ion irradiation with 1.8 MeV Kr^+ ions of different fluences induce a phase transformation along the whole Bain transformation path ranging from FCC to FCT to BCC. The orientation relationship between austenite and martensite was determined to be according to Nishiyama-Wassermann [2].

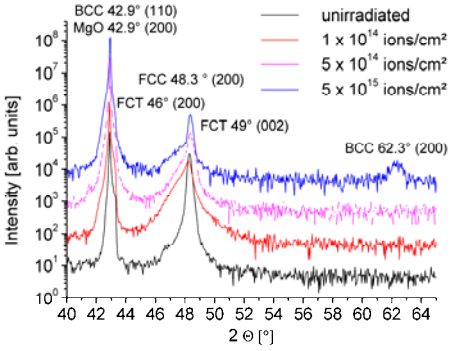

Figure 1: XRD measurements showing the FCC to FCT phase transformation for 10^{14} ions/cm² and the transformation to BCC for 5 x 10^{15} ions/cm².

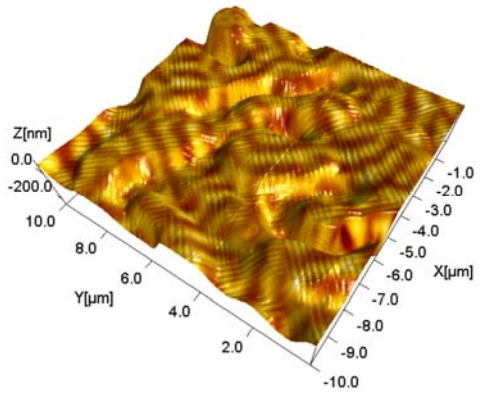

Figure 2: Stacked AFM and MFM image of a martensitic FCT Fe_7Pd_3 sample. Different magnetic domains (yellow and red), run predominantly perpendicular to the martensitic twinning boundaries.

The right orientation of the FCT martensitic cell constitutes an essential prerequisite for magnetic actuation. Therefore it is necessary to systematically examine the relation between the magnetic domain pattern and the underlying structure. During our studies we found experimental evidence that magnetic domain appearance is strongly affected by the presence and absence of nanotwinning [3-5]. While the martensite–austenite transformation upon temperature variation of as-deposited films is clearly reflected in topography, the magnetic domain pattern is hardly affected. These observations are strongly influenced by significant thermal stresses arising in the austenite phase due to the Invar properties of Fe_7Pd_3. Meanwhile freestanding martensitic films exhibit a hierarchical structure of micro- and nanotwinning with a more complex associated domain configuration, since the dominance of magnetic energy contributors alters within this length scale regime.

The foregoing characteristics and the biocompatibility of the films also suggest applications in biomedicine. Thus we test their interaction with coatings, i.e. the RGD amino acid sequence, which is crucial to cellular adhesion. Through delamination tests and cell culture assays we proved decent adhesion of RGD to the substrate, and cells to the RGD, respectively. Theoretical ab initio calculations via density functional theory confirm the experimental results and explain the strong connection between RGD and Fe_7Pd_3 in a fundamental physical way: it is mainly mediated by coordinate bonds between iron atoms of the films and nitrogen/oxygen atoms of the RGD [6]. Thus surface functionalization with biological coatings is possible and desirable.

Literature

[1] S. G. Mayr, Phys. Rev. B 85 (2012) 14105 (2012).
[2] A. Arabi-Hashemi and S. G. Mayr, Phys. Rev. Lett. 109, 195704 (2012).
[3] A. Landgraf, A. M. Jakob, Y. Ma and S.G. Mayr, Sci. Technol. Adv. Mat. 14 (2013) 045003.
[4] Y. Ma, A. Setzer, J.W. Gerlach, F. Frost, P. Esquinazi and S.G. Mayr, Adv. Funct. Mater. 22 (2012) 2429.
[5] A. M. Jakob, M. Hennes, M. Müller, D. Speeman and S.G. Mayr, Adv. Funct. Mater. 23 (2013) 4694.
[6] M. Zink, F. Szillat, U. Allenstein, S.G. Mayr, Adv. Funct. Mater. 23 (2013) 1383.

Two step reactive ion beam etching process for the realization of imaging gratings with modulated blaze

R. Fechner, A. Schindler, F. Frost
in collaboration with
M. Burkhardt, L. Erdmann, R. Steiner, O. Sandfuchs, A. Gatto, Carl Zeiss Jena GmbH

Blazed optical gratings are in general the best choice for attaining the maximal diffraction efficiencies in narrow spectral wavelength ranges. For many applications, e. g. in spectrometer systems, broader spectral windows are desirable. This can be realized by blazed gratings with different blazed areas on the same surface.

Here a combination of interference lithography and a two-step reactive ion beam etching (RIBE) is used to fabricate such gratings on curved glass substrates [1].

The initial saw tooth shaped resist mask pattern depth is about 100 nm over the whole substrate and has a period of 1.9 µm in the centre and a slight local variation of the line density outside. To achieve the desired grating profile depth in the glass by RIBE pattern transfer the etch selectivity can be adjusted between 0.1 and 10. Two RIBE steps have been performed on different parts of the grating using an aligned thin metal aperture mask mounted in two positions very close to the surface. In Fig. 1 the two-step ion etching process is schematicaly shown. To avoid an inhomogeneous illumination of the spectrometer pupil plane the different blazed grating areas have to be distributed in a appropiate pattern. Therefore a slit array like mask is used. Fig. 2 shows the mechanical parts together with the master grating with a usable diameter of 25 mm. The mask was mounted in a distance to the substrate of < 0.1 mm. The overlay error is about 10 micron. By rotating the mask by 180° the formerly covered areas are then exposed to the ion beam. In this way, certain regions can be

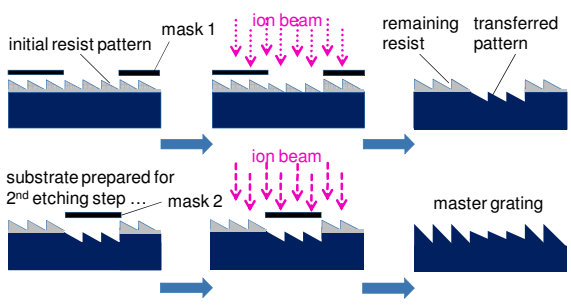

Figure 1: Modified transfer process of the resist pattern by integration of complementary structured masks.

Figure 2: Etching mask (left), substrate holder (middle) and Al-coated master grating with two different blazed regions arranged in a stripe pattern (right).

etched with different transfer ratio and the final element shows novel interesting properties. The grating depths of the two differently blazed areas are 130 nm and 360 nm, respectively. Thus, 50% of the optical active area shows the behaviour like a DUV-grating with a peak in the diffraction efficiency (approx. 75%) slightly above 300 nm wavelength. The remaining grating portion corresponds to a VIS/NIR-grating with a broader peak between wavelengths of 800 nm and 1 µm (diffraction efficiency of nearly 80%). Therefore, integrated in the spectrometer this grating would provide an overall efficiency between 30% and 50% that corresponds to the mean value of the two efficiency curves of the two gratings. It shows clearly a more balanced efficiency over the spectral region of interest. Further, two spectral separated maxima can be identified in the efficiency curve which are not obtained by known alternative profiles like that of binary or sinusoidal gratings.

Based on the two-step-RIBE-transfer process a blazed imaging grating with optical properties equivalent to a conventional holographic type and an ‘artificial’ spectral characteristic was realized. This approach has still potential for further improvement.

Literature

[1] M. Burkhardt, R. Fechner, L. Erdmann, F. Frost, R. Steiner, O. Sandfuchs, A. Schindler, A. Gatto, S. Sinzinger, DGaO-Proceedings 2012, Paper Nr. A003; http://www.dgao-proceedings.de/download/113/113_a3.p

Plasma jet generated slope normals for Nano-Optic-Measuring Machine (NOM) characterization

Th. Arnold, G. Böhm, H. Paetzelt
in collaboration with
F. Siewert, Helmholzzentrum Berlin (HZB)

Autocollimator-based slope measuring profilers like the Nanometer Optical Component Measuring Machine (NOM) [1] at BESSY-II have become standard instrumentations for the ultra-precise characterization of synchrotron optics with sub-nanometer accuracy. Recent experience has shown that a careful characterization and calibration of slope measuring profilers is essential to achieve the accuracy requirements for synchrotron optics of today. A further issue of discussion is the spatial resolution achievable by slope measuring deflectometry.

The knowledge of spatial resolution characteristics in the performance of autocollimator based slope measuring profilers is an important point to consider, e.g. when applying slope-measurement based mapping data to calculate the removal simulation for deterministic surface finishing applications like Ion Beam Figuring.

In past publications it was proposed to perform investigations on this topic by use of dedicated test samples of periodic and chirped profiles.

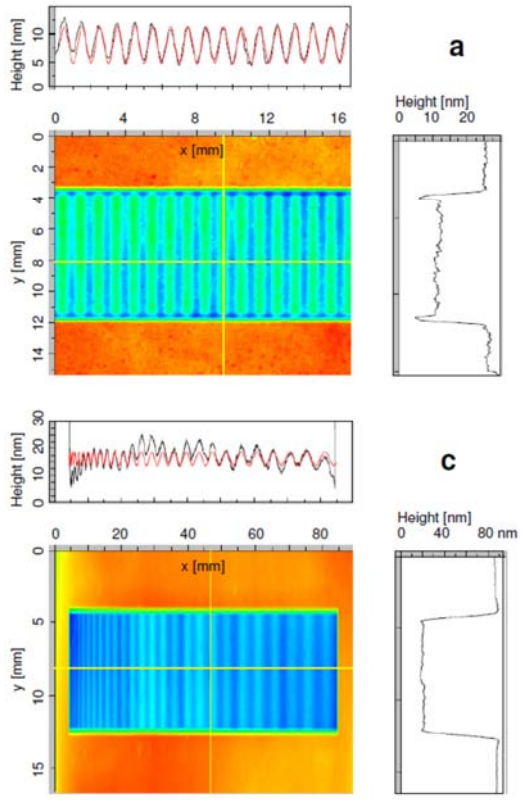

Figure 1: (a) Plasma jet generated sinusoidal surface profile with period of 1 mm and PV of 5 nm, (c) chirped profile.

The purpose of slope measurements in X-ray optics is to identify figure deviations in the range of only a few nanometer PV. Thus, the intention was to prepare a sample with periodic and chirped profiles of 5 nm amplitude. Atmospheric Plasma Jet Etching using a RF excited reactive plasma jet fed with He/CF_4 gas mixture and with a narrow beam size of 0.4 mm FWHM was applied for deterministic local etching of shallow sinusoidal profiles with a nominal PV of 5 nm on a flat silicon disc.

A lateral period of 0.5, 1.0 and 2.0 mm has been realized for three profiles [2]. Furthermore, a chirped profile was made with a spatial variation of 0.5 – 10.0 mm, described by the following equation:

$$y = A\,(\cos(2\pi\, p^{-1}\, x)+1))$$

where A = 2.5 nm and the period $p = 0.3(1+x^{0.5})$. The sample is made on a super-polished single crystal Si-substrate of 100 mm in diameter and 10 mm thickness. The initial substrate flatness was measured with λ/20 peak to valley (λ=633 nm) and the micro-roughness was <0.1nm rms (measured by use of an interference microscope). The interferometric measurement of the 1 mm sinusoidal and the chirped profiles are shown in Fig. 1. (a) and (c). The comparison between theoretical (red) and measured (black) height modulation in the horizontal cross sections prove a sufficient accuracy and a PV of 5 nm, provided that the background long spatial wavelength figure error is subtracted.

Slope measurements of the profiles have been performed on NOM using different circular diaphragm sizes from 1.8 mm to 10 mm. The results reveal a clear correlation between diaphragm size, beam diameter respectively, and spatial resolution.

Literature

[1] F. Siewert, J. Buchheim, S. Boutet, G. Williams, P. A. Montanez, J. Krzywinski, R. Signorato, Optics Express, 20, (2012) 4525.
[2] F. Siewert, J. Buchheim, T. Höft ,T. Zeschke, A. Schindler, Th. Arnold, Nucl. Instrum. Meth. A 710 (2013) 42-47.

Personal Activities

Doctoral Theses

Diploma and Master Theses

Activities in Scientific Organisations

Honours and Awards

Doctoral Theses

2012

Khare, Chinmay
Growth of Ge, Ag and multilayered Si/Ge nanostructures by ion beam sputter glancing angle deposition
Universität Leipzig, Fakultät für Physik und Geowissenschaften, 2012

Luteran, Johannes
Prozesssimulation für die deterministische Oberflächenpräzisionsbearbeitung mittels lokalen chemischen Plasmajettätzens
Universität Leipzig, Fakultät für Physik und Geowissenschaften, 2012

2013

Eichentopf, Inga-Maria
Grundlagenuntersuchung zur Plasmajet-gestützten Bearbeitung von SiC
Universität Leipzig, Fakultät für Physik und Geowissenschaften, 2013

Ma, Yanhong
Miniaturized Fe-Pd ferromagnetic shape memory alloys
Universität Leipzig, Fakultät für Physik und Geowissenschaften, 2013

Neumann, Lena
Anfangsstadien des ionenstrahlgestützten epitaktischen Wachstums von GaN-Schichten auf Siliziumkarbid
Universität Leipzig, Fakultät für Physik und Geowissenschaften, 2013

Perlt, Susanne
Microstructure analyses and structure-property relationships of Ag_1-x$Pb_{18}Sb_1$+yTe_{20}
Universität Leipzig, Fakultät für Physik und Geowissenschaften, 2013

Szillat, Florian
Von oligomierbasierten Beschichtungen zu biokompatiblen Oberflächen
Universität Leipzig, Fakultät für Physik und Geowissenschaften, 2013

Wang, Xi
The thermal and mechanical effects during laser interaction with semiconductor materialsand the application of laser scribing on the CIGS-TFSC thin film solar cell
University Nanjing, China, 2013

Diploma and Master Theses

2012

Abe, Christian
Elektronenstrahlinduzierte Synthese von Cryogelen und deren Anwendung als Enzymreaktoren
Hochschule Fresenius, Zwickau, 2012

Allenstein, Uta
Biocompatibility of $Fe_{70}Pd_{30}$ ferromagnetic shape memory alloys
Universität Leipzig, Fakultät für Physik und Geowissenschaften, 2012

Breite, Daniel
Stabilität und Schaltbarkeit von Polymermembranen
Universität Leipzig, Fakultät für Chemie und Mineralogie, 2012

Dietrich, Corinna
Herstellung photokatalytisch aktiver TiO_2/PES-Membranen
Universität Leipzig, Fakultät für Chemie und Mineralogie, 2012

Dunkel, Robin
Untersuchungen zum Ionennitrieren von rostfreien Edelstählen und CoCr-Legierungen und CoCr-Legierungen
Friedrich-Schiller-Universität Jena, Institut für Werkstoffwissenschaften, 2012

Grüner, Christoph
Glanzwinkeldeposition amorpher Si- und Ge-Nanostrukturen zur Entwicklung innovativer, thermoelektrischer Basismaterialkonzepte
Universität Leipzig, Fakultät für Physik und Geowissenschaften, 2012

Günther, Christian
In situ XRD investigation on the phase formation of the expanded phase of austenitic stainless steel during LEII
Universität Leipzig, Fakultät für Physik und Geowissenschaften, 2012

Hainich, Stefan
Untersuchungen zur Herstellung und Modifizierung von Goldnanopartikeln für biologische Anwendungen
Technische Universität Zwickau, 2012

Heinz, Daniel
Untersuchungen zur Integration poröser Polymerstrukturen in miniaturisierte Systeme und deren Funktionalisierung
Hochschule Fresenius Zwickau, 2012

Jha, Diwaker
Optimization of photoactive TiO_2 thin films
Universität Leipzig, Fakultät für Physik und Geowissenschaften, 2012

Kauerhoff, Tilo
Material und HF-Einkopplungsoptimierung an einem Hochfrequenz- Triebwerk
HTWK Leipzig, Fakultät für Elektrotechnik u. Informationstechnologie, 2012

Müller, Marcus
Biokompatibilität metallischer Oberflächen
Universität Leipzig, Fakultät für Physik und Geowissenschaften, 2012

2013

Bulst, Martin
Dynamische Charakterisierung organischer Dünnfilme
Universität Leipzig, Fakultät für Physik und Geowissenschaften, 2013

Fleischer, Dorena
Elektrische Charakterisierung von flexiblen CIGS-Dünnschichtsolarzellen nach Strukturierung mittels Pikosekundenlaser
Fachhochschule Mittweida, Fakultät für Mathematik, Naturwissenschaften und Informatik, 2013

Fuchs, Maria
Charakterisierung von biokompatiblen Schichten auf Fe-Pd
Universität Leipzig, Fakultät für Physik und Geowissenschaften, 2013

Herold, Benjamin
Hyperthermal ion beam assisted deposition of thin gallium nitride layers on polyimide substrates
Fachhochschule Jena, Fachbereich SciTec, 2013

Lohmann, Felix
Monolithische und partikiläre Cryogelsysteme für Bioanwendungen
Universität Leipzig, Fakultät für Chemie und Mineralogie, 2013

Nilsson, Johan
Time- and angle-resolved photoelectron spectroscopy on liquid surfaces
Universität Leipzig, Fakultät für Chemie und Mineralogie, 2013

Panchani, Satishkumar
Microelectromechanical functional elements on flexible substrates – Fundamental and application of laser-based manufacturing
Hochschule Bremen, Institut für Mikroelektronik, Mikromechanik und Mikrooptik (I3M), 2013

Warmer, Felix
Reactor extrapolation of Wendelstein 7-X
Universität Leipzig, Fakultät für Physik und Geowissenschaften, 2013

Wesemann, Christian
In situ XRD investigations of phase formation during nitriding of CrCo and austenitic steel
Universität Leipzig, Fakultät für Physik und Geowissenschaften, 2013

Activities in Scientific Organisations

Abel, Bernd

- Mitherausgeber der Zeitschrift für Physikalische Chemie, De Gruyter Verlag
- Fachgutachter im Fachkollegium „Physikalische Chemie“ der DFG

Lotnyk, Andriy

- Member of Editorial Board: Materials Science of “The Scientific World Journal“

Mändl, Stephan

- Member of the Int. Committee “Plasma Based Ion Implantation and Deposition“

Neumann, Horst

- Leiter der Arbeitsgruppe „Electric Propulsion“ des DGLR-Fachausschuss "Chemische und Elektrische Raketenantriebe"

Rauschenbach, Bernd

- Member of the Curatorship for “Innovation and Science”
- Member of the Coordination Board “Plasma Surface Technologies”
- Mitglied des Leipziger Forschungsforums an der Universität Leipzig
- Member of the Advisory Board of the International Conference on Plasma Surface Engineering
- Member of the Editorial Board "Journal of Materials"
- Member of the Advisory Board of the International Conference on Ion, Electron and Laser Physics
- Sprecher der DFG-Forschergruppe 845 „Selbstorganisierte Nanostrukturen durch niederenergetische Ionenstrahlerosion"
- Member of Internal Advisory Committee of the Translational Centre for Regenerative Medicine (TRM)
- Member of the Scientific Committee of the International Conference of Surface Modification of Materials
- Member of the Editorial Board "Dataset of Material Sciences"
- Member of the Editorial Board "Condensed Matter Physics"
- Member of the Scientific Committee "Nanomaterials: Applications and Properties"

Zimmer, Klaus

- Member of the Scientific Committee of the EMRS Spring Meeting "Laser Materials Processing for Micro and Nano Applications" 2012

Honours and Awards

Frost, Frank

- Wissenschafts- und Technologiepreis des IOM Leipzig (Institutspreis) 2012

Helmstedt, Ulrike

- Leibniz Mentoring Programm für exzellente Frauen der Leibniz-Gemeinschaft

Jakob, Alexander M.

- Nachwuchsforscherpreis des IOM Leipzig 2013

Khare, Chinmay

- Nachwuchsforscherpreis des IOM Leipzig 2012

Ma, Yanhong

- Chinese Government Award for Outstanding Students Abroad from China Scholarship Council 2012

Neumann, Horst

- Wissenschafts- und Technologiepreis des IOM Leipzig (Institutspreis) 2013

Reichelt, Senta

- Scientific Award from Irradiation Association (IIA), IRAP 2012

Scientific Events

Scientific Meetings

Institute Colloquia

Lectures

Seminars

Scientific Meetings

XIX. Workshop „Oberflächentechnologien mit Plasma- und Ionenstrahlprozessen“
06.-08.03.2012, Mühlleithen, H. Neumann (organisation)

Bunsentagung „Ionic Liquids“ der Deutschen Bunsen-Gesellschaft für Physikalische Chemie e.V.
17.-19.05.2012, Leipzig, B. Abel (co-organisation)

BuildMoNa module „Analysis of Surfaces“
09.-10.07.2012, Leipzig, B. Rauschenbach, S.G. Mayr (organisation)

XX. Workshop „Oberflächentechnologien mit Plasma- und Ionenstrahlprozessen“
05.-08.03.2013, Mühlleithen, H. Neumann (organisation)

3rd European NanoMill User Group Workshop
06.06.13, Dresden, A. Lotnyk (organisation)

Nationaler Workshop „Ionenstrahlen in Forschung und Anwendung“
12.-14.06.2013, Leipzig, B. Rauschenbach, Y. Bohne, D. Manova, S. Mändl, F. Frost, J.W. Gerlach, Th. Arnold, S.G. Mayr (organisation)

BuildMoNa Module “Quantum Structures for Energy Applications”
30.9.-01.10.13, Leipzig, B. Rauschenbach (co-organisation)

Herbsttagung des Gemeinschaftsausschusses Plasma Germany
29.-30.11.13, Leipzig, H. Neumann (organisation)

Institute Colloquia

Prof. Dr. F. Rosei (09.01.2012)
Université du Québec, Canada
Strategies for controlled assembly at the nanoscale

Prof. Dr. F. Giessibl (12.01.2012)
Universität Regensburg, Institut für Experimentelle und Angewandte Physik, Germany
The art and science of atomic force microscopy

Prof. Dr. K. Nordlund (19.01.2012)
University of Helsinki, Finnland
Molecular dynamics simulations of ion beam processing of GaAsN, GaN and ZnO

Dr. J. Schubert (24.01.2012)
Forschungszentrum Jülich, Germany
Growth of ternary rare-earth based high-k dielectrics using pulsed laser deposition

Prof. R. Liska (26.01.2012)
TU Wien, Institut für Angewandte Synthesechemie, Österreich
Advanced Monomers and Photoinitiators for Radical Photopolymerization

Prof. Dr. G. Jakob (02.02.2012)
Universität Mainz, Germany
Magnetic Shape Memory Materials: Changing Shape by Magnetic Field

Dr. A. Markaki (24.05.2012)
Lecturer, Dept. of Engineering, University of Cambridge, United Kingdom
Advanced Transmission electron microscopy: Structure and composition of complex oxide interfaces

Prof. Dr. H. Winter (31.05.2012)
Institut für Physik der Humboldt-Universität zu Berlin, Germany
Oberflächenanalytik mittels streifender Ionen-Streuung

Prof. Dr. F. Postberg (04.06.2012)
Universtät Heidelberg, Institut für Geowissenschaften, Universität Stuttgart, Institut für Raumfahrtsysteme, Germany
Die Eisvulkane des Enceladus - die Raumsonde Cassini erforscht den spektakulären Saturnmond

Dr. J. Bonse (07.06.2012)
Bundesanstalt für Materialforschung und –prüfung BAM, Berlin, Germany
Femtosecond laser-induced periodic surface structures

Prof. Dr. K. Liefeith (14.06.2012)
Institute for Bioprocessing and Analytical Measurement Techniques e.V., Heilbad Heiligenstadt, Germany
Mikro- und nanostrukturierte bioanaloge Oberflächen und Strukturen für Diagnostik und Therapie

Dr. M. Luysberg (21.06.2012)
Forschungszentrum Jülich, Germany
Advanced Transmission electron microscopy: Structure and composition of complex oxide interfaces

Prof. Dr. X. Cheng (12.07.2012)
Shanghai Institute of Microsystems and Information Technology, China
Formation of high-k dielectrics by energetic PVD processes

Prof. M. Mehring (19.07.2012)
TU Chemnitz, Institut für Chemie, Germany
From Molecules and Metal Oxido Clusters towards Organic-Inorganic Hybrid Materials and Metal Oxide Nanoparticles

Prof. Dr. J. Lindner (26.07.2012)
Universität Paderborn, Germany
Nanolithographie von Oberflächen für das Wachstum optoelektronischer Strukturen

Prof. Dr. Bhupendra N. Dev (30.08.2012)
Department of Materials Science Indian Association for the Cultivation of Science, Kolkata, India
Pattern and morphology in growth on pristine and ion beam modified surfaces

Dr. T. Hosenfeldt (17.10.2012)
Schaeffler AG & Co.KG Schweinfurt, Germany
Oberflächentechnik als Konstruktionselement für innovative Produkte mit Mehrwert

Prof. H.-G. Löhmannsröben (15.11.2012)
Universität Potsdam (IAP), Germany
Laserspektroskopie und faseroptische Sensorik für (bio)chemische Diagnostik

Prof. Dr. R. Wolf (22.11.2012)
MPI für Plasmaphysik, Greifswald, Germany
Der Stellarator - ein alternatives Einschlusskonzept für ein stationäres Fusionsplasma

Prof. Dr. G. Marowsky (29.11.2012)
LLG Göttingen, Germany
New Developments in Laser Technology for Industrial and Analytical Applications

Dr. À. Varga (13.12.2012)
CALTECH, Pasadena, USA
Solid Acid Fuel Cells - From fundamental discovery to application

Prof. Dr. O. Oeckler (10.01.2013)
Universität Leipzig, Institut für Mineralogie, Kristallographie und Materialwissenschaft, Germany
Von Phasenwechselmaterialien zu Thermoelektrika - Realstruktur-Eigenschafts-Beziehungen bei fehlgeordneten Telluriden

Dr. J. Schubert (24.01.2013)
Forschungszentrum Jülich, Germany
Growth of ternary rare-earth based high-k dielectrics using pulsed laser deposition

Prof. Dr. C. Werner (31.01.2013)
IPF Dresden, Germany
Tailoring polymeric biomaterials for advanced medical therapies

Dr. A. Kahnt (07.02.2013)
Universität Erlangen, Germany
Time-resolved investigation of reactions between nanomaterials and highly reactive species - kinetics, intermediates and mechanisms

Dr. Y. Leterrier (18.04.2013)
EPFL Lausanne, Schweiz
Photopolymerized Nanocomposites and Nanostructures

Prof. Dr. A. Meyer (16.05.2013)
DLR Köln, Institut für Materialphysik im Weltraum, Germany
Materialphysik im Weltraum - Materialdesign aus der Schmelze

Prof. Dr. K. Saalwächter (23.05.2013)
Universität Halle, Institut für Physik, Germany
Dynamics and structure of interphases in nanostructured polymer systems

Prof. Dr. J.W. Bartha (30.05.2013)
TU Dresden, Germany
Untersuchungen von ALD Prozessen in-situ und in-vakuo

Prof. Dr. H. Kohlmann (06.06.2013)
Universität Leipzig, Institut für Anorganische Chemie, Germany
Wasserstoff als Chamäleon im Festkörper

Prof. Dr. B. Kersting (20.06.2013)
Universität Leipzig, Institut für Anorganische Chemie, Germany
Container Molecules: Properties and Applications

Prof. Dr. J. Colligon (25.06.2013)
Metropolitan University, Dalton Research Institute Manchester, UK
MAX-phase and super-hard coatings: formation, properties and applications

Dr. P. Schwaller (11.07.2013)
Bern University of Applied Science, Institute for Applied Laser, Photonics & Surface Technologies ALPS, Schweiz
Laser-induced processes on transparent materials using $CuSO_4$-based solutions

Prof. Dr. B. de Groot (18.07.2013)
MPI für Biophysikalische Chemie, Göttingen, Germany
Molecular dynamics of inhibition, permeation and recognition

Prof. Dr. J. Matysik (07.11.2013)
Universität Leipzig, Institut für Analytische Chemie, Germany
Cofactor-Protein interaction in photoreceptor phytochrome

H. J. Risselada (28.11.2013)
MPI for Biophysical Chemistry, Göttingen, Germany
Simulation of collective phenomenain liquid membranes

Prof. Dr. K.-M. Weitzel (05.12.2013)
Philipps-Universität Marburg, Germany
Low energy bombardement induced ion transport through glasses, polymer films and polyelectrolyte membranes

Prof. Dr. G. Seifert (12.12.2013)
TU Dresden, Germany
Energie- und Wasserstoffspeicherung in Kohlenstoffnanostrukturen

Lectures

B. Abel

- *Einführung in die Physikalische Chemie*
  Universität Leipzig, Fakultät für Chemie und Mineralogie
  winter 13/14, winter 12/13

- *Chemie für das Nebenfach*
  Universität Leipzig, Fakultät für Chemie und Mineralogie
  winter 13/14, winter 12/13

- *Physikalische Chemie für Fortgeschrittene*
  Universität Leipzig, Fakultät für Chemie und Mineralogie
  summer 13, summer 12

- *Aktuelle Themen der Physikalischen Chemie*
  Universität Leipzig, Fakultät für Chemie und Mineralogie
  summer 13, summer 12

- *Methoden der Charakterisierung von Photopolymerisationsreaktionen*
  Beijing University of Technology
  summer 12 (one week lecture)

S. Mändl

- *Quantenphysikalische Grundlagen der Nanotechnologie*
  Westsächsische Hochschule Zwickau
  winter 13/14, winter 12/13

- *Plasmaphysik*
  Universität Leipzig, Fakultät für Physik und Geowissenschaften
  winter 12/13

S.G. Mayr

- *Einführung in die Materialphysik*
  Universität Leipzig, Fakultät für Physik und Geowissenschaften
  winter 13/14

- *Festkörperphysik*
  Universität Leipzig, Fakultät für Physik und Geowissenschaften
  summer 13

- *Einführung in die Oberflächenphysik*
  Universität Leipzig, Fakultät für Physik und Geowissenschaften
  winter 12/13

- *Einführung in die Materialphysik*
  Universität Leipzig, Fakultät für Physik und Geowissenschaften
  summer 12

B. Rauschenbach

- *Einführung in Nanophysik und -technologie*
  Universität Leipzig, Fakultät für Physik und Geowissenschaften
  winter 13/14

- *Surface and Thin Film Analysis*
  Universität Leipzig, Fakultät für Physik und Geowissenschaften
  summer 13

- *Ionen- und Laserstrahl induzierte Nanostrukturen*
  Universität Leipzig, Fakultät für Physik und Geowissenschaften
  winter 12/13

- *Physics of Thin Films*
  Universität Leipzig, Fakultät für Physik und Geowissenschaften
  summer 12

K. Zimmer

- *Mikro- und Nanotechnologie*
  Fachhochschule Mittweida
  winter 12/13

Seminars

S.G. Mayr

- *Materialwissenschaftliches Seminar*
  Universität Leipzig, Fakultät für Physik und Geowissenschaften
  winter 13/14, summer 13, winter 12/13, summer 13

B. Rauschenbach

- *Materialwissenschaftliches Seminar*
  Universität Leipzig, Fakultät für Physik und Geowissenschaften
  winter 13/14, summer 13, winter 12/13, summer 13

K. Zimmer

- *Mikro- und Nanotechnologie*
  Fachhochschule Mittweida
  winter 12/13

Publications and Presentations

Publications in Journals and Books

Conference Proceedings

Talks

Posters

Patents

Publications in Journals and Books

2012

B. Abel, U. Buck, A.L. Sobolewski, W. Domcke
On the nature and signatures of the solvated electron in water
Phys. Chem. Phys. **14** (2012) 22-34

D. Abou-Ras, T. Rissom, B. Marsen, F. Frost, H. Schulz, F. Bauer, V. Efimova, V. Hoffmann, A. Eicke
Enhancements in specimen preparation of Cu(In,Ga)(S,Se)$_2$ thin films
Micron **43** (2012) 470

A. Arabi-Hashemi, S.G. Mayr
Ion-irradiation-assisted phase selection in single crystalline Fe_7Pd_3 ferromagnetic shape memory alloy thin films: From fcc to bcc along the Nishiyama-Wassermann path
Phys. Rev. Lett. **109** (2012) 195704

Th. Arnold, G. Böhm
Application of atmospheric plasma jet machining (PJM) for effective surface figuring of SiC
Precision Engineering **36** (2012) 546-553

T. Bahners, L. Prager, S. Kriehn, J. S. Gutmann
Super-hydrophilic surfaces by photo-induced micro-folding
Appl. Surf. Sci. **259** (2012) 847-852

J. Bauer, M. Weise, B. Rauschenbach, N. Geyer B. Fuhrmann
Shape evolution in glancing angle deposition of arranged germanium nonocolumns
J. Appl. Phys. **111** (2012) 104309

J. Bauer, J. Weise, M. Khare, B. Rauschenbach
Ordered Si-Ge nanostructures by glancing angle deposition via ion beam sputtering
Proceed. MRS Symp. **1329** (2012) 81-87

C. Bechtold, A. Lotnyk, B. Erkartal, L. Kienle, E. Quandt
Structural characterization of sputtered $Fe_{70}Pd_{30}$ thin films during ex situ and in situ TEM heating
Adv. Eng. Mater. **14** (2012) 716-723

S.N. Britvin, O.I. Siidra, A. Lotnyk, L. Kienle, S.V. Krivovichev, W. Depmeier
The fluoride route to Lindqvist clusters: Synthesis and crystal structure of layered hexatantalate $Na_8Ta_6O_{19}{\cdot}26H_2O$
Inorganic Chemistry Comm. **25** (2012) 18-20

I. Claussen, R.A. Brand, H. Hahn, S.G. Mayr
Relaxation scenarios in Fe-Pd and Fe-Pd-Cu magnetic shape memory splats short range order and microstructure
Scripta Mater **66** (2012) 163

V. Dallacasagrande, M. Zink, S. Huth, A. Jakob, M. Müller, A. Reichenbach, J.A. Käs, S.G. Mayr
Tailoring substrates for long-term organotypic culture of adult neuronal tissue
Adv. Mater. **24** (2012) 2399-2403

C. Díaz, J.A. García, S. Mändl, R. Pereiro, B. Fernández, R.J. Rodríguez
Plasma immersion ion implantation for reducing metal ion release
AIP Conf. Proceed. **1496** (2012) 284-287

M. Ehrhardt, P. Lorenz, F. Frost, K. Zimmer
Laser embossing of micro- and submicrometer surface structures in copper
Physics Procedia **39** (2012) 735-742

M. Ehrhardt, P. Lorenz, K. Zimmer
Surface modification by laser etching using a surface-adsorbed layer
Thin Solid Films **520** (2012) 3629-3633

L. Escalada, J. Lutz, S. Mändl, S. Simison, D. Manova, H. Neumann
Corrosion properties of stainless steel 316L after energetic nitrogen insertion
Surf. Coat. Tech. **211** (2012) 76-79

M. Faubel, K. R. Siefermann, Y. Liu, B. Abel
Ultrafast soft x-ray photoelectron spectroscopy at liquid water microjets
Acc. Chem. Res. **45** (2012) 120

J.W. Gerlach, T. Ivanov, L. Neumann, Th. Höche, D. Hirsch, B. Rauschenbach
Epitaxial GaN films by hyperthermal ion-beam nitridation of Ga droplets
J. Appl. Phys. **111** (2012) 113521

R. Hassert, M. Pagel, Z. Ming, T. Häupl, B. Abel, K. Braun, M. Wiessler, A.G. Beck-Sickinger
Biocompatible silicon surfaces through orthogonal click chemistries and a high affinity silicon oxide binding peptide
Bioconjugate Chem. **23** (2012) 2129-2137

U. Helmstedt, E. Clot
Hydride ligands make the difference: Density functional study of the mechanism of the Murai reaction catalyzed by $[Ru(H)_2(H_2)_2(PR_3)_2]$ (R=cyclohexyl)
Chem. Eur. J. **18** (2012) 11449-11458

M. Hennes, J. Buchwald, S.G. Mayr
Structural properties of spherical Cu/Ni nanoparticles
Cryst. Eng. Comm. **14** (2012) 7633-7638

A. Henriquez, H. Bhuyan, M. Favre, B. Bora, E. Wyndham, H. Chuaqui, S. Mändl, J.W. Gerlach, D. Manova
Nitriding of Ti substrate using energetic ions from plasma focus device
J. Phys. Conf. Ser. **370** (2012) 012010

J. A. Jacob, S. Naumov, T. Mukherjee, S. Kapoor
Possible binding sites for Indole acids stabilized water soluble Ag Nanoparticles: An experimental and theoretical study
Int. J. Chem. **4** (1) (2012) 451-458

A.M. Jakob, M. Müller, B. Rauschenbach, S.G. Mayr
Nanoscale mechanical surface properties of single crystalline martensitic Ni-Mn-Ga ferromagnetic shape memory alloys
New J. Phys. **14** (2012) 033029

A. Jenichen, C. Engler
Reconstructions and surface facets of the GaAs(112)A and (112)B surfaces: First-principles DFT supercell calculations
Surf. Sci. **608** (2012) 204-211

R. Joshi, T. K. Ghanty, T. Mukherjee, S. Naumov
Structure, hydrogen bonding and binding energies of neutral and cation dimers of H_2Se with H_2Se, H_2S and H_2O
J. Phys. Chem. **116** (2012) 11965-11972

P. Junghans, B. Wagner, A. Nickel, H. Faust
Tracer kinetics and metabolic models in medicine
Isot Environ Healt S 48 / 2 (2012) 226238

A. Karabchevsky, C. Khare, B. Rauschenbach, I. Abdulhalim
Microspot sensing based on surface enhanced fluorescence from nanosclptured thin films
J. Nanophotonics **6** (2012) 061508

S. Kempf, R. Srama, E. Grün, A. Mocker, F. Postberg, Jon K. Hillier, M. Horányi, Z. Sternovsky, B. Abel, A. Beinsen, R. Thissen, J. Schmidt, F. Spahn, N. Altobelli
Linear high resolution dust mass spectrometer for a mission to the Galilean satellites
Planet Space Sci **65** (2012) 10-20

C. Khare, J.W. Gerlach, Th. Höche, B. Fuhrmann, H.S. Leipner, B. Rauschenbach
Effects of annealing on arrays of Ge nanocolumns formed by glancing angle deposition
Appl. Surf. Sci. **258** (2012) 9762-9769

C. Khare, J.W. Gerlach, C. Patzig, B. Rauschenbach
Ion beam sputter deposition of epitaxial Ag films on native oxide covered Si(100) substrates
Appl. Surf. Sci. **258** (2012) 9617-9622

P. Lorenz, M. Ehrhardt, K. Zimmer
Laser-induced front side and back side etching of fused silica with KrF and XeF excimer lasers using metallic absorber layers: A comparison
Appl. Surf. Sci. **258** (2012) 9742-9748

P. Lorenz, M. Ehrhardt, K. Zimmer
Laser-induced front side etching of fused silica with KrF excimer laser using thin chromium layers
Phys. Status Solidi A **209** (2012) 1114-1118

P. Lorenz, M. Ehrhardt, K. Zimmer
Laser-induced front side etching: An easy and fast method for Sub-¼m structuring of dielectrics
Physics Procedia **39** (2012) 542-547

P. Lorenz, M. Ehrhardt, K. Zimmer
Laser-induced front side etching: An easy and fast method for sub-µm structuring of dielectrics
Physics Procedia **39** (2012) 542-547

P. Lorenz, M. Ehrhardt, A. Wehrmann, K. Zimmer
Laser-induced front side etching of fused silica with XeF excimer laser using thin metal layers
Appl. Surf. Sci. **258** (2012) 9138-9142

H. Lu, E. Thelander, J.W. Gerlach, D. Hirsch, U. Decker, B. Rauschenbach
$Ge_2Sb_2Te_5$ phase-change films on polyimide substrates by laser deposition
Appl. Phys. Lett. **101** (2012) 031905

Y. Ma, A. Setzer, J.W. Gerlach, F. Frost, P. Esquinazi, S.G. Mayr
Freestanding single crystalline FePd ferromagnetic shape memory membranes role of mechanical and magnetic constraints across the martensite transition
Adv. Funct. Mater. **22** (2012) 2529

S. Macko, J. Grenzer, F. Frost, M. Engler, D. Hirsch, M. Fritzsche, A. Mücklich, T. Michely
Iron assisted ion beam patterning of Si(001) in the crystalline regime
New J. Phys. **14** (2012) 073003

M. Mäder, Th. Höche, B. Rauschenbach
Non-periodic nanoscale templates by diffration mask projection laser ablation
Phys. Status Solidi A **209** (2012) 2208-2211

D. Manova, A. Bergmann, S. Mändl, H. Neumann, B. Rauschenbach
Integration of a broad beam ion source with a high-temperature x-ray diffraction vacuum chamber
Rev. Sci. Instrum. **83** (2012) 113901

S.G. Mayr
Energetic and thermodynamic aspects of structural transitions in Fe-Pd ferromagnetic shape memory thin films: An ab initio study
Phys. Rev. B **85** (2012) 014105

S.G. Mayr, A. Arabi-Hashemi
Structural defects in Fe-Pd-based ferromagnetic shape memory alloys: tuning transformation properties by ion irradiation and severe plastic deformation
New J. Phys. **14** (2012) 103006

M. Mecklenburg, A. Schuchardt, Y.K. Mishra, S. Kaps, R. Adelung, A. Lotnyk, L. Kienle, K. Schulte
Aerographite: Ultra lightweight, flexible nanowall, carbon microtube material with outstanding mechanical performance
Adv. Mater. **24** (2012) 34863490

A. Meiners, G. Ohms, M. Leck, U. Vetter, B. Abel
Plasma treatment of glass fiber size to optimize fiber matric adhesion
Adhes. Sci. Technol. **26** (2012) 1611-1627

G. Mirschel, O. Savchuk, T. Scherzer, B. Genest
The effect of different gloss levels on in-line monitoring of the thickness of printed layers by NIR spectroscopy
Anal. Bioanal. Chem. **404** (2012) 573-583

G. Mirschel, K. Heymann, O. Savchuk, T. Scherzer, B. Genest
In-line monitoring of the thickness of printed layers by NIR spectroscopy at a printing press
Appl. Spectrosc. **66** (2012) 765-772

S. Naumov, M. R. Buchmeiser
On the regioselectivity of insertion and the role of the anionic ligands in the Ru-alkylidene catalyzed cyclopolymerization of 1,6-heptadiynes
Organometallics **31** (2012) 847-856

L. Neumann, J.W. Gerlach, B. Rauschenbach
Initial stages of the ion-beam assisted epitaxial GaN film growth on 6H-SiC(0001)
Thin Solid Films **520** (2012) 3936-3945

L. Prager, L. Wennrich, W. Knolle, S. Naumov, A. Prager
Absorption of acrylates and polysilazanes in the far UVC and VUV regions
Mater. Chem. Phys. **134** (2012) 235-242

S. Reichelt, C. Elsner, A. Prager, S. Naumov, J. Kuballa, M. R. Buchmeiser
Amino-functionalized monolithic spin-type columns for high-throughput lectin affinity chromatography of glycoproteins
Analyst **137** (2012) 2600-2607

T. Scherzer
VUV-induced photopolymerization of acrylates
Macromol. Chem. Phys. **213** (2012) 324334

A. Schulze, B. Marquardt, M. Went, A. Prager, M. R. Buchmeiser
Electron beam-based functionalization of polymer membranes
Water Sci. Technol. **65** (2012) 574-580

A. Shalabney, C. Khare, B. Rauschenbach, I. Abdulhalim
Detailed study of surface enhanced Raman scattering from metallic nano sculptured thin films and their potential for biosensing
J. of Nanophotonics **6** (2012) 48-55

M. Sivis, M. Duwe, B. Abel, C. Ropers
Nanostructure-enhanced atomic line emission
Nature Physics **6** (2012) 485

M. Stockmann, D. Hirsch, J. Lippmann-Pipke, H. Kupsch
Geochemical study of different-aged mining dump materials in the Freiberg mining district, Germany
Environ. Earth Sci. **68** (2012) 1153-1168

E. Thelander, B. Rauschenbach
Influence of burst pulses on the film topography in picosecond pulsed laser deposition of $LaALO_3$
J. of Physics: Conf. Series **356** (2012) 012015

H. v. Wenckstern, R. Schmidt-Grund, C. Bundesmann, A. Müller, C.P. Dietrich, M. Stölzel, M. Lange, M. Grundmann
The (Mg,Zn)O alloy
'Handbook of Zinc Oxide and Related Materials: Volume One, Materials'; Z.C. Feng (Ed.); ISBN 978-1-43-985570-6; Taylor and Francis/CRC Press, Boca Raton, Florida, USA (2012) 251-313

A. Wehrmann, S. Puttnins, L. Hartmann, M. Ehrhardt, P. Lorenz, K. Zimmer
Analysis of laser scribes at CIGS thin-film solar cells by localized electrical and optical measurements
Opt. Laser Technol. **44** (2012) 1753-1757

A. Zado, J.W. Gerlach, D.J. As
Low interface trapped charge density in MBE in situ grown Si_3N_4 cubic GaN MIS structures
Semicond. Sci. Technol. **27** (2012) 035020

J. Zajadacz, R. Fechner, K. Zimmer
Fabrication of high aspect ratio sub-100 nm patterns in fused silica
J. Mater. Sci. Eng. A **2** (2012) 458-462

J. Zajadacz, R. Fechner, K. Zimmer
Fabrication of high aspect ratio sub-100 nm patterns in fused silica
J. Mater. Sci. **2** (5) (2012) (2012) 458-462

J. Zajadacz
Measurement and simulation of the pull-off strength at the separation of miniaturized 3D connectors consisting of silicon masters with undercuts and PDMS replicas
Microelectron Eng. **101** (2012) 31-35

P. Gecys, G. Raciukaitis, A. Wehrmann, K. Zimmer, A. Braun, St. Ragnow
Scribing of thin-film solar cells with picosecond and femtosecond lasers
Journal of Laser Micro/Nanoengineering **7** (2012) 33-37

K. Zimmer, M. Ehrhardt, R. Böhme
Laser-induced backside wet etching: Processes, results, and applications
Laser Ablation in Liquids, Ed. Ed. G. Yang, Pan Stanford Publishing (2012) 1013 - 1132

K. Zimmer, J. Zajadacz, R. Fechner, K. Dhima, H.C. Scheer
Fabrication of optimized 3D microstructures with undercuts in fused silica for replication
Microelectron. Eng. **98** (2012) 163-166

2013

B. Abel
Hydrated interfacial ions and electrons
Annu. Rev. Phys. Chem. **64** (2013) 533-552

U. Allenstein, Y. Ma, A. Arabi-Hashemi, M. Zink, S.G. Mayr
Fe-Pd based ferromagnetic shape memory actuators for medical applications: biocompatibility, effect of surface roughness and protein coatings
Acta Biomaterialia **9** (2013) 5845

E. B. Anderson, P. S. Kumar, D. Schawaller, S. Mavila, M. Voss, A. Freyer, W. Knolle, F. Hermanutz, M. R. Buchmeiser
p-Doping and fiber spinning of poly(heptadiyne)s
Macromol. Chem. Phys. **214** (2013) 1047-1051

T. Bahners, L. Prager, A. Pender, J. Gutmann
Super-wetting surfaces by plasma- and UV-based grafting of micro-rough acrylate coatings
Prog. Org. Coat. **76** (2013)

A. Boulares-Pender, I. Thomas, A. Prager, A. Schulze
Surface modification of polyamide and poly(vinylidene fluoride) membranes
J. Appl. Polym. Sci. **128** (2013) 322-331

D. Cao, X. Cheng, Y. Yu, X. Li, C. Liu, D. Shen, S. Mändl
Competitive Si and La effect in HfO_2 phase stabilization in multi-layer $(La_2O_3)_{0.08}(HfO_2)$ films
Appl. Phys. Lett. **103** (2013)

M. Cyris, W. Knolle, J. Richard, E. Dopp, C. von Sonntag, T. C. Schmidt
Reaction of gadolinium chelates with ozone and hydroxyl radicals
Environ. Sci. Technol. **47** (2013) 9942-9949

O. Daikos, G. Mirschel, B. Genest, T. Scherzer
In-line monitoring of the thickness of printed layers by NIR spectroscopy: Elimination of the effect of the Varnish formulation on the prediction of the coating weight
Ind. Eng. Chem. Res. **52** (2013) 17735-17743

M. Ehrhardt, C. Scheit, S. Ragnow, P. Lorenz, A. Wehrmann, A. Braun, K. Zimmer
Fabrication of contact holes by rear side laser ablation of polyimide foils for CIGS solar modules
Appl. Surf. Sci. **278** (2013) 219-222

M. Ehrhardt, A. Wehrmann, P. Lorenz, K. Zimmer
Patterning of CIGS thin films induced by rear-side laser ablation of polyimide carrier foil
Appl. Phys. A **113** (2013) 309-313

M. Ehrhardt, P. Lorenz, F. Frost, K. Zimmer
Fabrication of sub-microstructures in solid copper surfaces by inverse laser microembossing
Appl. Phys. A **111** (2013) 517-523

M. Ehrhardt, P. Lorenz, M. Teichmann, J. Lorbeer, F. Frost, K. Zimmer
Laser embossing of self-organized nanostructures into metal surfaces by KrF laser irradiation
J. of Laser Micro / Nanoeng. **8** (2013) 85-89

L. Escalada, J. Lutz, S.P. Brühl, A: Márquez, S. Mändl, D. Manova, S.N. Simison
Microstructure and corrosion behaviour of AISI 316L duplex treated by means of ion nitriding and plasma based ion implantation and deposition
Surf. Coat. Tech. **223** (2013) 41-46

R. Feder, C. Bundesmann, H. Neumann, B. Rauschenbach
Ion beam sputtering of Ag angular and energetic distributions of sputtered and scattered particles
Nucl. Instrum. Meth. B **316** (2013) 198204

R. Feder, F. Frost, H. Neumann, C. Bundesmann, B. Rauschenbach
Systematic investigations of low energy Ar ion beam sputtering of Si and Ag
Nucl. Instrum. Meth. B **317** (2013) 137-142

R. Fernandes, M. Hüls, M.-J. Nadeau, P.M. Grootes, C.-D. Garbe-Schönberg, H.I. Hollund, A. Lotnyk, L. Kienle
Assessing screening criteria for the radiocarbon dating of bone mineral
Nucl. Instrum. Meth. B **294** (2013) 226-232

A. Fischbacher, J. von Sonntag, C. von Sonntag, T. C. Schmidt
The $^{\cdot}OH$ radical yield in the $H_2O_2 + O_3$
Environ. Sci. Technol. **47** (2013) 9959-9964

Y. Gloaguen, G. Bénac-Lestrille, L. Vendier, U. Helmstedt, E. Clot, Gilles Alcaraz, S. Sabo-Etienne
Monosubstituted borane ruthenium complexes $RuH_2(\cdot^2:\cdot^2\text{-}H_2BR)(PR2_3)_2$: A general approach to the geminal Bis(Ã-BH) coordination mode
Organometallics **32** (2013) 4868-4877

M. Golecki, J. Lach, A. Jeremies, F. Lungwitz, M. Fronk, G. Salvan, D.R.T. Zahn, J. Park, Y. Krupskaya, V. Kataev, R. Klingeler, B. Büchner, B. Mahns, M. Knupfer, P.F. Siles, D. Grimm, O.G. Schmidt, A. Reis, W.R. Thiel, D. Breite, B. Abel, B. Kerstin
Chemisorption of exchange-coupled (Ni_2L(dppba)* complexes on gold by using ambidentate 4-(diphenylphosphino)benzoate co-ligands
Chem. Eur. J. **19** (2013) 7787-7801

F. Guzmán, M. Favre, H.M. Ruiz, S. Hevia, L.S. Caballero, E.S. Wyndham, H. Bhuyan, M. Flores, S. Mändl
Pulsed laser deposition of thin carbon films in a neutral gas background
J. Phys. D Appl. Phys. **46** (2013) 215202

P. Hartmann, T. Brezesinski, J. Sann, A. Lotnyk, J.-P. Eufinger, L. Kienle, J. Janek
Defect chemistry of oxide nanomaterials with high surface area: Ordered mesoporous thin films of the oxygen storage catalyst CeO_2ZrO_2
ACS Nano **7** (2013) 2999-3013

B. Hopp, T. Smausz, T. Csizmadia, C. Vass, C. Tápai, B. Kiss, M. Ehrhardt, P. Lorenz, K. Zimmer
Production of nanostructures on bulk metal samples by laser ablation for fabrication of low-reflective surfaces
Appl. Phys. A **113** (2013) 291-296

V. Hrkac, L. Kienle, S. Kaps, A. Lotnyk, Y.K. Mishra, U. Schürmann, V. Duppel, B.V. Lotsch, R. Adelung
Superposition twinning supported by texture in ZnO nanospikes
J. Appl. Crystallogr. **46** (2013) 396-403

A. N. Idlibi, F. Al-Marrawi, M. Hannig, A. Lehmann, A. Rueppell, A. Schindler, H. Jentsch, S. Rupf
Destruction of oral biofilms formed in situ on machined titanium (Ti) surfaces by cold atmospheric plasma
Biofouling **29** (2013) 369-379

A.M. Jakob, M. Hennes, M. Müller, D. Spemann, S.G. Mayr
Coupling of micromagnetic and structural properties across the martensite and Curie temperatures in miniaturized Ni-Mn-Ga ferromagnetic shape memory alloys
Adv. Func. Mat. (2013)

A. Jenichen, C. Engler, B. Rauschenbach
Comparison of wurzite and zinc-blende GaAs surfaces as possible nanowire side walls: DFT stability calculations
Surf. Sci. **613** (2013) 74-79

B. Khanbabaee, B. Arezki, A. Biermanns, M. Cornejo, D. Hirsch, D. Lützenkirchen-Hecht, F. Frost, U. Pietsch
Depth profile investigation of the incorporated iron atoms during Kr^+ ion beam sputtering on Si(001)
Thin Solid Films **527** (2013) 349

J. Kullmann, C. Küster, T. Titze, C. Chmelik, R. Gläser, D. Enke, L. Prager
Potential des Micro-Imaging zur in-situ-Untersuchung von chemischen Reaktionen in nanoporösen Katalysatoren
Chem. Ing. Tech. 85 / **11** (2013) 1768-1773

A. Landgraf, A.M. Jakob, Y. Ma, S.G. Mayr
Nanoscale magneto-structural coupling in as-deposited and freestanding single-crystalline Fe_7Pd_3 ferromagnetic shape memory alloy thin films
Sci. Technol. Adv. Mater. **14** (2013) 045003

Q.T. Le, S. Naumov, T. Conard, A. Franquet, M. Müller, B. Beckhoff, C. Adelmann, H. Struyf, S. De Gendt, M. R. Baklanov
Mechanism of modification of fluorocarbon polymer by ultraviolet irradiation in oxygen atmosphere
ECS, J. Solid State Sci. Technol. **2** (2013) N93-N98

A. Lehmann, A. Rueppell, A. Schindler, I.-M. Zylla, H. J. Seifert, F. Nothdurft, M. Hannig, S. Rupf
Modification of enamel and dentin surfaces by non-thermal atmospheric plasma
Plasma Process. Polym. **10** (2013) 262-270

Z. Li, N. Pucher, K. Cicha, J. Torgersen, S. C. Ligon, A. Ajami, W. Husinsky, A. Rosspeintner, E. Vauthey, S. Naumov, T. Scherzer, J. Stampfl, R. Liska
A straightforward synthesis and structure-activity relationship of highly efficient initiators for two-photon polymerization
Macromolecules **46** (2013) 352-361

P. Lorenz, M. Ehrhardt, K. Zimmer
Laser-induced front side etching of fused silica with femtosecond laser using thin metal layers
Appl. Surf. Sci. **278** (2013)

P. Lorenz, M. Ehrhardt, K. Zimmer
Laser-induced front side etching of CaF_2 crystals with KrF excimer laser
Appl. Surf. Sci. **265** (2013)

P. Lorenz, F. Frost, M. Ehrhardt, K. Zimmer
Laser-induced fabrication of randomly distributed nanostructures in fused silica surfaces
Appl. Phys. A **111** (2013) 1025-1030

P. Lorenz, M. Klöppel, F. Frost, M. Ehrhardt, K. Zimmer, P. Li
Laser-induced circular nanostructures in fused silica assisted by a self-assembling chromium layer
Appl. Surf. Sci. **280** (2013)

A. Lotnyk
Analytisches S/TEM am IOM in Leipzig
Elektronenmikroskopie - Mitteilungen der Deutschen Gesellschaft für Elektronenmikroskopie e.V. **36** (2013) 18

H. Lu, E. Thelander, J.W. Gerlach, U. Decker, B. Zhu, B. Rauschenbach
Single pulse laser-induced phase transitions of PLD-deposited $Ge_2Sb_2Te_5$ films
Adv. Funct. Mater. **23** (2013)

Y. Ma, S.G. Mayr
Nanoindentation response of substrate-attached and freestanding single-crystalline Fe_7Pd_3 ferromagnetic shape memory thin films around the martensite transition: The impact of constraints and beyond
Acta Materialia **61** (2013)

S. Mändl, C. Díaz, J.W. Gerlach, J.A. García
Near surface analysis of duplex PIII treated CoCr alloys
Nucl. Instrum. Meth. B **307** (2013) 305-309

D. Manova, C. Günther, A. Bergmann, S. Mändl, H. Neumann, B. Rauschenbach
Influence of temperature on layer growth as measured by in-situ XRD observation of nitriding austenitic stainless steel
Nucl. Instrum. Meth. B **307** (2013) 310-314

G. Mirschel, O. Savchuk, T. Scherzer, B. Genest
Process control of printing processes with in-line NIR spectroscopy and elimi nation of the influence of the substrate on the prediction of the coating weight
Progr. Org. Coat. **76** (2013) 86-93

P. Nalawade, S. Naumov, S. Kapoor
Comparative study of p-amino benzhydrazide and m-amino benzhydrazide by free radicals and free electron transfer
J. Phys. Org. Chem. **26** (2013) 870-878

H. Paetzelt, Th. Arnold, G. Böhm, F. Pietag, A. Schindler
Surface patterning by local plasma jet sacrificial oxidation of silicon
Plasma Process. Polym. **10** (2013) 416-421

S. Perlt, Th. Höche, J. Dadda, E. Müller, B. Rauschenbach
Compositional sensitivity of microstructures and thermoelectric properties of Ag_1-$xPb_{18}Sb_1$-yTe_{20} compounds
J. Electronic Mat. **42** (2013)

B. Rauschenbach, Ch. Grüner
Glanzwinkeldeposition ein materialunabhängiges Verfahren zur Herstellung von Nanostrukturen
Nanotechnologie aktuell **6** (2013) 68-73

B. Rauschenbach
Entwicklungstrends für neuartige funktionelle Oberflächen
Technik in Bayern **5** (2013)

S. Reichelt, C. Abe, S. Hainich, W. Knolle, U. Decker, A. Prager, R. Konieczny
Electron-beam derived polymeric cryogels
Soft Matter **9** (2013) 2484-2492

A. Schulze, M. F. Maitz, R. Zimmermann, B. Marquardt, M. Fischer, C. Werner, M. Went, I. Thomas
Permanent surface modication by electron-beam-induced grafting of hydrophilic polymers to PVDF membranes
Royal Soc.Chem. Adv. **3** (2013) 22518-22526

A. Shalabney, Ch. Khare, B. Rauschenbach, I. Abdulhalim
Metallic nanosculptured thin films for biosensing applications using surface plasmon resonance and enhanced spectroscopies
Proceed. IEEE 2013 (2013)

F. Siewert, J. Buchheim, T. Höft , T. Zeschke, A. Schindler, Th. Arnold
Investigations on the spatial resolution of autocollimator-based slope measuring profilers
Nucl. Instrum. Meth. A **710** (2013) 42-47

M. Sivis, M. Duwe, B. Abel, C. Ropers
Extreme-ultraviolet-light generation in plasmonic nanostructures
Nat. Phys. Doi:10.1038 (2013) 1-6.

S. Starke, M. Went, A. Prager, A. Schulze
A Novel electron beam-based method for the immobilization of trypsin on poly(ethersulfone) and poly(vinylidene fluoride) membranes
React. Funct. Polym. **73** (2013) 698-702

F. Szillat, R. Fechner, S.G. Mayr
Pattern transfer during deposition and fixation of oligomeric bisphenol A on pre-structured copper surfaces
Chem. Phys. **15** (2013) 14017-14025

M. Teichmann, J. Lorbeer, B. Ziberi, F. Frost, B. Rauschenbach
Pattern formation on Ge by low energy ion beam erosion
New J. Phys. **15** (2013) 103029

X. Wang, M. Ehrhardt, P. Lorenz, C. Scheit, S. Ragnow, X. Ni, K. Zimmer
In-process measuring of the electrical shunt resistance of laser-scribed thin-film stacks by nested circular scribes
Rev. Sci. Instrum. **84** (2013)

L. Wennrich, H. Khalil, C. Bundesmann, U. Decker, J.W. Gerlach, U. Helmstedt, D. Manova, S. Naumov, L. Prager
Photochemical preparation of aluminium oxide layers via vacuum ultraviolet irradiation of a polymeric hexanoato aluminium complex
Mater. Chem. Phys. **137** (2013) 1046-1052

J. Zajadacz, P. Lorenz, M. Ehrhardt, K. Zimmer, S. Möllenbeck, K. Dhima, H.C.K. Scheer
Measurement and simulation of the pull-off strength at the separation of miniaturized 3D connectors consisting of silicon masters with undercuts and PDMS replicas
Microelectron. Eng. **101** (2013) 31-36

K. Zimmer, M. Ehrhardt, P. Lorenz, T. Stephan, R. Ebert, A. Braun
Joining of molybdenum thin films with copper printed circuit board by laser micro-riveting
Opt. Laser Technol. **49** (2013) 320-324

M. Zink, F. Szillat, U. Allenstein S.G. Mayr
Interaction of ferromagnetic shape memory alloys and RGD peptides for mechanical coupling to cells: From ab initio calculations to cell studies
Adv. Func. Mat. **23** (2013) 1383-139

Conference Proceedings

2012

Th. Arnold, G. Böhm, H. Paetzelt
Plasma jet machining based process chain for the manufacturing of complex shaped synchrotron mirrors
Paper Nr. P6.05, 12. Euspen International Conference, Stockholm, 04.-08.6. (2012) 71V2

C. Bundesmann, F. Scholze, H. Neumann
Advanced electric propulsion diagnostics
Electronic Journal of the Moscow Aviation Institute 'Trudy MAI' 60 (2012)

M. Burkhardt, R. Fechner, L. Erdmann, F. Frost, R. Steiner, O. Sandfuchs, A. Schindler, A. Gatto, S. Sinzinger
Imaging gratings with modulated blaze - realized by a combination of holography and reactive ion beam etching
Paper Nr. A003, DGaO-Proceedings 2012, Eindhoven, Niederlande, 29.05.-02.06.2012

C. Díaz, J.A. García, S. Mändl, R. Pereiro, B. Fernández
Nanoscale plasma treatment for improvement behavior of F-799 alloys for MoM prosthesis application
Int. Conf. on Nanotechnol. in Medicine, London, U.K., 07.-09.11. (2012)

M. Ehrhardt, P. Lorenz, K. Zimmer
Nanometerpräzises Abformen in Metalloberflächen mit gepulster Laserstrahlung
Proc. 3. Kolloquium “Dünne Schichten in der Optik“, Leipzig, 04.06.09. (2012) 390-394

K. Fischer, M. Müller, J.W. Gerlach, A. Prager, A. Schulze
Photocatalytic membrane for water purification
Euromembrane 2012, London, 23.-27.9. (2012) 1807

K. Fischer, A. Prager, P. Hertel, J. W. Gerlach, A. Schulze
Photocatalytic membrane for water purification
Aachener Membran Kolloqium, Aachen, 7.-8.11. (2012) 368

F. Frost, R. Fechner, J. Lorbeer, M. Teichmann, A. Schindler, R. Steiner, M. Burkhardt, L. Erdmann, T. Gase, T. Glaser, A. Gatto
Mikro- und Nanostrukturierung optischer Oberflächen durch Ionenstrahlprozesse
8. ThGOT Thementage Grenz- und Oberflächentechnik und 3. Optik-Kolloquium „Dünne Schichten in der Optik“, Leipzig, 04.-06.09. (2012) 345 - 349

D. Lellinger, S. Agarwal, T. Scherzer, H. Oehler, I. Alig
Simultaneous recording of conversion and shear modulus
Adhäsion 3/2012 (2012) 48-51

D. Lellinger, S. Agarwal, T. Scherzer, H. Oehler, I. Alig
Simultane Erfassung von Umsatz und Schubmodul
Adhäsion 6/2012 (2012) 38-42

P. Lorenz, M. Ehrhardt, K. Zimmer
Laser-induced front side etching of fused silica with short and ultra-short laser pulses
Paper Nr. 82430Y, SPIE Photonics West, San Francisco, 21.-26.1. (2012) 82430Y

P. Lorenz, M. Ehrhardt, K. Zimmer
Status des laserinduzierten Rückseitenätzens optischer Materialien
8. ThGOT Thementage Grenz- und Oberflächentechnik und 3. Kolloquium „Dünne Schichten in der Optik“, Leipzig, 04.-06.09. (2012) 415-416

P. Lorenz, M. Ehrhardt, K. Zimmer
Laserinduziertes Vorderseitenätzen (LIFE) von Quarzglas
Proc. 3. Kolloquium „Dünne Schichten in der Optik“, Leipzig, 04.-06.09. (2012) 413-414

R. Mehnert, E. Mai, A. Freyer, E. Bilz
Freisetzung von SiO_2-Nanopartikeln aus UV-gehärteten Nanokompositen
Farbe + Lack 118-4 (2012) 31-35

H. Neumann, R. Feder, C. Bundesmann
Thruster relevant material sputter investigations
Electronic Journal of the Moscow Aviation Institute “Trudy MAI” 60 (2012)

G. Raiukaitis, P. Geys, S. Grubinskas, K. Zimmer, M. Ehrhardt, A. Wehrmann, A. Braun
Laser structuring of thin films for flexible CIGS solar cells
Photovoltaics International 17 (2012) 91-98

S. Reichelt, C. Abe, S. Hainich, C. Elsner, W. Knolle
Charakterisierung und Anwendung elektronenstrahlgenerierter poröser Cryogele
8. ThGOT Thementage Grenz- und Oberflächentechnik und, Leipzig, 04.-06.09. (2012) 255

S. Reichelt, C. Abe, A. Prager, R. Konieczny, W. Knolle, U. Decker
Electron-beam derived macroporus polymeric cryogels
IRaP, Krakau, 14.-19.10. (2012) 24

S. Reichelt, C. Elsner
Electron-beam assisted synthesis of polymer based macroporous scaffolds for biotechnological applications
NanoBiomed, Frankfurt, 06.-07.03. (2012) 30

T. Scherzer, O. Savchuk, S. Naumov, W. Knolle, K. Heymann
Self-initiation of photopolymerization reactions using halogenated (meth)acrylates
RadTech Report 26 (2012) 18-26

A. Schulze, A. Boulares-Pender, M. Went, I. Thomas, B. Marquardt, A. Prager
Permanente Hydrophilierung von Polymermembranen mittels Plasma- und Elektronenstrahlbehandlung
13. Wörlitzer Workshop: Membrantechnologien und Modifizierung von Membranen, Wörlitz, 04.07. (2012)

A. Schulze, A. Boulares-Pender, M. Went, I. Thomas, B. Marquardt, A. Prager
Membrane hydrophilization using electron beam and plasma techniques
Paper Nr. P013, 11th World Filtration Congress, Graz, Österreich, 16.-20.04. (2012)

A. Schulze, B. Marquardt, M. Went, A. Prager
Elektronenstrahlmodifizierung von Polymermembranen
20. NDVaK, Dreden, 25.-26.10. (2012) 35

A. Schulze, S. Starke, A. Prager, M. Went
A novel electron beam-based method for the immobilization of trypsin on polymer membranes
14. Aachener Membrankolloquium, Aachen, Germany, 07.-08.11. (2012) 532

A. Schulze, S. Starke, A. Prager, M. Went
Immobilization of trypsin on polymer membranes via electron beam irradiation
Paper Nr. P2.153, Euromembrane 2012, London, UK, 23.-27.09. (2012)

M. Sivis, M. Duwe, Y. Liu, K. Siefermann, B. Abel, C. Ropers
High Intensity Lasers and High Field Phenomena
Atomic and Molecular Physics, Berlin, 12.03. (2012)

2013

Th. Arnold, G. Böhm, H. Paetzelt
Plasma jet polishing of rough fused silica surfaces
13. Euspen International Conference, Stockholm, Conf. Proceed. V2 (2013) 19-22

C. Díaz, S. Mändl, J.A. García, R. Rodríguez
Biotribology analysis of a surface modified CoCr alloy for use in metal-on-metal hip prosthesis
VII Iberian Conference on Tribology, Porto, Portugal, 20.-21.06. (2013)

C. Eichhorn, F. Scholze, C. Bundesmann, H. Neumann
Plasmadiagnostics in the plume of a radiofrequency ion thruster
Paper Nr. IEPC-2013-295, 33. International Electric Propulsion Conference, Washington, DC, 06.-10.10. (2013)

K. Fischer, M. Müller, J. Gerlach, A. Schulze
Photocatalytic mixed matrix membrane for water purification
3. International Conference on Multifunctional, Hybrid and Nanomaterials, Sorrento, 03.-07.03. (2013)

K. Fischer, D. Meinhard, R. Gläser, A. Schulze
Nanoporous photocatalytic TiO_2 PES mixed matrix membrane for water purification
11. International Conference on Materials Chemistry, University of Warwick, 08.-11.06. (2013)

P. Lorenz, M Klöppel, F. Frost, M. Ehrhardt, P. Li, K. Zimmer
Nanostructuring of fused silica surfaces induced by KrF excimer laser radiation: Experiment and theory
NSTI - Nanotech 1 (2013)

A. Lotnyk, D. Poppitz, J. Gerlach, B. Rauschenbach
Low-energy Ar+-polishing of FIB prepared GaN-SiC interfaces for Cs-corrected STEM
MC 2013 Proceedings, Eed. R. Rachel, Regensburg, Germany, 25.-30.08 (2013) 305-306

D. Poppitz, A. Lotnyk, J. Gerlach, B. Rauschenbach
Microstructure investigation of porous gallium-nitride thin films
MC 2013 Proceedings, Ed. R. Rachel, Regensburg, Germany, 25.-30.08 (2013) 617-618

B. Rauschenbach, Ch. Grüner, Ch. Khare
Ion beam sputtering induced nano-scluptured thin films
Proceed. XXI. Intern. Conference “Ion-Surfce Interaction”, Jaroslavel, 22.-26.08. (2013) 233-238

B. Rauschenbach
Preparation of ion beam induced nanostructures on surface
3. Int. Conf. Nanomaterials: Applications and Properties, Vol. 2, no. 1, pp. 01001, Alushta, 16.-21.09 (2013)

S. Reichelt, S. Oehmichen, F. Lohmann, J. Becher, J. Weisser, M. Schnabelrauch, W. Knolle
Elektronenstrahl-induzierte Synthese von makroporösen Cryogelen für biotechnologische Anwendungen
Beschichtungungen für Biotechnologie und Medizintechnik, Dresden, 14.-17.10. (2013) 49

S. Reichelt, C. Abe, S. Oehmichen, W. Knolle, A. Prager, M. Schnabelrauch, J. Becher, S. Möller, A. Berg, J. Weisser
Tailor made electron-beam generated polymeric cryogels and their biotechnological application
International Meeting on Radiation Processing, Shanghai, 04.-08.11. (2013) 74

S. Reichelt, S. Oehmichen, F. Lohmann, J. Becher, J. Weisser, M. Schnabelrauch, W. Knolle
Biokompatible makroporöse Cryogele: Synthese, Charakterisierung und Anwendungen
9. Thüringer Biomaterial-Kolloquium, Zeulenroda, 03.-05.09 (2013) 348-352

S. Reichelt, C. Abe, M. Kühnert, C. Elsner
Electron-beam-derived polymeric macrporous scaffolds for biotechnological applications
Paper Nr. A3.13.3, 3. International Conference on Multifunctional, Hydbrid and Nanomaterials, Sorrento, Italien, 03.-07.03. (2013)

U. Roß, A. Lotnyk, E. Thelander, B. Rauschenbach
Characterization of laser-deposited Ge-Sb-Te thin films by Cs corrected STEM
MC 2013 Proceedings, Ed. R. Rachel, Regensburg, Germany, 25.-30.08 (2013) 435-436

T. Scherzer, G. Mirschel, O. Daikos, K. Heymann, B. Genest, C. Sommerer, C. Steckert
In-line monitoring of the conversion in an offset printing press
Proc. RadTech Europe 2013, Basel, 15.-17.10. (2013)

A. Schulze, A. Stoelzer, S. Starke, I. Thomas, M. Went
Self-cleaning polymer membrane surfaces
Paper Nr. C2.5.2, 3. International Conference on Multifunctional, Hydbrid and Nanomaterials, Sorrento, Italien, 03.-07.03. (2013)

A. Schulze, S. Starke, M. Went, A. Prager
Enzyme immobilization on polymer membranes by electron beam irradiation
Polym. Adv. Technol. 24 (S1) (2013)

A. Shavorskiy, A. Cordones, J. Vura-Weis, K. Siefermann, D. Slaughter, F. Sturm, F. Weise, H. Bluhm, M. Strader, H. Cho, M. Fu, C. Bacellar, C. Khurmi, M. Hertlein, J. Guo, T. Tyliszczak, D. Prendergast, G. Coslovich, J. Robinson, R. Kaindl, R. Schoe
Time-resolved x-ray photoelectron spectroscopy techniques for real-time studies of interfacial charge transfer dynamics
22. International Conference Application of Accelerators in Research and Industry, Ft. Worth, TX, USA , 05.-10.08. (2013) 475-479

M. Tromayer, Z. Li, J. Torgersen, A. Ajami, A. Rosspeintner, S. Naumov, T. Scherzer, J. Stampfl, R. Liska
Novel highly efficient initiators for two-photon induced photopolymerization
Proc. RadTech Europe, Basel, 15.-17.10. (2013)

Presentations

Talks

2012

U. Allenstein, Y. Ma, A. Arabi-Hashemi, S.G. Mayr, M. Zink
Biocompatibility of $Fe_{70}Pd_{30}$ ferromagnetic shape memory films for cell actuation
Frühjahrstagung der DPG, Berlin, 25.-30.03.2012

A. Arabi-Hashemi, M. Müller, T. Edler, A. Jakob, Y. Ma, L. Kühnemund, I. Claussen, A. Graumann, U. Allenstein, M. Zink, S.G. Mayr
Miniaturized ferromagnetic shape memory alloys - fundamentals, applications and challenges
Joint Colloquium of the Materials Science and Metallurgy/ Department of Engineering, University of Cambridge, Cambridge, UK, 11.9.2012

Th. Arnold, G. Böhm, M. Janietz, I.M. Eichentopf, H. Paetzelt, A. Schindler
Precision machining of optical surfaces with plasma jet tools in IOM Leipzig
Workshop on the Future of Particle and Energy Beam Processes in Europe, Cranfield, GB, 29.08.2012

Th. Arnold, G. Böhm, A. Schindler
Ultra-precision technology in IOM
Workshop on the Future of Particle and Energy Beam Processes in Europe, Cranfield, GB, 29.08.2012

Th. Arnold, G. Böhm, M. Janietz, I.M. Eichentopf, H. Paetzelt, A. Schindler
Plasma Jet Machining-Ultrapräzisions-Formgebung von Oberflächen
8. ThGOT Thementage Grenz- und Oberflächentechnik und 3. Optik-Kolloquium „Dünne Schichten in der Optik“, Leipzig, 04.-06.09.2012

J. Bauer, C. Grüner, B. Rauschenbach
Nanostrukturierte Dünnschichten mittels Glanzwinkeldeposition - Grundlagen und Anwendungen
XIX. Erfahrungsaustausch „Oberflächentechnologie mit Plasma- und Ionenstrahlprozessen“, Mühlleithen, 06.-08.03.2012

F. Bauer, U. Decker, C. Riedel
Improved properties of acrylate-based nanocomposites by 172 nm irradiation
2. IAEA RCM Meeting on Nanocomposites, Kairo, Ägypten, 26.-30.11.2012

G. Böhm, Th. Arnold, H. Paetzelt, F. Pietag, M. Volkmer, A. Schindler
Nanometer figure error correction
Optonet Workshop, Jena, 26.-27.09.2012

T. Böntgen, J. Lorbeer, F. Frost, M. Teichmann, R. Schmidt-Grund, M. Lorenz, M. Grundmann
Optische Untersuchung strukturierter Oberflächen
8. ThGOT Thementage Grenz- und Oberflächentechnik und 3. Optik-Kolloquium „Dünne Schichten in der Optik“, Leipzig, 04.-06.09.2012

T. Böntgen, J. Lorbeer, F. Frost, M. Teichmann, R. Schmidt-Grund, M. Lorenz, M. Grundmann
Ellipsometric study of nano patterned surfaces for structural investigation
7. Workshop Ellipsometry, Leipzig, 05.-07.03.2012

C. Bundesmann, R. Feder, F. Frost, F. Scholze, H. Neumann
Influence of process parameters on properties of Si thin films grown by Ar ion beam sputtering
Frühjahrstagung der DPG, Berlin, 25.-30.03.2012

C. Bundesmann, M. Tartz, F. Scholze, H.J. Leiter, F. Scortecci, D. Feili, R.Y. Gnizdor, H. Neumann
Advanced electric propulsion diagnostics
4. Russian-German Conference on Electric Propulsion and Their Application, Moskau, 25.-29.06.2012

C. Bundesmann, F. Scholze, H.J. Leiter, H. Neumann
In-situ EP thruster characterization with a thermocamera
Space Propulsion, Bordeaux, 07.-10.05.2012

M. Burkhardt, R. Fechner, L. Erdmann, F. Frost, R. Steiner, O. Sandfuchs, A. Schindler, A. Gatto, S. Sinzinger
Imaging gratings with modulated blaze realized by a combination of holography and reactive ion beam etching
113. Jahrestagung der DGaO, Eindhoven, Niederlande, 29.05.-02.06.2012

C. Chmelik, D. Enke, R. Gläser, J. Kärger, J. Kullmann, T. Titze, J. Weitkamp, L. Prager
The potentials of IR micro-imaging for in-situ studies of chemical reactions in nanoporous catalysts
45. Jahrestreffen Deutscher Katalytiker, Weimar, 14.-16.03.2012

C. Díaz, J.A. García, R. Pereiro, B. Fernández, S. Mändl, D. Manova, R.J. Rodríguez
Plasma immersion ion implantation for reducing metal ion release
19. Int. Conf. on Ion Implantation Technology, Valladolid, Spain, 25.-29.06.2012

C. Díaz, J.A. García, R. Periero, B. Fernandéz, S. Mändl, D. Manova, J.R. Rodrígues
Plasma immersion ion implantation for reducing metal ion release
19. Int. Conf. on Ion Implantation Technology, Valladolid, Spain, 25.-29.6.2012

T. Edler, S.G. Mayr
Fe-Pd ferromagnetic shape memory alloys
Preisträgervortrag anlässlich der Verleihung des Peter-Haasen-Preises, Göttingen, 23.01.2012

T. Edler, A. Jakob, Y. Ma, A. Arabi-Hashemi, M. Müller, L. Kühnemund, I. Claussen, A. Graumann, U. Allenstein, M. Zink, S.G. Mayr
Fe-Pd ferromagnetic shape memory membranes for biomedical applications - fundamentals, applications, challenges
Annual Meeting of the German Biophysical Society, Göttingen, 23-26.09.2012

M. Ehrhardt, P. Lorenz, K. Zimmer
Nanometerpräzises Abformen in Metalloberflächen mit gepulster Laserstrahlung
8. ThGOT Thementage Grenz- und Oberflächentechnik und 3. Optik-Kolloquium „Dünne Schichten in der Optik“, Leipzig, 04.-06.09.2012

M. Ehrhardt, P. Lorenz, F. Frost, K. Zimmer
Laser embossing of micro-and submicrometer surface structures in copper
LANE 2012, 7th International Conference and Exhibition, Fürth, 12.-15.10.2012

I.-M. Eichentopf, Th. Arnold
Untersuchung von Oberflächenprozessen bei der Plasmajetbearbeitung von Siliziumkarbid
Frühjahrstagung der DPG, Stuttgart, 12.-16.03.2012

C. Eichhorn, R. Feder, F. Scholze, C. Bundesmann, H. Neumann
Eine neue Diagnostikmethode auf der AEPD-Plattform
5. Deutscher Electric Propulsion Workshop, Göttingen, 06.-07.2012

M. Engler, S. Müller, F. Frost, R. Feder, D. Speemann, T. Michely
Silicide induced ion beam patterning of silicon(001)
19. International Workshop on Inelastic Ion-Surface Collisions, Frauenchiemsee, 16.-21.09.2012

R. Feder, C. Eichhorn, F. Scholze, C. Bundesmann, H. Neumann
Untersuchung zu Sputterprozessen - Nutzung für Thruster-Spacecraft Interaction
5. Deutscher Electric Propulsion Workshop, Göttingen, 06.-07.11.2012

R. Feder, F. Scholze, F. Frost, H. Neumann, C. Bundesmann
Systematic investigation of
ion beam sputtering of Si: First experimental and simulation results
XIX. Erfahrungsaustausch Oberflächentechnologie mit Plasma- und Ionenstrahlprozessen, Mühlleithen, 06.-08.03.2012

T. Fischer, L. Prager, J. Hohage, H. Ruelke, S. E. Schulz, R. Richter, T. Gessner
A two-step UV curing process for producing high tensile stressed silicon nitride layers
MRS Spring Meeting & Exhibition, San Francisco, 09.-13.04.2012

K. Fischer, S.G. Mayr
In-plane mechanical response of TiO_2 nanotube arrays - intrinsic properties and impact of adsorbates for sensor applications
MRS, Fall Meeting, Boston, 26.11.2012

F. Frost, R. Fechner, J. Lorbeer, M. Teichmann, A. Schindler, R. Steiner, M. Burkhardt, L. Erdmann, T. Gase, T. Glaser, A. Gatto
Mikro- und Nanostrukturierung optischer Oberflächen durch Ionenstrahlprozesse
8. ThGOT Thementage Grenz- und Oberflächentechnik und 3. Optik-Kolloquium „Dünne Schichten in der Optik“, Leipzig, 04.-06.09.2012

F. Frost
Mikro- und Nanostrukturierung sowie Oberflächenglättung mit Ionenstrahlen
CC-UPOB-Workshop, Leipzig, 02.02.2012

F. Frost, R. Fechner, A. Schindler
Reaktives Ionenstrahlätzen (RIBE) von strukturierten Oberflächen für die Optik
XIX. Erfahrungsaustausch Oberflächentechnologie mit Plasma- und Ionenstrahlprozessen, Mühlleithen, 06.-08.03.2012

F. Frost
Der Energieumsatz beim Menschen
XIX. Erfahrungsaustausch Oberflächentechnologie mit Plasma- und Ionenstrahlprozessen, Mühlleithen, 06.-08.03.2012

F. Frost
Surface engineering with ion beams: From self-organized nanostructures to ultra-smooth surfaces
1. Workshop Leibniz Nano, Berlin, 30.-.31.01.2012

J.W. Gerlach, L. Neumann, Th. Höche, B. Rauschenbach
Ion-beam assisted epitaxy of ultrathin GaN films: in situ and ex situ structural characterization
18. Int. Conf. on Ion Beam Modifications of Materials (IBMM), Qingdao, China, 02.-07.09.2012

J.W. Gerlach
Two different low-energy ion beam based approaches for the synthesis of epitaxial gallium nitride films
Institute seminar, Institute of Physical Engineering, Brno University of Technology, Brno, Tschechien, 05.12.2012

J.W. Gerlach
Zu ultradünnen Metallnitrid-Schichten durch Anwendung ionenstrahlbasierter Epitaxietechniken
Forschungsseminar der Arbeitsgruppe „Physik der Grenzflächen und dünnen Schichten“ der Humboldt-Universität zu Berlin, Berlin, 08.02.2012

A. Graumann, S.G. Mayr
Magnetic force microscopy on single crystalline $Fe_{70}Pd_{30}$ ferromagnetic shape memory films
Frühjahrstagung der DPG, Berlin, 25.-30.3.2012

U. Helmstedt, M. Naumann, Y. Bohne, A. Freyer, W. Berthold, B. Rauschenbach
Direct laser ablation of polymers for a new rotogravure printing technology
ILaCoS 2012 International Laser and Coating Symposium, Dresden, 17.-18.10.2012

H. Hildebrand, K. Franke, A. Freyer, E. Bilz, R. Mehnert, E. Mai, C. Isaacson, K. Schirmer, A. Ammann, L. Sigg
Investigation of the life cycle of nanoparticles be means of $[^{44,45}Ti]TiO_2$ and $[^{110m}Ag]Ag^0$ research project NanoTrack
Int. Conf. on Safe Production and Use of Nanomaterials, Nanosafe 2012, Minatec, Grenoble, France, 13.-15.11.2012

A.M. Jakob, Y. Ma, F. Szillat, J. Buchwald, A. Arabi-Hashemi, M. Hennes, A. Graumann, M. Müller, S. Huth, E. Lissek, M. Bulst, M. Fuchs, U. Allenstein, S.G. Mayr
New functional materials for biomedical applications
Fakultät für Biowissenschaften, Pharmazie und Psychologie, University of Leipzig, Leipzig, 10.06.2012

A.M. Jakob, S.G. Mayr
Nano mechanical surface properties of the ferromagnetic shape memory alloy Ni-Mn-Ga
Frühjahrstagung der DPG, Berlin, 25.-30.03.2012

A.M. Jakob, B. Rauschenbach, S.G. Mayr
Contact resonance atomic force microsc: Nanometerresolved mechanical surface properties of Ni-Mn-Ga single crystal films
Materials Science and Engineering (DGM), Darmstadt, 25.-27.09.2012

A.M. Jakob, S.G. Mayr
Nanometer-resolved mechanical surface properties of single crystalline martensitic Ni-Mn-Ga ferromagnetic shape memory alloy thin films
MRS, Fall Meeting, Boston, 29.12.2012

A.M. Jakob, S.G. Mayr
Probing nanomechanics with contact-resonance atomic force microscopy - Fundamentals, applications and challenges
MRS, Fall Meeting, Boston, 28.11.2012

B. Khanbabaee, A. Biermanns, M. Cornejo, D. Hirsch, F. Frost, U. Pietsch
Investigation of the Fe incorporation in ion-beam induced patterning on Si (100)
Frühjahrstagung der DPG, Berlin, 25.-30.03.2012

M. Krause, T. Höche, M. Naumann
Structural damage imposed by laser machining
ILaCoS 2012 International Laser and Coating Symposium, Dresden, 17.-18.10.2012

P. Lorenz, M. Ehrhardt, K. Zimmer
Laser-induced front side etching: An easy and fast method for sub-¼m structuring of dielectrics
LANE 2012, 7. Int. Conf. & Exhibition, 12.-15.10.2012

P. Lorenz, M. Ehrhardt, K. Zimmer
Structuring of dielectrics by laser-induced front and back side etching: A review
ALT, Thun, 02.-06.09.2012

P. Lorenz, D. Spemann, M. Ehrhardt, K. Zimmer
Laser-induced front side etching (LIFE) of crystalline silica
Frühjahrstagung der DPG, Stuttgart, 12.-16.3.2012

P. Lorenz, M. Ehrhardt, A. Wehrmann, K. Zimmer
Laser-induced front side etching of commercial glasses with short and ultra-short laser pulses
SPIE Photonic West, San Francisco, 21.-26.1.2012

Y. Ma, A. Setzer, J.W. Gerlach, F. Frost, P. Esquinazi, S.G. Mayr
Freestanding single crystalline Fe-Pd ferromagnetic shape memory membranes: Structural, morphological and magnetic characterization
Frühjahrstagung der DPG, Berlin, 25.-30.03.2012

Y. Ma, S.G. Mayr
Miniaturization of Fe-Pd based ferromagnetic shape memory alloys - role of surfaces, dimensionality and constraints
MRS, Fall Meeting, Boston, 27.11.2012

S. Mändl
Surface modification by plasma focus device
XIX. Erfahrungsaustausch Oberflächentechnologie mit Plasmaprozessen, Mühlleithen, 06.-08.03.2012

D. Manova, C. Günter, S. Mändl, H. Neumann, B. Rauschenbach
Formation and stability of expanded austenite
XIX. Erfahrungsaustausch Oberflächentechnologie mit Plasma- und Ionenstrahlprozessen, Mühlleithen, 06.-08.03.2012

D. Manova, C. Günther, A. Bergman, S. Mändl, H. Neumann, B. Rauschenbach
In-situ observation of layer growth during low energy nitriding of austenitic stainless steel
14. Int. Conf. on Plasma Surface Engineering, Garmisch-Partenkirchen, Germany, 15.-19.09.2012

S.G. Mayr
Ferromagnetic shape memory alloys - fundamentals, synthesis, challenges
TU Chemnitz, Abteilungskolloquium, Chemnitz, 28.10.2012

S.G. Mayr, M. Zink, A. Reichenbach, V. Dallacasagrande, J. Käs
TiO_2 nanotube arrays as substrates for neuronal tissue
RWTH Aachen, Aachen, 26.06.2012

A. Miessler, Th. Arnold
Pattern transfer on fused silica samples using sub-aperture Reactive Ion Beam Etching
Frühjahrstagung der DPG, Berlin, 25.-30.03.2012

A. Miessler, Th. Arnold
Oberflächenbearbeitung durch reaktive Ionenstrahlen
XIX. Erfahrungsaustausch Oberflächentechnologie mit Plasma- und Ionenstrahlprozessen, Mühlleithen, 6.-8.03.2012

S. Müller, M. Engler, F. Frost, T. Michely
Is silicide formation the decisive factor in impurity induced ion beam pattern formation?
Frühjahrstagung der DPG, Berlin, 25.-30.03.2012

S. Naumov, T. Scherzer, W. Knolle, O. Savchuk
Quantum chemical modeling of the primary processes by radiation-induced polymerisation
4. Asia-Pacific Symposium on Radiation Chemistry (APSRC-12), Huangshan, China, 30.10.-04.11.2012

H. Neumann, R. Feder, C. Bundesmann
Thruster relevant material sputter investigations
IV. Russian-German Conference “Electric Propulsion”, Moskau, 25.-30.06.2012

L. Neumann, J.W. Gerlach, B. Rauschenbach
Growth study: ultrathin GaN films on 6H-SiC(0001)
Frühjahrstagung der DPG, Berlin, 25.-30.03.2012

L. Prager, W. Knolle, S. Naumov, L. Wennrich, F. Kita, R. Grottenmüller
Photo-induced conversion of silazanes into Si-O-Si-(R) networks
European Symposium of Photopolymer Science, Torino, Italien, 4.-7.09.2012

B. Rauschenbach
Sculptured thin films by glancing-angle ion beam deposition
Physikalisches Kolloquium, MPI Greifswald, 14.06.2012

B. Rauschenbach
Sputter induced glancing angle deposition
Colloquium, Israel Institute of Technology, Technion, Haifa/Israel, 21.02.2012

S. Reichelt, C. Abe, U. Decker, C. Elsner
Elektronenstrahlinduzierte Synthese makroporöser Cryogele
Abteilungskolloquium bei Innovent, Jena, 22.06.2012

S. Reichelt, C. Abe, U. Decker, W. Knolle, C. Elsner
Electron-beam-assisted synthesis of polymer based macroporous scaffolds for biotechnological applications
Nanobiomed 2012, Frankfurt Dechema, 06.-07.03.2012

S. Reichelt, C. Abe, S. Hainich, C. Elsner,W. Knolle, U. Decker, A. Prager
Electron-beam derived macroporous polymeric cryogels
10. Meeting of the ionizing radiation and polymers symposium, Krakau, 14.-19.10.2012

S. Reichelt, C. Abe, S. Hainich, W. Knolle, U. Decker, C. Elsner
Charakterisierung und Anwendung elektronenstrahlgenerierter poröser Cryogele
8. ThGOT Thementage Grenz- und Oberflächentechnik und 3. Optik-Kolloquium „Dünne Schichten in der Optik“, Leipzig, 04.-06.09.2012

T. Scherzer, S. Naumov, O. Savchuk, W. Knolle, K. Heymann
Halogenated (meth)acrylates as initiators for photopolymerization reactions
European Symposium of Photopolymer Science, Torino, Italien, 04.-07.9.2012

A. Schindler
Ultra-precision surface processing using ion beams and plasma jets
6. Sino-German Symposium on Micro- and Nano-Production, Measurement and Application, Braunschweig, 12.-14.09.2012

A. Schindler
Tutorial recent advances in ion beam and plasma jet processing
Imaging and Applied Optics Congress, OSA, Monterey Plaza Hotel, Monterey, California, USA, 24.-28.06.2012

A. Schindler
Aktuelle FuE-Arbeiten zur Ionenstrahl-Präzisionsbearbeitung und neue Anwendungen der Atmosphären-Plasmajet-Technik
CC-UPOB-Workshop, Leipzig, 02.02.2012

F. Scholze, T. Kauerhoff, H.J. Leiter, H. Neumann
Useful AEPD applications - example RIT-¼X breadboard
Space Propulsion 2012, Bordeaux, 07.-10.05.2012

F. Scholze, T.Kauerhoff, H. Leiter, H. Neumann
Charakterisierung eines Ionentriebwerkes vom Typ RIT-¼X
XIX. Erfahrungsaustausch Oberflächentechnologie mit Plasma- und Ionenstrahlprozessen, Mühlleithen, 06.-08.03.2012

F. Scholze, M. Tartz, H. Leiter, E. Hartmann, H. Neumann
Gridded thruster dynamic lifetime modelling
4. Russian-German Conference on Electric Propulsion and their Application, Moskau, 25.-29.06.2012

F. Scholze, H. Neumann
Gridded thruster dynamic life time modelling
IV. Russian-German Conference “Electric Propulsion”, Moskau, 25.-30.06.2012

A. Schulze, A. Boulares-Pender, M. Went, I. Thomas, B. Marquardt, A. Prager
Membrane hydrophilization using electron beam and plasma techniques
11. World Filtration Congress, Graz, Österreich, 16.-20.04.2012

A. Schulze, A. Boulares-Pender, M. Went, I. Thomas, B. Marquardt, A. Prager
Permanente Hydrophilierung von Polymermembranen mittels Plasma- und Elektronen-strahlbehandlung
13. Wörlitzer Workshop: Membrantechnologien und Modifizierung von Membranen, Wörlitz, 04.07.2012

A. Schulze, B. Marquardt, M. Went, A. Prager
Elektronenstrahlmodifizierung von Polymermembranen
20. NDVaK, Dresden, 25.-26.10.2012

M. Teichmann, J. Lorbeer, M. Cornejo, F. Frost, B. Rauschenbach
Ionenstrahl-induzierte Musterbildung auf Si mit und ohne simultane Fe-Kodeposition
XIX. Erfahrungsaustausch Oberflächentechnologie mit Plasma- und Ionenstrahlprozessen, Mühlleithen, 06.-08.03.2012

K. Zimmer, M. Ehrhardt, R. Böhme, P. Lorenz
Precise processing of optical surfaces by pulsed laser radiation
CC-UPOB-Workshop, Leipzig, 02.02.2012

K. Zimmer
Mikro-, Nano- und Laserstrukturierung am IOM
Kolloquium des Lehrstuhls für Laseranwendungstechnik an der Ruhr-Universität Bochum, Bochum, 22.02.2012

M. Zink, V. Dallacasagrande, S. Huth, A.M. Jakob, M. Müller, A. Reichenbach, J. Käs, S.G. Mayr
Longterm organotypic culture of adult neuronal tissue
Gruppenseminar Neuroanatomie, Universität Leipzig, Leipzig, 07.02.2012

M. Zink, Y. Ma, U. Allenstein, S.G. Mayr
Fe-Pd based ferromagnetic shape memory alloy membranes as sensors and actuators in biomedical applications - fundamentals, applications and challenges
MRS, Fall Meeting, Boston, 29.11.2012

2013

A. Arabi-Hashemi, S.G. Mayr
Ion-irradiation-assisted phase selection in single crystalline Fe_7Pd_3 ferromagnetic shape memory alloy thin films: From fcc to bcc along the Nishiyama-Wassermann path
6. BuildMoNa Workshop for doctoral candidates, Leipzig, 04.-05.03.2013

A. Arabi-Hashemi, S.G. Mayr
Ion-irradiation-assisted phase selection in single crystalline Fe_7Pd_3 ferromagnetic shape memory alloy thin films: From fcc to bcc along the Nishiyama-Wassermann path
2013 MRS Spring Meeting & Exhibit, San Francisco, California, USA, 01.-05.04.2013

A. Arabi-Hashemi, S.G. Mayr
Ion-irradiation-assisted phase selection in single crystalline Fe_7Pd_3 ferromagnetic shape memory alloy thin films: From fcc to bcc along the Nishiyama-Wassermann path
Frühjahrstagung der DPG, Regensburg, Germany, 11.-15.03.2013

A. Arabi-Hashemi, S.G. Mayr
Ion assisted tuning of ferromagnetic shape memory alloys for biomedical applications
Workshop „Ionenstrahlen in Forschung und Anwendung“, Leipzig, 12.-14.06.2013

A. Arabi-Hashemi, S.G. Mayr
On-irradiation driven Fe-Pd based ferromagnetic shape memory alloys - tuning phase along the Nishiyama-Wassermann path
MRS, Fall Meeting, Boston, MA, USA, 01.-06.12.2013

Th. Arnold. G. Böhm, H. Paetzelt
Plasma Jet Machining-Ultrapräzisions-Oberflächenbearbeitung mit reaktiven Plasmajets
16. Fachtagung für Plasmatechnolgie, Greifswald, 18.-20.02.2013

Th. Arnold. G. Böhm, H. Paetzelt
Ultrapräzisions-Oberflächenbearbeitung mit Plasma Jet Machining
6. Optikseminar, Deggendorf, 12.-13.03.2013

Th. Arnold, G. Böhm, H. Paetzelt
Plasma jet polishing of rough fused silica surfaces
Euspen International Conference, Berlin, 27.-31.05.2013

Th. Arnold, G. Böhm, H. Paetzelt
Atmospheric plasma jet treatment of optical surfaces
3. EOS Conference on Manufacturing of Optical Components, München, 13.-15.05.2013

Th. Arnold, F. Pietag, A. Nickel
Correction of precision optics using low-energy ion beams - Si sphere machining
Workshop „Ionenstrahlen in Forschung und Anwendung“, Leipzig, 12.-14.06.2013

G. Böhm, H. Paetzelt, Th. Arnold, P. Lorenz, M. Ehrhardt, K. Zimmer
Laser and plasma processing for direct writing of high quality optical surfaces
3. EOS Conference on Manufacturing of Optical Components (EOSMOC 2013), International Congress Centre Munich (ICM), Munich, Germany, 13.05.2013

C. Bundesmann, R. Feder, H. Neumann
Ion beam deposition of Ag films: Influence of process parameters on optical and electrical film properties
XX. Erfahrungsaustausch Oberflächentechnologie mit Plasma- und Ionenstrahlprozessen, Mühlleithen, 05.-08.03. 2013

C. Bundesmann, R. Feder, H. Neumann
Tailoring of thin film properties by (dual) ion beam sputter deposition
Workshop „Ionenstrahlen in Forschung und Anwendung“, Leipzig, 12.-14.06.2013

C. Bundesmann, F. Scholze, R. Feder, H. Neumann
Ion beam sputtering: Principle, instrumentation, applications
Kolloquium Abteilung Halbleiterphysik, Universität Leipzig, Leipzig, 11.12.2013

C. Bundesmann, F. Scholze, C. Eichhorn, R. Feder, H. Neumann
In-situ diagnostics of ion beam sources for terrestrial and space applications
Plasma Germany, Herbstsitzung, Leipzig, 11.-12.11.2013

C. Díaz, S. Mändl, J.A. García, R. Rodríguez
Biotribology analysis of a surface modified CoCr alloy for use in metal-on-metal hip prosthesis
VII. Iberian Conference on Tribology, Porto, Portugal, 20.-21.06.2013

C. Díaz, J.W. Gerlach, S. Mändl, J.A. García
Reduction of corrosion current of CoCr alloys by post-PIII oxidation
12. Int. Workshop on Plasma Based Ion Implantation & Deposition, Poitiers, Frankreich, 01.-05.07.2013

M. Ehrhardt, P. Lorenz, A. Wehrmann, C. Scheit, X. Wang, S. Ragnow, A. Braun, K. Zimmer
Scribing of CIGS thin films for solar module fabrication by external integrated interconnection
Photonic West, San Francisco, 02.-07.02.2013

M. Ehrhardt, P. Lorenz, J. Zajadacz, F. Frost, R. Fechner, K. Zimmer
Fabrication of grating structures into copper surfaces by laser embossing
3. EOS Conference on Manufacturing of Optical Components (EOSMOC 2013), International Congress Centre Munich (ICM), Munich, Germany, 13.05.2013

C. Eichhorn, F. Scholze, C. Bundesmann, H. Neumann
Plasmadiagnostics in the plume of a radiofrequency ion thruster
33. International Electric Propulsion Conference, Washington, DC, 06.-10.10.2013

C. Elsner
Nichtkonventionelle Synthese poröser, monolithischer Chromatographiephasen und deren Modifizierung
6. Workshop „Gut getrennt?“ HPLC in Theorie und Praxis, Dresden-Rossendorf, 26.03.2013

C. Elsner, B. Abel
Hochauflösende bildgebende MALDI-TOF-Massenspektrometrie zur topologischen und chemischen Analytik von Fingerabdruckspuren
EFDS-Workshop „Analyse von Spurenverunreinigungen auf Oberflächen und in Gasen“, Dresden, 03.12.2013

M. Engler, S. Müller, M. Will, F. Frost, R. Feder, D. Spemann, R. Hübner, S.Facsko, T. Michely
Is silicide formation the decisive factor in impurity induced ion beam pattern formation?
International Symposium on Nanoscale Pattern Formation at Surfaces, Copenhagen, Dänemark, 26.-30.05.2013

R. Feder, H. Neumann, C. Bundesmann, B. Rauschenbach
Ion beam sputtering of Ag: Influence of process parameters on secondary particle properties
Workshop on Particle - Surface Interactions (PASI 2013), Luxenburg, 03.-05.06.2013

R. Feder, H. Neumann, C. Bundesmann, B. Rauschenbach
Ion beam sputtering of Ag and Ge: properties of sputtered and scattered particles
Workshop „Ionenstrahlen in Forschung und Anwendung“, Leipzig, 12.-14.06.2013

R. Feder, H. Neumann, C. Bundesmann
Ion beam sputtering of Ag: Properties of sputtered and scattered particles
XX. Erfahrungsaustausch Oberflächentechnologie mit Plasma- und Ionenstrahlprozessen, Mühlleithen, 05.-08.03.2013

R. Feder, F. Frost, H. Neumann, C. Bundesmann, B. Rauschenbach
Systematic investigations of low energy Ar ion beam sputtering of Ag
Frühjahrstagung der DPG, Regensburg, 10.-15.03.2013

K. Fischer, D. Meinhard, R. Gläser, A. Schulze
Nanoporous photocatalytic TiO_2 PES mixed matrix membrane for water purification
11. International Conference on Materials Chemistry, University of Warwick, 08.-11.06.2013

R. Flyunt, W. Knolle, A. Prager, B. Abel
Efficient reduction of graphene oxide in aqueous dispersions by means of EB- or UV-irradiation
Symposium in Memory of Klaus-Dieter Asmus, Poznan, Poland, 22.03.2013

F. Frost, R. Fechner, M. Emmrich, A. Schindler
Reaktives Ionenstrahlätzen (RIBE) von mikrooptischen Oberflächen: Fortschrittsbericht
XX. Erfahrungsaustausch Oberflächentechnologie mit Plasma- und Ionenstrahlprozessen, Mühlleithen, 05.-08.03.2013

F. Frost, R. Fechner, J. Lorbeer, M. Teichmann, A. Schindler
Ionengestützte Strukturierung optischer Oberflächen mit Sub-Nanometer-Präzision
Plasma Germany, Leipzig, 11.-12.11.2013

J.W. Gerlach, Th. Höche, D. Hirsch, B. Rauschenbach
Structural characterization of thin epitaxial GaN films prepared by low-energy ion-beam nitridation of Ga droplets
21. Jahrestagung der Deutschen Gesellschaft für Kristallographie (DGK), Freiberg (Sachsen), 19.-22.03. 013

J.W. Gerlach, L. Neumann, Th. Höche, B. Rauschenbach
Anfangsstadien des ionenstrahl-gestützten Wachstums von GaN
Workshop „Ionenstrahlen in Forschung und Anwendung“, Leipzig, 12.-13.06.2013

J.W. Gerlach, L. Neumann, B. Rauschenbach
Ion-beam based pathways for the epitaxial growth of thin nitride semiconductor films
18. International Summer School on Vacuum, Electron and Ion Technlologies (VEIT 2013), Sozopol, Bulgarien, 07.-11.10.2013

J.W. Gerlach, L. Neumann, Th. Höche, B. Rauschenbach
Growth study: Ultra-thin GaN films by ion-beam assisted molecular beam epitaxy
19. International Vacuum Congress (IVC), Paris, 09.-13.09.2013

M. Hennes, A. Lotnyk, S.G. Mayr
Synthesis and characterization of magnetic core-shell nanoparticles
Frühjahrstagung der DPG, Regensburg, 10.-15.03.2013

A.M. Jakob, S.G. Mayr
Probing nanomechanics of single-crystalline Ni-Mn-Ga ferromagnetic shape memory alloy surfaces with atomic force acoustic microscopy (AFAM)
MRS, Fall Meeting, Boston, USA, 01.-06.12.2013

A.M. Jakob, M. Müller, B. Rauschenbach, S.G. Mayr
Contact resonance atomic force microscopy: nanometer-resolved mechanical surface properties of Ni-Mn-Ga single crystal films
MRS Spring Meeting & Exhibit 2013, San Francisco, 01.-05.04.2013

A.M. Jakob, A. Landgraf, Y. Ma, A. Arabi-Hashemi, M. Hennes, S.G. Mayr
Twin and magnetic domain patterns in miniaturized ferromagnetic shape memory alloys: self-organized formation and coupling at the nanoscale
MRS, Fall Meeting, Boston, USA, 01.-06.12.2013

A. Graumann, A.M. Jakob, Y. Ma, S.G. Mayr
Magnetic properties of single crystalline Fe_7Pd_3 ferromagnetic shape memory alloy thin films - A magnetic force microscopy study
Annual BuildMoNa Conference, Leipzig, 04.-05.03.2013

A. Lehmann, A. Schubert, S. Rupf, A. Schindler, G. Böhm, T. Arnold, D. Hirsch
Biofunktionale Schichten für die Zahnmedizin mittels lokaler Plasmaabscheidung
ak-adp, 3. Workshop Plasmamedizin, Berlin, 03.-04.06.2013

J. Lorbeer, M. Teichmann, F. Frost
Ionenstrahlgestützte Musterbildung auf oxidischen Materialien: SiO_2 vs. Al_2O_3
XX. Erfahrungsaustausch Oberflächentechnologie mit Plasma- und Ionenstrahlprozessen, Mühlleithen, 05.-08.03.2013

J. Lorbeer, M. Teichmann, F. Frost, B. Rauschenbach
Pattern formation on sapphire by low energy ion beam erosion
Frühjahrstagung der DPG, Regensburg, 10.-15.03.2013

P. Lorenz, F. Frost, M. Ehrhardt, K. Zimmer
Fabrication of optical elements by laser-induced front side etching methods
3. EOS Conference on Manufacturing of Optical Components (EOSMOC 2013), International Congress Centre Munich (ICM), Munich, Germany, 13.05.2013

P. Lorenz, F. Frost, M. Ehrhardt, K. Zimmer
Nanosecond laser-induced nano-structuring of fused silica
Frühjahrstagung der DPG, Regensburg, 10.-15.03.2013

A. Lotnyk
Transmissionselektronenmikroskopie am IOM
1. Sächsisches TEM-Präparatorentreffen, Dresden, 16.05.2013

A. Lotnyk, D. Poppitz, J. Gerlach, B. Rauschenbach
Low-energy ion milling of TEM lamellae for Cs-corrected HRSTEM
International Multidisciplinary Microscopy Congress (InterM 2013), Antalya, Turkei, 10.-13.10.2013

A. Lotnyk, D. Poppitz, J. W. Gerlach, B. Rauschenbach
TEM sample preparation of GaN-SiC interfaces for Cs-corrected STEM
2. NanoMill Group User Meeting, Halle (Saale), 05.-06.06.2013

E. Lugovoy, T. Gladytz, J. Nilsson, B. Abel, K. Siefermann
Time-resolved photoelectron spectroscopy on liquids: How fast is the evaporation of water
112. Bunsentagung, Karlsruhe, 09.-11.05.2013

J. Lutz, C. Díaz, J.W. Gerlach, S. Mändl
Sequentielle Implantation von Stickstoff und Sauerstoff in medizinische CoCr-Legierungen für kombinierten Verschleiß- und Korrosionsschutz
Workshop „Ionenstrahlen in Forschung und Anwendung“, Leipzig, 12.-14.06.2013

S. Mändl
Surface hardening of austenitic stainless steel and CoCr alloys
Coloquio del Departamento de Física, Pontificia Universidad Católica de Chile, Santiago, Chile, 20.03.2013

S. Mändl, J. Lutz, C. Díaz, J.W. Gerlach, J.A. García
Influence of reduced current density on PIII nitriding of austenitic stainless steel and CoCr alloys
12. Int. Workshop on Plasma Based Ion Implantation & Deposition, Poitiers, Frankreich, 01.-05.07.2013

S. Mändl
Verbesserung der Biokompatibilität von CoCr-Legierungen
XX. Erfahrungsaustausch Oberflächentechnologie mit Plasma- und Ionenstrahlprozessen, Mühlleithen, 05.-08.03.2013

D. Manova, S. Mändl, H. Neumann, B. Rauschenbach
In situ XRD investigations during low energy ion nitriding of austenitic stainless steel
Institute for Plasma Physics (INFIP), Departamento de Fisica, Universidad de Buenos Aires, Buenos Aires, 20.11.2013

D. Manova, D. Hirsch, S. Mändl, H. Neumann, B. Rauschenbach
In situ XRD investigations during low energy nitriding of austenitic stainless steel
XX. Erfahrungsaustausch Oberflächentechnologie mit Plasma- und Ionenstrahlprozessen, Mühlleithen, 05.-08.03.2013

D. Manova, S. Mändl, H. Neumann, B. Rauschenbach
Observation of decay of expanded austenite in CoCr alloys after nitriding
18. Int. Conf. on Surface Modification of Materials by Ion Beams, Kuşadası, Türkei, 15.-20.09.2013

D. Manova, S. Mändl, H. Neumann, B. Rauschenbach
Analysis of in-situ XRD measurements for nitriding of fcc metals
12. Int. Workshop on Plasma Based Ion Implantation & Deposition, Poitiers, Frankreich, 01.-05.07.2013

A. Mießler
Subaperture reactive ion beam etching (RIBE)
Workshop „Ionenstrahlen in Forschung und Anwendung“, Leipzig, 12.-14.06.2013

S. Naumov, T. Scherzer, W. Knolle, O. Daikos, K. Heymann
Primary processes by self-initiation of photopolymerization reactions using halogenated (meth)acrylates Molecular modelling
European Polymer Congress - EPF 2013, Pisa, Italien, 16.-21.06.2013

S. Naumov, T. Scherzer, W. Knolle, O. Daikos, K. Heymann
Computational modelling of the primary processes by photo- and electron-induced polymerization
13. European Conference on Molecular Electronics (ECME2013), London, 03.-07.09.2013

O. Öztürk, M. Fidan, S. Mändl
Hard, magnetic layers on stainless steel and CoCr alloys by nitrogen plasma immersion ion implantation
18. Int. Conf. on Surface Modification of Materials by Ion Beams, Kuşadası, Türkei, 15.-20.09.2013

L. Prager, U. Helmstedt, H. Herrnberger, M. Münch, O. Kahle, F. Kita, A. Pender, M. Stasiak
Photochemical approach to thin barrier films for the encapsulation of flexible laminar electronic devices
Pro Flex 2013 Vacuum Roll-To-Roll Processing of Flexible Materials, Dresden, 24.-25.09.2013

L. Prager, U. Helmstedt, H. Herrnberger, M. Münch, O. Kahle, F. Kita, A. Pender, M. Stasiak
Design, Herstellung und Eigenschaften von Hochbarriere-Verkapselungsfolien für flexible PV-Module auf photochemischem Wege
21. NDVaK, Dresden, 16.-17.10.2013

B. Rauschenbach
Funktionelle Oberflächen - Herausforderung für die Technologieentwicklung
12. Symposium Bayern Innovativ, Aschaffenburg, 11.04.2013

B. Rauschenbach
Nanostructures on surfaces by ion beam sputtering
18. International Summer School on Vacuum, Electron and Ion Technlologies (VEIT 2013), Sozopol, Bulgarien, 07.-11.10.2013

B. Rauschenbach
Surface modification of insulators by ion beams
17. Intern. Conference Radiation Effects in Insulators, Helsinki, 30.06.-05.07.2013

B. Rauschenbach, C. Grüner, Ch. Khare
Ion beam sputtering induced nano-sculperted thin films
XXI. Intern. Conference 'Ion-Surface Interaction', Jaroslavl, 22.-26.2013

B. Rauschenbach
Ion beam induced nanostructures on surfaces
3. Intern. Conference Nanomaterials: Applications & Properties, Alushta, 16.-21.06.2013

B. Rauschenbach
Low-energy ion beam interaction with solid surfaces
Kolloquium der TUHH, Hamburg, 20.06.2013

B. Rauschenbach
Ion beam assisted deposition - Methods, film growth and application
WE-Heraeus-Seminar on Ionized- and Ion Assisted Physical Vapor Deposition, Helmholtz Zentrum Dresden-Rossendorf, 26.-28.06.2013

S. Reichelt, S. Oehmichen, F. Lohmann, J. Becher, J. Weisser, M. Schnabelrauch, W. Knolle
Biokompatible makroporöse Cryogele: Synthese, Charakterisierung und Anwendungen
9. Thüringer Biomaterial-Kolloquium, Zeulenroda, 03.-05.09.2013

S. Reichelt, S. Oehmichen, F. Lohmann, J. Becher, J. Weisser, M. Schnabelrauch, W. Knolle
Elektronenstrahl-induzierte Synthese von makroporösen Cryogelen für biotechnologische Anwendungen
V2013 - WS1: Beschichtung für Biotechnologie und Medizintechnik, Dresden, 14.-17.10.2013

S. Reichelt, S. Oehmichen, F. Lohmann, A. Prager, W. Knolle
Cryogele - Trägermaterialien für die Biotechnologie und Medizintechnik
Kolloquium in der Arbeitsgruppe Photobiophysik, Institut für Physik, HU Berlin, Berlin, 28.10.2013

S. Reichelt, C. Abe, S. Oehmichen, W. Knolle, A. Prager, M. Schnabelrauch, J. Becher, S. Möller, A. Berg, J. Weisser
Tailor made electron-beam generated polymeric cryogels and their biotechnological application
International Meeting on radiation processing, Shanghai, 04.-08.11.2013

T. Scherzer, G. Mirschel, O. Daikos, K. Heymann, B. Genest, C. Sommerer, C. Steckert
In-line monitoring of the conversion in an offset printing press
RadTech Europe, Basel, 15.-17.10.2013

T. Scherzer, G. Mirschel, K. Heymann, O. Daikos
In-line-Überwachung von Druck- und Beschichtungsprozessen mittels Nahinfrarot-Spektroskopie
3. Oberflächenseminar der VBLF event, Würzburg, 12.-13.09.2013

R. Schmidt-Grund, T. Böntgen, L. Fricke, J. Lorbeer, C. Grüner, J. Bauer, C. Sturm, M. Teichmann, J. Lenzner, C. Bundesmann, F. Frost, M. Grundmann
Ellipsometric investigation of natural and functional nano-structured surfaces
6. Int. Conf. Spectroscopic Ellipsometry, Kyoto, Japan, 26.-31.05.2013

A. Schulze, S. Starke, M. Went, A. Prager
Enzyme immobilization on polymer membranes by electron beam irradiation
12. Int. Conf. Polymers for Advanced Technologies, Berlin, Germany, 29.09.-02.10.2013

K. Siefermann, F. Weise, M. Lin, C. Bacellar, A. Belkacem, T. Weber, F. Sturm, D. Slaughter, C. Khurmi, T. Wright, B. Schoenlein
Ultrafast x-ray photoelectron spectroscopy studies of photoinduced electronic dynamics in dye sensitized semiconductor nanocrystals
Frühjahrstagung der DPG, Hannover, 18.-22.03.2013

M. Teichmann, J. Lorbeer, F. Frost
Musterbildung auf Germanium mit niederenergetischen Edelgasionen
XX. Erfahrungsaustausch Oberflächentechnologie mit Plasma- und Ionenstrahlprozessen, Mühlleithen, 05.-08.03.2013

M. Teichmann, J. Lorbeer, F. Frost, B. Rauschenbach
Evolution of Ge surface topography during low energy ion beam erosion
Frühjahrstagung der DPG, Regensburg, 10.-15.03.2013

M. Teichmann
Stabilization and destabilization of ion beam eroded Ge surfaces
Workshop „Ionenstrahlen in Forschung und Anwendun“, Leipzig, 12.-14.06.2013

M. Tromayer, Z. Li, J. Torgersen, A. Ajami, A. Rosspeintner, S. Naumov, T. Scherzer, J. Stampfl, R. Liska
Novel highly efficient initiators for two-photon induced photopolymerization
RadTech Europe, Basel, 15.-17.10.2013

E. I. Wisotzki, M. Hennes, S.G. Mayr
Plasma synthesized magnetic nanoparticles fixed in radiation optimized hydrogels
1. Colloquium of SPP 1681, Benediktbeuern, 24.-25.09.2013

K. Zimmer
Precise patterning of dielectrics by lasers: Processes, mechanism, and applications
ALPS-Seminar, Berner University of Applied Science, Burgsdorf, Schweiz, 22.05.2013

M. Zink, F. Szillat, U. Allenstein, S.G. Mayr
Interaction of ferromagnetic shape memory alloys and RGD peptides for promotion of cell adhesion: From ab-initio-calculations to cell studies
MRS, Fall Meeting, Boston, USA, 01.-06.12.2013

M. Zink, V. Dallacasagrande, A. Reichenbach, J. Käs, S.G. Mayr
Investigating super-hydrophilic nanotube arrays for long-term organotypic culture of adult retina and brain tissue
MRS, Fall Meeting, Boston, USA, 01.-06.12.2013

Posters

2012

A. Arabi-Hashemi, S.G. Mayr
Ion beam induced phase transformations in the ferromagnetic shape memory alloy $Fe_{70}Pd_{30}$
5. Scientific Symposium of the Graduate School BuildMoNa, Leipzig, 12.03.2012

Th. Arnold, G. Böhm, H. Paetzelt
Plasma jet machining based process chain for the manufacturing of complex shaped synchrotron mirrors
12. Euspen International Conference, Stockholm, 04.-08.06.2012

Th. Arnold, H. Paetzelt, G. Böhm
Numerically controlled local plasma jet oxidation of silicon
13. International Conference on Plasma Surface Engineering, Garmisch-Partenkirchen, 10.-14.09.2012

J. Bauer, C. Grüner, B. Rauschenbach
Doped amorphous Si/Ge nanostructured thin films via glancing angle deposition
Frühjahrstagung der DPG, Berlin, 25.-30.03 2012

J. Bauer, C. Grüner, M. Weise, B. Rauschenbach
Glancing angle deposition: Customized shaping of self-assembled nanostructures
1. Workshop Leibniz Nano, Berlin, 30.-31.01.2012

F. Bauer, U. Decker, S. Naumov, C. Riedel
Photoinitiator-free UV curing of acrylate-based nanocomposites
2. European Symposium of Photopolymer Science, Turin, Italien, 04.-07.09.2012

T. Böntgen, J. Lorbeer, M. Teichmann, F. Frost, R. Schmidt-Grund, M. Lorenz, M. Grundmann
Optical investigation of Au coated nanostructured surfaces
Frühjahrstagung der DPG, Berlin, 25.-30.03.2012

T. Böntgen, J. Lorbeer, F. Frost, M. Teichmann, R. Schmidt-Grund, M. Lorenz, M. Grundmann
Ellipsometric study of nano patterned surfaces for structural investigation
7. Workshop Ellipsometry, Leipzig, 05.-07.03.2012

J. Buchwald, S.G. Mayr
Elastic properties of surfaces at nanoscale
5. Scientific Symposium of the Graduate School BuildMoNa, Leipzig, 12.03.2012

C. Bundesmann, H. Neumann
Optical properties of stress-minimized optical multi-layer coatings grown by dual ion beam deposition
7. Workshop Ellipsometry, Leipzig, 05.-07.03.2012

D. Cao, X. Cheng, D. Manova, S. Mändl, T. Jia, Y. Yu
Characterization of HfAlO film deposited by plasma enhanced atomic layer deposition
18. Int. Conf. on Ion Beam Modification of Materials, Qingdao, China, 02.-07.09.2012

V. Dallacasagrande, M. Zink, S. Huth, A.M. Jakob, M. Müller, J.A. Käs, S.G. Mayr, A. Reichenbach
Tailoring substrates for long-term organotypic culture of adult neuronal tissue
3. Edu-GLIA Annual Meeting, Margaux, Frankreich, 24.-25.08.2012

V. Dallacasagrande, M. Zink, S. Huth, A.M. Jakob, M. Müller, J.A. Käs, S.G. Mayr, A. Reichenbach
Tailoring substrates for long-term organotypic culture of adult neuronal tissue
8. FENS Forum of Neuroscience, Barcelona, Spanien, 14.-18.07.2012

C. Diaz, J.A. García, R. Pereiro, B. Fernández, S. Mändl, R.J. Rodríguez
Nanoscale plasma treatment for improvement behavior of F-799 alloys for MoM prosthesis application
Int. Conf. on Nanotechnology in Medicine, London, U.K., 07.-09.11.2012

C. Díaz, J.A. García, R. Pereiro, B. Fernández, S. Mändl, D. Manova, R.J. Rodríguez
Advanced plasma treatments for improving orthopaedic surfaces
22. Annual Biointerface Conf., Dublin, Ireland, 23.-25.10.2012

M. Ehrhardt, P. Lorenz, K. Zimmer
Replication of sub micrometer size structures by laser embossing in thin metal foils
Frühjahrstagung der DPG, Berlin, 25-30.03.2012

M. Ehrhardt, C. Scheit, S. Ragnow, P. Lorenz, A. Wehrmann, A. Braun, K. Zimmer
Fabrication of contact holes by backside laser ablation of PI foils for CIGS solar modules
EMRS, Spring Meeting, Straßburg, 14.-18.05.2012

M. Ehrhardt, P. Lorenz, K. Zimmer
Microembossing of thin metal foils with UV excimer laser pulses
EMRS, Spring Meeting, Straßburg, 14.-18.05.2012

M. Ehrhardt, A. Wehrmann, C. Scheit, S. Ragnow, P. Lorenz, A. Braun, K. Zimmer
Scribing of CIGS thin film solar cells for external integrated interconnection
EMRS, Spring Meeting, Straßburg, 14.-18.05.2012

M. Ehrhardt, P. Lorenz, K. Zimmer
Microembossing of thin metal foils with UV excimer laser pulses
EMRS, Spring Meeting, Symp. V, Straßburg, 14.-18.05.2012

M. Ehrhardt, C. Scheit, S. Ragnow, P. Lorenz, A. Wehrmann, A. Braun, K. Zimmer
Fabrication of contact holes by rear side laser ablation of polyimide foils for CIGS solar modules
EMRS, Spring Meeting, Straßburg, 14.-18.05.2012

C. Elsner, S. Reichelt, C. Abe, S. Hainich
Surface functionalized porous polymeric materials for bioapplications
CELLMAT 2012, Dresden, 07.-09.11.2012

C. Elsner, S. Reichelt, A. Pender
Polymer synthesis and modification by radiation-induced processes for biological applications
1. Workshop Leibniz Nano, Berlin, 30.-31.01.2012

L. Escalada, L. Vaca, S. Simison, S. Brühl, D. Manova, H. Neumann, S. Mändl
Influence of processing conditions on corrosion results of nitrided stainless steel AISI 316L
Corrosion 2012, Salt Lake City, Utah, USA, 11.-15.03.2012

L. Escalada, E. L. Dalibon, L. S. Vaca, D. Manova, S. Mändl, H. Neumann, S.P. Brühl, S. Simison
Corrosion behaviour of AISI 316L stainless steel nitrided by three different processes using different ion energies
18. Int. Conf. on Ion Beam Modification of Materials, Qingdao, China, 02.-07.09.2012

R. Feder, F. Frost, H. Neumann, C. Bundesmann, B. Rauschenbach
Systematic investigations of ion beam sputtering of Si and Ag: First experimental and simulation results
IISC-19, Frauenchiemsee, 16.-21.09.2012

R. Feder, F. Scholze, F. Frost, H. Neumann, C. Bundesmann
Monte Carlo simulations of silicon sputtering by argon ions and an approach for comparison with experimental results
Frühjahrstagung der DPG, Berlin, 25.-30.03.2012

K. Fischer, M. Müller, J.W. Gerlach, A. Prager, A. Schulze
Photocatalytic membrane for water purification
Euromembrane 2012, London, UK, 23.-27.09.2012

T. Fischer, L. Prager, J. Hohage, H. Ruelke, S. E. Schulz, R. Richter, T. Gessner
A complimentary study of vacuum ultraviolet curing procedures on high tensile stress Si N H PECVD silicon nitride layers
17. Workshop on Dielectrics in Microelectronics (WoDiM2012), Dresden, 25.-27.06.2012

K. Fischer, A. Prager, P. Hertel, J. W. Gerlach, A. Schulze
Photocatalytic membrane for water purification
Aachener Membran Kolloquium, Aachen, 07.-08.11.2012

A. Freyer, E. Bilz, H. Hildebrand, K. Franke, R. Mehnert, E. Mai
Investigation of nanoparticle release from UV-curable polymeric nanocomposites
Int. Conf. on safe production and use of nanomaterials, Nanosafe 2012, Minatec, Grenoble, France, 13.-15.11.2012

A. Freyer, E. Bilz, A. Prager, I. Reinhardt
Verfolgung des Abbaus von Ag-haltigen Nanokompositen – NanoTrack
2. Clustertreffen der BMBF-Fördermaßnahmen NanoCare und NanoNature, Frankfurt/Main, 13.-14. 03.2012

A. Graumann, S.G. Mayr
Magnetic force microscopy on single crystalline $Fe_{70}Pd_{30}$ ferromagnetic shape memory thin films
5. Scientific Symposium of the Graduate School BuildMoNa, Leipzig, 12.03.2012

C. Grüner, J. Bauer, B. Rauschenbach
Glancing angle deposition: Structural aspects and growth modeling
Frühjahrstagung der DPG, Berlin, 25.-30.3.2012

H. Hildebrand, K. Franke, N. Gibson, I. Cydzik, F. Simonelli, A. Bulgheroni, U. Holzwarth, E. Bilz, A. Freyer
Radiolabelling of engineered silver and titania nanoparticles as a tool for sensitive detection of nanoparticle release from surface coatings
Int. Conf. on Safe Production and Use of Nanomaterials, Nanosafe 2012, Minatec, Grenoble, France, 13.-15.11.2012

D. Jha, D. Manova, J.W. Gerlach, W. Assmann, E. Valcheva, S. Mändl
Influence of Ti interlayer on photoactive properties of TiO_2
14. Int. Conf. on Plasma Surface Engineering, Garmisch-Partenkirchen, Germany, 15.-19.09.2012

J. Kullmann, T. Titze, C. Chmelik, J. Kärger, D. Enke, L. Prager
The potentials of IR micro-imaging for in-situ studies of chemical reactions in nanoporous catalyst
24. Deutsche Zeolith-Tagung, Magdeburg, 07.-09.03.2012

J. Kullmann, T. Titze, C. Chmelik, J. Kärger, D. Enke, L. Prager
The potentials of IR micro-imaging for in-situ studies of chemical reactions in nanoporous catalyst
CPM-6, 6. International Workshop on Characterization of Porous Materials: From Angstroms to Millimeters, Delray Beach, Florida, 29.04.-02.05.2012

A. Lehmann, M. Volkmer, S. Rupf, G. Böhm, T. Arnold, A. Schindler
SiO_x-thin-film deposition on enamel by an atmospheric plasma jet (APJ)
4. International Conference on Plasma Medicine, Orléans, France, 17.-21.06.2012

Z. Li, N. Pucher, R. Liska, J. Stampfl, A. Rosspeinter, E. Vauthey, S. Naumov, T. Scherzer
A straightforward sythesis and structure-activity relationship of highly efficient initiators for two-photon polymerization
European Symposium of Photopolymer Science (ESPS 2012), Torino / Italien, 04.-07.9.2012

J. Lorbeer, M. Teichmann, F. Frost, B. Rauschenbach
Pattern formation on ion beam eroded quartz glass surfaces
Frühjahrstagung der DPG, Berlin, 25.-30.03.2012

P. Lorenz, M. Ehrhardt, K. Zimmer
Production of sub-µm to cm structures on fused silica by laser-induced front side etching using self-regenerating adsorbing layer (SAL-LIFE)
Frühjahrstagung der DPG, Berlin, 25.-30.03.2012

P. Lorenz, M. Ehrhardt, K. Zimmer
Laser-induced front side etching of fused silica with fs laser radiation using thin metal layers
EMRS, Spring Meeting, Straßburg, 14.-18.05.2012

P. Lorenz, M. Ehrhardt, K. Zimmer
Laser-induced front side etching using self-regenerating adsorbing layer (SAL-LIFE) of fused silica
Frühjahrstagung der DPG, Stuttgart, 12-16.03.2012

P. Lorenz, M. Ehrhardt, K. Zimmer
Laserinduziertes Vorderseitenätzen (LIFE) von Quarzglas
8. ThGOT Thementage Grenz- und Oberflächentechnik und 3. Optik-Kolloquium „Dünne Schichten in der Optik“, Leipzig, 04.-06.09.2012

P. Lorenz, M. Ehrhardt, K. Zimmer
Nanometerpräzises Abformen in Metalloberflächen mit gepulster Laserstrahlung
8. ThGOT Thementage Grenz- und Oberflächentechnik und 3. Optik-Kolloquium „Dünne Schichten in der Optik“, Leipzig, 04.-06.09.2012

A. Lotnyk, C. Bechtold, B. Erkarta, C. Szillus, E. Quandt, L. Kienle
FIB preparation of $Fe_{70}Pd_{30}$ films for in situ heating in TEM
7. FIB-Workshop: Focused Ion Beams in Research, Science and Technology, Dresden, 25.-27.06.2012

A. Lotnyk, C. Bechtold, B. Erkartal, C. Szillus, E. Quandt, L. Kienle
FIB preparation of $Fe_{70}Pd_{30}$ films for in situ heating in TEM
7. FIB-Workshop: Focused Ion Beams in Research, Science and Technology, Dresden, 25.-27.06.2012

Y. Ma, A. Setzer, P. Esquinazi, S.G. Mayr
Martensitic transformation and magnetic properties of freestanding single crystalline $Fe_{70}Pd_{30}$ thin films
5. Scientific Symposium of the Graduate School BuildMoNa, Leipzig, 12.03.2012

S. Mändl. C. Díaz, J.W. Gerlach, J.A. García
Near surface analysis of duplex PIII treated CoCr alloys
18. Int. Conf. on Ion Beam Modification of Materials, Qingdao, China, 02.-07.09.2012

D. Manova, A. Bergman, C. Günther, S. Mändl, H. Neumann, B. Rauschenbach
Influence of temperature on layer growth as measured by in situ XRD observation of austenitic stainless steel nitriding
18. Int. Conf. on Ion Beam Modification of Materials, Qingdao, China, 02.-07.09.2012

D. Meinhard, M. Kühnert, A. Prager, P. D. Esquinazi, A. Setzer
Preparation and magnetic properties of barium hexaferrite based nano-composites and their UV-curing behavior
Nanofair 2012, Dresden, 12.-13.06.2012

D. Meinhard, E. Bilz, W. Hovestadt, T. Büsgen, P. Reichert, N. Zöll
Graduelle photochemische Mattierung von Acrylatlacken mittels VUV-Strahlung: Ein neuer Ansatz für den Antiglare-Effekt?
8. ThGOT Thementage Grenz- und Oberflächentechnik und 3. Optik-Kolloquium „Dünne Schichten in der Optik“, Leipzig, 04.-06.09.2012

S. Naumov, W. Knolle, T. Scherzer, O. Savchuk
Molecular modeling of primary processes by photo- and electron-induced polymerization
European Symposium of Photopolymer Science, Torino / Italien, 04.-07.9.2012

S. Naumov, W. Knolle, T. Scherzer, O. Savchuk
Computational modelling of the primary processes by radiation-induced polymerization
7. Singapore International Chemical Conference, Singapore, 16.-20.12.2012

A. Schindler, F. Frost, R. Fechner, A. Nickel, T. Arnold, G. Böhm, H. Paetzelt, T. Hänsel
IOM competence in R&D for ultra-precision surface processing with ion beams and plasma jets
Precision Engineering at CERN: Future Challenges & Opportunities, Euspen, Thoiry, France 02.-03.05.2012

C. Schmidt, O. Savchuk, T. Scherzer
Shrinkage determination of UV-cured acrylates using photorheology
European Symposium of Photopolymer Science, Torino, Italien, 04.-07.9.2012

A. Schulze, S. Starke, A. Prager, M. Went
A novel electron beam-based method for the immobilization of trypsin on polymer membranes
14. Aachener Membrankolloquium, Aachen, Deutschland, 07.-08.11.2012

A. Schulze, S. Starke, A. Prager, M. Went
Immobilization of trypsin on polymer membranes via electron beam irradiation
Euromembrane 2012, London, UK, 23.-27.09.2012

F. Szillat, S.G. Mayr
Influence of pre-structuring on self-organized pattern formation at organic-metal interfaces - experiment vs. modeling
Frühjahrstagung der DPG, Berlin, 25.-30.03.2012

M. Teichmann, J. Lorbeer, F. Frost, B. Rauschenbach
Evolution of Si surface topography during ion beam erosion at high incidence angles
Frühjahrstagung der DPG, Berlin, 25.-30.03.2012

J. Zajadacz, P. Lorenz, M. Ehrhardt, K. Zimmer, S. Möllenbeck, K. Dhima, H.-C. Scheer
Separation of rigid 3D micromoulds with undercuts from PDMS replica: An experimental and theoretical study
38. International Conference on Micro and Nano Engineering, Toulouse, 16.-20.09.2012

M. Zink, V. Dallacasagrande, S. Huth, A.M. Jakob, M. Mueller, A. Reichenbach, J. Käs, S.G. Mayr
Tailoring substrates for long-term organotypic culture of adult neuronal tissue
MRS, Fall Meeting, Boston, 27.11.2012

M. Zink, V. Dallacasagrande, S. Huth, A.M. Jakob, M. Müller, A. Reichenbach, J. Käs, S.G. Mayr
Tailoring substrates for long-term organotypic culture of adult neuronal tissue
Annual Meeting of the German Biophysics Society, Göttingen, 23.-26.09.2012

2013

T. Böntgen, J. Lorbeer, M. Teichmann, F. Frost, R. Schmidt-Grund, M. Grundmann
Investigation of surface plasmons on structured surfaces
Frühjahrstagung der DPG, Regensburg, 10.-15.03.2013

S.P. Brühl, L.S. Vaca, E.L. Dalibon, D. Manova, S. Mändl, H. Neumann, L. Escalada, S.N. Simison
Comparison of three different nitriding bethods on AISI 316L stainless steel regarding wear and corrosion performance
12. Int. Workshop on Plasma Based Ion Implantation & Deposition, Poitiers, Frankreich, 01.-05.07.2013

C. Bundesmann, R. Feder, H. Neumann
Tailoring the properties of Ag thin films grown by ion beam sputter deposition
6. International Conference on Spectroscopic Ellipsometry, Kyoto, Japan, 26.-31.05.2013

C. Bundesmann, R. Feder, H. Neumann
Tailoring of thin film properties by (dual) ion beam sputter deposition
273. PTB-Seminar, VUV and EUV Metrology, BESSY II/HZB, Berlin, 24.-25.10.2013

M. Ehrhardt, P. Lorenz, K. Zimmer
Laser embossing: surface processing beyond the diffraction limit of the laser radiation
EMRS, Spring Meeting, Straßburg, 27.-31.05.2013

M. Ehrhardt, P. Lorenz, F. Frost, K. Zimmer
Surface nanostructuring of poly- and monocrystalline copper substrates by laser embossing
Nanotech 2013, Washington D.C., 11.-15.05.2013

M. Ehrhardt, F. Frost, P. Lorenz, K. Zimmer
Submicrometer precise machining of metal surfaces with excimer laser radiation
Frühjahrstagung der DPG, Regensburg, 10.-15.03.2013

C. Elsner, S. Hainich
Untersuchungen zur Polymer-Modifizierung von und mit Gold-Nanopartikeln mittels MALDI-TOF-MS
Bruker Anwendertreffen, Berlin, 25.-26.02.2013

C. Elsner, B. Abel
Schnelles molekulares Diagnostikverfahren zur Erzeugung von Täter- und Tätergruppenprofilen
Zivieler Sicherheits-Schutz vor organisierter Kriminalität, BMBF-Partnering Event, Düsseldorf, 24.10.2013

L. Escalada, S.P. Brühl, S. Suarez, D. Manova, S. Mändl, S. Simison
Influence of inclusions on the corrosion attack of plasma nitrided austenitic stainless steel
European Congress and Exhibition on Advanced Materials and Processess, Sevilla, Spanien, 08.-13.09.2013

R. Feder, H. Neumann, C. Bundesmann, B. Rauschenbach
Influence of process parameters on thin film properties of Ag films grown by ion beam sputter deposition
Wilhelm und Else Heraeus Seminar, Physics of Ionized and Ion-Assisted PVD: Principles and Current Trends, Helmholtz-Zentrum Dresden-Rossendorf, 26.-28.07.2013

B. Bacci Fernandes, S. Mändl, R. Moraes Oliveira, M. Ueda
Characterization of SS304 treated by plasma immersion ion implantation
18. Int. Conf. on Surface Modification of Materials by Ion Beams, Kuşadası, Türkei, 15.-20.09.2013

J. Fernández, C. Díaz, J.A. García, S. Mändl
Nitriding of maraging steel grade 300 by plasma immersion ion implantation
12. Int. Workshop on Plasma Based Ion Implantation & Deposition, Poitiers, Frankreich, 01.-05.07.2013

M. Fidan, O. Öztürk, S. Mändl
MFM imaging of expanded austenite formed in stainless steel and CoCr alloys
12. Int. Workshop on Plasma Based Ion Implantation & Deposition, Poitiers, Frankreich, 01.-05.07.2013

A. Finzel, J. W. Gerlach, F. Frost, J. Lorbeer, B. Rauschenbach
Ion-beam assisted molecular-beam epitaxy of gallium nitride - initial stages of ion irradiation
18. International Summer School on Vacuum, Electron and Ion Technlologies (VEIT 2013), Sozopol, Bulgarien, 07.-11.10.2013

K. Fischer, M. Müller, J. Gerlach, A. Schulze
Photocatalytic mixed matrix membrane for water purification
Photocatalytic Mixed Matrix Membrane for Water Purification, Sorrento, 03.-07.03.2013

A. Freyer, E. Bilz, A. Prager, H. Hildebrand, K. Franke, E. Mai, R. Mehnert
Investigation of TiO_2-nanoparticle release from UV-curable polymeric nanocomposites NanoTrack
3. Clustertreffen der BMBF-Fördermaßnahmen NanoCare und NanoNature, Frankfurt/Main, 14.-15.01.2013

L. Fricke, T. Böntgen, J. Lorbeer, J. Lenzner, R. Schmidt-Grund, M.Grundmann
Surface modification of ZnO bulk single crystals in vacuum
Frühjahrstagung der DPG, Regensburg, 10.-15.03.2013

T. Gladytz, E. Lugovoy, K. Siefermann, B. Abel
A new multivariate method to disentangle complex spectra
112. Bunsentagung, Karlsruhe, 09.-11.05.2013

C. Grüner, B. Rauschenbach
Glancing angle deposited silicon/germanium nanostructures for electronic applications
Frühjahrstagung der DPG, Regensburg, 10.-15.03.2013

C. Grüner, J. Bauer, B. Rauschenbach
Nanoscale Si/Ge heterostructures prepared by glancing angle deposition
19. International Vacuum Congress IVC-19/ICN+T, Paris, 09.-13.09.2013

U. Helmstedt, L. Wennrich, H. Khalil, C. Bundesmann, U. Decker, J. W. Gerlach, D. Manova, S. Naumov, L. Prager
A pure photochemical preparation of aluminium oxide thin films
MRS Spring Meeting & Exhibit, San Francisco, 01.-05.04.2013

M. Hennes, A. Lotnyk, S.G. Mayr
Structural properties of bimetallic magnetic nanoparticles
Doktorandenforum der Leibniz-Gemeinschaft, Sektion D, Berlin, 06.-07.06.2013

H. Hildebrand, K. Franke, N. Gibson, I. Cydzik, F. Simonelli, A. Bulgheroni, U. Holzwarth, E. Bilz, A. Freyer
Radiolabelling of silver and titania nanoparticles as a tool for sensitive detection of nanoparticle release from surface coatings
3. Clustertreffen der BMBF-Fördermaßnahmen NanoCare und NanoNature, Frankfurt/Main, 14.-15.01.2013

D. Hintzen, M. Jorewitz, Y. Riyad, J. Griebel, B. Abel, K. Siefermann
Towards understanding ultrafast dynamics in light-switchable polymers
DPG Physics School: Innovative concepts in photovoltaics, Bad Honnef, 22.-27.09.2013

B. Hopp, T. Csizmadia, T. Smausz, C. Tápai, J. Kopniczky, X. Wang, M. Ehrhardt, P. Lorenz, K. Zimmer
Production of low-reflective surface structures on metal films
12. International Conference on Laser Ablation (COLA 2013), Ischia, Italien, 06.-11.10.2013

A. Lehmann, S. Rupf, M. Hannig and A. Schindler
Plasma jet treatment of tooth surfaces for bonding improvement in composite restoration
16. Fachtagung für Plasmatechnologie (PT-16), Greifswald, 18.-20.02.2013

F. Lehnert, J. Zajadacz, S.G. Mayr
Nanoporous materials by ion processing
BuildMoNa Conference: Quantum Structures for Energy Applications, Leipzig, 30.9.-01.10.2013

J. Lorbeer, M. Teichmann, F. Frost, B. Rauschenbach
Surface evolution on fused silica by low energy ion beam erosion: smoothing, ripple formation, faceting and coarsening
International Symposium on Nanoscale Pattern Formation at Surfaces, Copenhagen, Dänemark, 26.-30.05.2013

J. Lorbeer, M. Teichmann, F. Frost, B. Rauschenbach
Ion beam induced pattern formation on oxidic materials: SiO_2 vs. Al_2O_3
International Symposium on Nanoscale Pattern Formation at Surfaces, Copenhagen, Dänemark, 26.-30.05.2013

P. Lorenz, M. Ehrhardt, K. Zimmer
Laser-induced front side etching using self-regenerationg adsorbing layer (SAL-LIFE) of commercial glasses
Photonic West, San Francisco, 02.-07.02.2013

P. Lorenz, F. Frost, M. Ehrhardt, K. Zimmer
Laser-induced nanostructure fabrication in fused silica surfaces: experiment and theory
Frühjahrstagung der DPG, Regensburg, 10.-15.03.2013

P. Lorenz, M. Ehrhardt, K. Zimmer
Structuring of glass fibre surfaces by laser-induced front side etching
EMRS, Spring Meeting, Straßburg, 27.-31.05.2013

P. Lorenz, M. Klöppel, F. Frost, M. Ehrhardt, P. Li, K. Zimmer
Nanostructuring of dielectric surfaces induced by KrF excimer laser radiation: Experiment and theory
Nanotech 2013, Washington D.C., 11.-15.05.2013

A. Lotnyk, D. Poppitz, U. Roß, J.W. Gerlach, B. Rauschenbach
Ultrathin TEM lamellae for low voltage Cs-corrected STEM
Frühjahrstagung der DPG, Regensburg, 10.-15.03.2013

A. Lotnyk, D. Poppitz, J. W. Gerlach, B. Rauschenbach
Low-energy Ar^+-polishing of FIB prepared GaN-SiC interfaces for Cs-corrected STEM
Microscopy Conference 2013 (MC 2013), Regensburg, 25.-30.08.2013

Y. Ma, A. Jakob, and S.G. Mayr
Nanoindentation response of freestanding epitaxially grown Fe-Pd ferromagnetic shape memory thin films
Annual Conference of the Graduate School BuildMoNa, Leipzig, 04.-05.03.2013

S. Mändl, D. Manova, E. Valcheva
Influence of layer thickness on photo-induced hydrophilicity of TiO_2 thin films
18. Int. Conf. on Surface Modification of Materials by Ion Beams, Kuşadası, Türkei, 15.-20.09.2013

D. Manova, S. Mändl, H. Neumann, B. Rauschenbach
Reduction of layer growth in expanded austenite for reduced ion current densities
18. Int. Conf. on Surface Modification of Materials by Ion Beams, Kuşadası, Türkei, 15.-20.09.2013

S. Naumov, T. Scherzer, W. Knolle, O. Daikos, K. Heymann, L. Prager
Computational modelling of the primary processes by photo- and electron-induced polymerization
ECME13 12. European Conference on Molecular Electronics, London, UK, 03.-07.09.2013

A. Pender, A. Prager
Plasma surface treatment as polymerization promoter
16. Fachtagung für Plasmatechnologie (PT-16), Greifswald, 18.-20.02.2013

D. Poppitz, A. Lotnyk, J.W. Gerlach, L. Neumann, B. Rauschenbach
Microstructural investigation of epitaxial GaN thin films grown using hyperthermal ions
Frühjahrstagung der DPG, Regensburg, 10.-15.03.2013

D. Poppitz, A. Lotnyk, J.W. Gerlach, B. Rauschenbach
Microstructure investigation of porous gallium nitride thin films
Microscopy Conference (MC) 2013, Regensburg, 25.-30.08.2013

S. Reichelt, C. Abe, M. Kühnert, C. Elsner
Electron-beam-derived macroporous scaffolds for biotechnolgical applications
3. International Conference on Multifunctional, Hydbrid and Nanomaterials, Sorrento, Italien, 03.-07.03.2013

U. Roß, A. Lotnyk, E. Thelander, B. Rauschenbach
Quantitative investigation of laser-deposited $Ge_2Sb_2Te_5$ phase change films by Cs-corrected STEM
Microscopy Conference MC 2013, Regensburg, 25.-30.08.2013

U. Roß, A. Lotnyk, E. Thelander, B. Rauschenbach
Quantitative investigation of laser-deposited $Ge_2Sb_2Te_5$ by abberation-corrected STEM/EELS
Frühjahratagung der DPG, Regensburg, 10.-15.03.2013

U. Roß, D. Poppitz, A. Lotnyk, B. Rauschenbach
Aberration-corrected transmission electron microscopy of thin films
Leibniz Doktorandenforum 2013, Sektion D, Berlin, 06.-07.06.2013

M. Sarmanova, E. Thelander, A. Jakob, J. W. Gerlach, S.G. Mayr, B. Rauschenbach
Measurements of elastic properties of surfaces with nanometer resolution
Frühjahrstagung der DPG, Regensburg, 10.-15.03.2013

A. Schulze, A. Stoelzer, S. Starke, I. Thomas, M. Went
Self-cleaning polymer membrane surfaces
3. International Conference on Multifunctional Hybrid and Nanomaterials, Sorrento, Italien, 03. -07.3.2013

X. Sun, E. Thelander, H. Lu, J.W. Gerlach, U. Decker, D. Hirsch, B. Rauschenbach
Structural investigation of pulsed laser deposited phase-change films
18. International Summer School on Vacuum, Electron and Ion Technlologies (VEIT 2013), Sozopol, Bulgarien, 07.-11.10.2013

M. Teichmann, J. Lorbeer, F. Frost, B. Rauschenbach
Ion mass dependent pattern formation on Si by low energy ion beam erosion
International Symposium on Nanoscale Pattern Formation at Surfaces, Kopenhagen, 26.-30.05.2013

M. Teichmann, J. Lorbeer, F. Frost, B. Rauschenbach
Stabilization and destabilization of ion beam eroded Ge surfaces
International Symposium on Nanoscale Pattern Formation at Surfaces, Kopenhagen, 26.-30.05.2013

M. Teichmann, J. Lorbeer, F. Frost, B. Rauschenbach
Stabilization and destabilization of ion beam eroded Ge surfaces
International Symposium on Nanoscale Pattern Formation at Surfaces, Copenhagen, Dänemark, 26.-30.05.2013

M. Teichmann, J. Lorbeer, F. Frost, B. Rauschenbach
Ion mass dependent pattern formation on Si by low energy ion beam erosion
International Symposium on Nanoscale Pattern Formation at Surfaces, Copenhagen, Dänemark, 26.-30.05.2013

E. Thelander, H. Lu, J.W. Gerlach, B. Rauschenbach
Phase ransitions in GST-films using single nanosecond UV pulses
Frühjahrstagung der DPG, Regensburg, 10.-15.03.2013

E. Thelander, H. Lu, J.W. Gerlach, B. Rauschenbach
Laser-induced phase transitions in PLD-deposited $Ge_2Sb_2Te_5$-films using single nanosecond UV-pulses
Annual Conference of the Graduate School BuildMoNa, Leipzig, 04.-05.03.2013

E. Thelander, U. Ross, X. Sun, A.Lotnyk, H.Lu and B. Rauschenbach
Pulsed laser deposition of $Ge_2Sb_2Te_5$ thin films for phase change data storage applications
12. International Conference on Laser Ablation, Ischia, Italien, 06.-11.10.2013

X. Wang, D. Fleischer, P. Lorenz, M. Ehrhardt, C. Scheit, S. Ragnow, X. Ni, K. Zimmer
Alteration of electrical properties from CIGS thin-film solar cells after laser irradiation
EMRS, Spring Meeting, Straßburg, 27.-31.05.2013

X. Wang, X. Ni, D. Fleischer, M. Ehrhardt, P. Lorenz, K. Zimmer
Laser processing for CIGS thin-film solar cells
Frühjahrstagung der DPG, Regensburg, 10.-15.03.2013

E. I. Wisotzki, M. Hennes, S.G. Mayr
Plasma synthesized magnetic nanoparticles arrested in radiation optimized hydrogels
1. Colloquium of SPP 1681/13. German Ferrofluid Workshop, Benediktbeuern, 24.-27.09.2013

K. Zimmer, M. Ehrhardt, P. Lorenz, C. Vass, T. Csizmadia, B. Hopp
Reducing the incubation effects for rear side laser etching of fused silica
EMRS, Spring Meeting, Straßburg, 27.-31.05.2013

M. Zink, F. Szillat, U. Allenstein, S.G. Mayr
Tuning biocompatibility of single crystalline $Fe_{70}Pd_{30}$ ferromagnetic shape memory films for cell sensing
MRS, Fall Meeting, Boston, MA, USA, 01.-06.12.2013

Patents

K. Zimmer, A. Braun, D. Ruthe
Laserritzen von Dünnschichthalbleiterbauelementen
Patent granted Germany DE 103 26 505.8

Th. Hänsel, P. Seidel, A. Nickel, I. Bucsi
Verfahren und Vorrichtung zur präzisen Positionierung eines Ionenstrahles bei gleichzeitiger Bestimmung seines Abtragsprofiles
Patent granted Germany DE 10 2007 015 351.3

Leibniz-Institut für Oberflächenmodifizierung e. V.
Permoserstraße 15 / D-04318 Leipzig / Germany

Telefon: +49 (0) 341 235-2308
Telefax: +49 (0) 341 235-2313

www.iom-leipzig.de